UNIVERSITY OF CALIFORNIA,
IRVINE

Vaccine-induced adaptive T cell immunity enhances protective responses against *Coxiella burnetii*

DISSERTATION

submitted in partial satisfaction of the requirements
for the degree of

DOCTOR OF PHILOSOPHY

in Biomedical Sciences

by

Sharon Jan

Dissertation Committee:
Professor-in-Residence Philip Felgner, Chair
Professor Eric Pearlman
Professor Szu-Wen Wang
Professor Rongsheng Jin

2023

DEDICATION

To

my family and friends

for always loving and supporting me

TABLE OF CONTENTS

	PAGE
LIST OF FIGURES	iii
LIST OF TABLES	v
ACKNOWLEDGEMENTS	vi
VITA	viii
ABSTRACT OF THE DISSERTATION	xi
CHAPTER 1	1
Introduction	
CHAPTER 2	24
Bacteria-like particle bead complexes as an immunostimulatory platform for high-throughput vaccine antigen capture and delivery	
CHAPTER 3	55
Multivalent vaccines demonstrate immunogenicity and protect against *Coxiella burnetii* aerosol challenge	
CHAPTER 4	99
Conclusions and perspectives	
REFERENCES	106

LIST OF FIGURES

FIGURE **PAGE**

Figure 1.1 12

PAMP activation of NF-κB in antigen presenting cells (APC) result in immune cell recruitment and upregulation of cellular and humoral responses.

Figure 1.2 18

Antigen-specific T cells induced by antigen presentation activate macrophages.

Figure 1.3 20

$CD4^+$ T cells and macrophages are important in controlling C. burnetii infection.

Figure 1.4 23

Simplified overview of examples of toll-like receptors and agonists.

Figure 2.1 38

Schematic for antigen capture system capturing His-tagged proteins from in vitro protein synthesis via IVTT.

Figure 2.2 39

Efficient and high-throughput extraction of purified His-tagged proteins expressed in the cell-free system demonstrates immunogenicity.

Figure 2.3 43

IVAX-1 (MPLA, CpG1018, AddaVAX) increases immunogenicity of multiplex bead formulation.

Figure 2.4 46

Feasibility of modification, isolation, and purification of the bacterial sacculus.

Figure 2.5 49

The sacculus increases immunogenicity of subunit vaccine formulations and demonstrates synergy with AddaVAX.

Figure 3.1 65

Antibody and T cell profiling after administration of Q-VAX.

Figure 3.2 73

Immunogenicity screen of candidate *C. burnetii* antigens.

Figure 3.3 78

IVAX-1 (MPLA, CpG1018, AddaVAX) is a potent combination adjuvant for enhancing IgG2c responses and increasing proinflammatory cytokine production.

Figure 3.4 82

Guinea pig vaccine formulations were evaluated for reactogenicity.

Figure 3.5 86

Multiple antigens induce IgG responses in Hartley guinea pigs.

Figure 3.6 89

An intratracheal aerosol challenge study with *Coxiella burnetii* strain NMI RSA493 was performed in Hartley guinea pigs (n=5).

Figure S3.1 96

Splenocytes from mice immunized with Q-VAX generate responses to purified protein.

Figure S3.2 97

Coxiella proteins expressed in IVTT were captured on Sepharose beads for mouse immunizations.

Figure S3.3 98

Guinea pig vaccine formulations were evaluated for reactogenicity.

LIST OF TABLES

TABLE	PAGE
Table 3.1 Literature, proteomics, and protein microarray selection of *Coxiella burnetii* protein antigen candidates.	67
Table 3.2 Vaccine formulations including adjuvants for immunogenicity studies in C57BL/6 mice.	77
Table 3.3 Vaccine formulations used in Hartley guinea pig challenge and reactogenicity studies.	81

ACKNOWLEDGEMENTS

I would like to express the deepest appreciation to my committee chair, Dr. Philip Felgner. You've been so supporting and encouraging throughout my graduate career, and I sincerely appreciate your patience and optimism. Without your guidance and wild ideas, this would not have been possible.

I'd like to thank the members of my dissertation committee, Dr. Eric Pearlman, Dr. Szu Wang, and Dr. Rongsheng Jin. I am forever grateful for your insight and periodic check ins that kept me going. You encouraged critical thinking and gave me valuable feedback on my research.

Thank you to Dr. Huw Davies and Dr. Anthony Gregory for all the mentorship you've provided in guiding the direction of my thesis. You were readily available for chats on experiment planning and data interpretation. I could always count on the both of you for immunology and *Coxiella* know-how. Anthony, you're a great BSL-3 buddy and you certainly have made the experiences memorable. Thank you for showing me the ropes and forcing me out of my scientific comfort zone.

I am very thankful to the friends I've made in the Felgner lab, both past and present. I'd like to start off with Jiin Felgner, our formulation star, an amazing scientist, and also an amazing cook! Thank you for always helping me with my projects and providing the lab with snacks. Thank you to Dr. Jenny Hernandez-Davies, my food partner-in-crime, for always being down to fulfill my never-ending cravings. And of course the rest of the Boba Crew – Rie Nakajima, Emily Silzel, and Sarai Ochoa. Dr. Rafael Ramiro de Assis, thank you for adopting me as your temporary science daughter and for teaching me R. Thank you Dr. E.J. Pone, for your overflowing enthusiasm and guidance in immunology and flow cytometry. Thank you to Dr. Al Jasinskas, Dr. Erwin

Strahsburger, Dr. Joshua Obiero, Andrew Sy, and Medalyn Supnet for the good talks and the fun times. I also must thank my wonderful collaborators for making this possible. Dr. Alycia Fratzke, Dr. Sean Fan, Dr. Tyler Albin, Dr. Amanda Burkhardt, and Aaron Ramirez, thank you for all your hard work in seeing things through.

Special shout-out to Dr. Harinder Singh and Dr. Joanne Ly of GPS-STEM for your support and advice. It was wonderful working with you both and you've taught me so much.

And lastly, thank you to the dear friends I have made in graduate school, for I have shown great growth thanks to all of you. We'll call it character development. Thank you so much for all the fun and I will always treasure our tea breaks and adventures that got me through both graduate school and the pandemic.

It's been an absolutely wild ride, full of ups and downs, but I'm so glad I made the journey and will come out a better scientist and person for it. Thank you, UCI, for giving me this opportunity of a lifetime.

VITA

Sharon Jan

EDUCATION

2023 **Ph.D.** in Biomedical Sciences, University of California, Irvine, Irvine, CA

2015 **B.S.** in Microbiology, University of California, Davis, Davis, CA

EXPERIENCE

2017-23 Graduate Student Researcher, University of California, Irvine, Irvine, CA
Advisor: Philip Felgner

2015-16 Research Assistant, Stanford University, Palo Alto, CA
Advisor: Stanley Rockson

2015 Research Intern, Animal Health Research Institute, Taipei, Taiwan
Advisor: Tzu-Ming Huang

2012 - 15 Student Research Assistant, University of California, Davis, Davis, CA
Advisor: Scott Dawson

PUBLICATIONS

1. **Jan S.**, Fratzke A.P., Felgner J., Hernandez-Davies J.E., Liang L., Nakajima R., Jasinskas A., Supnet M., Jain A., Felgner P.L., Davies, D.H., Gregory, A.E. Multivalent vaccines demonstrate immunogenicity and protect against *Coxiella burnetii* aerosol challenge. Front. Immunol. *manuscript under revision*

2. Pone E.J., Hernandez-Davies J.E., **Jan S.**, Silzel E., Felgner P.L., Davies, D.H. Multimericity amplifies the synergy of BCR and TLR4 for B cell activation and antibody class switching. Front Immunol. 2022 May 19;13:882502.

3. Hernandez-Davies J.E., Dollinger E., Pone E., Felgner J., Strohmeier S., **Jan S.**, Albin T., Jain A., Nakajima R., Jasinskas A., Krammer F., Esser-Kahn A., Felgner P., Nie Q., Davies D.H. Magnitude and breadth of antibody cross-reactivity induced by recombinant influenza hemagglutinin trimer vaccine is enhanced by combination adjuvants. Sci Rep. 2022 Jun 2;12(1):9198.

4. Fan Z., **Jan S.**, Hickey J.C., Davies D.H., Felgner J., Felgner P.L., Guan Z. Multifunctional Dendronized Polypeptides for Controlled Adjuvanticity. Biomacromolecules. 2021 Dec 13;22(12):5074-5086.

5. Fratzke A.P., **Jan S.**, Felgner J., Liang L., Nakajima R., Jasinskas A., Manna S., Nihesh F.N., Maiti S., Albin T.J., Esser-Kahn A.P., Davies D.H., Samuel J.E., Felgner P.L., Gregory A.E.. Subunit Vaccines Using TLR Triagonist Combination Adjuvants Provide Protection Against *Coxiella burnetii* While Minimizing Reactogenic Responses. Front Immunol. 2021 Mar 17;12:653092.

6. Hernandez-Davies J.E., Felgner J., Strohmeier S., Pone E.J., Jain A., **Jan S.**, Nakajima R., Jasinskas A., Strahsburger E., Krammer F., Felgner P.L., Davies D.H. Administration of Multivalent Influenza Virus Recombinant Hemagglutinin Vaccine in Combination-Adjuvant Elicits Broad Reactivity Beyond the Vaccine Components. Front Immunol. 2021 Jul 14;12:692151.

7. Ma C., Titorahardjo J.A., **Jan S.**, Schweizer S.S., Rosario S. A.C., Du Y., Zhang J.J., Morrissette N.S., Andrade R.M. Auranofin Resistance in *Toxoplasma gondii* Decreases the Accumulation of Reactive Oxygen Species but Does Not Target Parasite Thioredoxin Reductase. Front Cell Infect Microbiol. 2021 Mar 19;11:618994.

8. Khan S., Jain A., Taghavian O., Nakajima R., Jasinskas A., Supnet M., Felgner J., Davies J., de Assis R.R., **Jan S.**, Obiero J., Strahsburger E., Pone E.J., Liang L., Davies D.H., Felgner P.L. Use of an Influenza Antigen Microarray to Measure the Breadth of Serum Antibodies Across Virus Subtypes. J Vis Exp. 2019 Jul 26;(149).

ABSTRACTS AND PRESENTATIONS

Jan S., Gregory A., Liang L., Felgner J., Ramirez A., Duong T., Kwon Y.J., Wang S.W., Davies D.H., Felgner P.L. Development of Single Dose Nanoparticle Vaccines against Select Agent *Coxiella burnetii*.

- 2022 CBD S&T (San Francisco, CA) – Poster presentation

Jan S., Gregory A., Felgner J., Davies J., Nakajima R., Jasinskas A., Davies D.H., Felgner P.L. Assessing Immunogenicity of Vaccines and Adjuvant Combinations for Q Fever.

- 2022 AAI Immunology (Portland, OR) – Poster presentation

- 2021 UCI Immunology Fair (Irvine, CA) – Poster presentation

Jan S., Felgner J., Assis R.R., Davies J., Albin T., Nakajima R., Jasinskas A., Davies D.H., Felgner P.L. Bacteria-like particle bead complexes as an immunostimulatory platform for high-throughput vaccine antigen capture and delivery.

- 2020 AAI Immunology (Honolulu, HI) – Poster presentation (meeting canceled)
- 2019 UCI Immunology Fair (Irvine, CA) – Poster presentation

Jan S., Felgner J., Pone E.J., Nakajima R., Davies D.H., Felgner P.L. Combination Q fever vaccine antigen capture and in vivo delivery using microspheres.

- 2019 Immunology LA (Irvine, CA) – Poster presentation
- 2019 DTRA Coxiella Workshop (Arlington, VA) – Oral presentation
- 2019 ASM Biothreats (Arlington, VA) – Poster presentation

MEMBERSHIPS

- Trainee Council Member and BESTern (Broadening Experiences in Scientific Training Intern) of UCI GPS-STEM (formerly GPS-BIOMED), funded by NIH-BEST, 2017 – 2023.
- Department Representative for UCI Diverse Educational Community and Doctoral Experience (DECADE), 2019 – 2023.

ABSTRACT OF THE DISSERTATION

Vaccine-induced adaptive T cell immunity enhances protective responses against *Coxiella burnetii*

by

Sharon Jan

Doctor of Philosophy in Biomedical Sciences

University of California, Irvine, 2023

Professor Philip Felgner, Chair

Coxiella burnetii is an intracellular Gram-negative bacterium responsible for Q fever, a zoonotic disease with significant global health implications courtesy of its endemic status worldwide. This tier 2 select agent has the potential for use as a bioweapon due to low infectious dose and aerosol transmissibility. The development of a vaccine against *C. burnetii* is of great interest, particularly for people who are in close contact with ruminants and military personnel who may be exposed to the pathogen in the field. The Q-VAX vaccine, an inactivated whole-cell vaccine, has shown efficacy in preventing Q fever and has been used in high-risk populations. However, challenges remain in its widespread implementation due to limited availability and adverse reactions.

Immunological studies have demonstrated the crucial role of macrophages in the host's defense against *C. burnetii*, with these cells playing a central role in phagocytosis, antigen presentation, and the production of pro-inflammatory cytokines. Interferon gamma (IFNγ), a key cytokine produced by T lymphocytes and natural killer cells, plays a significant role in controlling *C. burnetii* infection by activating macrophages and enhancing their antimicrobial activity.

The use of nanoparticles as chemically programmable scaffolds in bead design shows promise in *C. burnetii* vaccine development. These nanoparticles can be engineered to display multiple proteins and epitopes, increasing immunogenicity and broadening the immune response. We showcased a high-throughput method of capturing expressed proteins onto bead scaffolds, which were directly administered to animals for *in vivo* evaluation. Additionally, the bacterial sacculus, the highly ordered peptidoglycan structure of bacteria, was explored as a vaccine scaffold and adjuvant. Muramyl dipeptide (MDP), the main component of the sacculus, acts as a pathogen-associated molecular pattern (PAMP) and activates innate immune responses through recognition by NOD-like receptors. The sacculus's immunogenicity as an adjuvant was also evaluated *in vivo*.

Adjuvants, such as toll-like receptor (TLR) agonists, are investigated here to enhance the immunogenicity of Q fever vaccines by increasing Th1 responses and IFNγ production. Challenge studies were conducted to evaluate subunit vaccine formulations containing downselected antigen candidates combined with optimized adjuvant combinations, including *C. burnetii* lipopolysaccharide.

In conclusion, understanding the immunology of *C. burnetii* infection and the challenges associated with vaccine development is essential for effectively combating Q fever. Continued research into novel vaccine strategies, adjuvants, and delivery systems holds promise for improving vaccine efficacy, reducing the global burden of Q fever, and protecting at-risk individuals.

CHAPTER 1:

INTRODUCTION

Coxiella burnetii

Overview

Coxiella burnetii is an intracellular, gram-negative bacterium that causes the zoonotic disease Q (for query) fever. Transmission to humans occurs primarily through inhalation of contaminated aerosols from infected ruminants, such as cattle, sheep, and goats (1). Q fever can manifest acutely or chronically and ranges in severity from mild flu-like symptoms to severe pneumonia, hepatitis, or endocarditis. Acute Q fever is the most common form of the disease and typically occurs after an incubation period of 2 to 3 weeks. The symptoms of acute Q fever may include fever, headache, muscle aches, fatigue, and chills, and the disease is usually self-limiting and resolves without treatment within a few weeks.

Chronic Q fever, on the other hand, is less common but a more severe form of the disease that can develop weeks to months after the initial infection. Chronic Q fever can occur in individuals with pre-existing heart valve disease or compromised immune systems, as well as those who have undergone heart valve surgery or have a history of vascular grafting. If left untreated, chronic Q fever can lead to endocarditis, an infection of the heart valves, which can be life-threatening with a considerable mortality of up to 60% (2). Other complications can include hepatitis, osteomyelitis, and granulomatous inflammation of various organs. Chronic Q fever can be treated with prolonged therapy of doxycycline and hydroxychloroquine (3).

History and phylogeny

Coxiella burnetii belongs to the phylum Pseudomonadota, renamed from Proteobacteria in 2021, and within that, the class Gammaproteobacteria (4). Phylogenetically, *Coxiella burnetii* is part of the order Legionellales, which comprises of *Legionella* and *Coxiella* families. These bacteria share

certain commonalities in terms of their intracellular lifestyle and association with host-associated infections. *Legionella pneumophila* is an intracellular parasite that shares similar properties in *Coxiella burnetii* in that it favors replication within macrophages and makes use of a type IVB secretion system to inject effector proteins into the host cell (5).

Coxiella burnetii is specifically classified within the family Coxiellaceae, containing the *Coxiella* genus. This family is characterized by bacteria that are obligate intracellular parasites capable of infecting a wide range of hosts, including mammals, birds, and arthropods (6). *Rickettsiella grylli*, an intracellular pathogen of arthropods, similarly to *C. burnetii*, was also previously categorized under the order Rickettsiales prior to 16S rRNA gene analysis before being placed into the Coxiellaceae family (7,8). Drs. Herald Cox and Gordon Davis of the Rocky Mountain Laboratory in Hamilton, Montana, and Dr. Rolla Dyer of the National Institutes of Health of the United States, pioneered the discovery of the pathogen and studies in human transmission of the newfound agent of Q fever in 1938, with Dyer contracting a laboratory infection (9). Meanwhile, Sir Frank Macfarlane Burnet and Dr. Edward Holbrook Derrick at the Queensland Health Department in Australia encountered a similar disease affecting abattoirs and worked tirelessly to identify the causative agent (10). Dyer and Burnet were in correspondence about their respective research and quickly realized that they were working on the same pathogenic organism. After many iterations, including *Rickettsia burneti*, *Rickettsia diaporica*, in 1948, the designation of *Coxiella burnetii* was settled upon, honoring those who discovered and characterized it (11,12).

At a broader level, *Coxiella burnetii* shares a lot of similarities to the phylogenetically distinct endosymbiotic Rickettsiaceae family within the Rickettsiales order, which is within the Alphaproteobacteria class of the Pseudomonadota phylum (13). The mitochondrion is believed to

have evolved from the predecessor of obligate bacterial parasite *Rickettsia prowazekii* (14,15). Along with their similar morphologies and intracellular natures, *Orienta tsutsugamushi* of the Rickettsiaceae family also exhibits differential developmental stages, similar to *C. burnetii*'s small and large cell variants (16,17). Despite their originally classification under the *Rickettsia* genus, *C. burnetii* differs in containing higher guanine-cytosine content in their genomes, with 42.2% compared to the ~30% of representative *Rickettsia* species (18). Their cell tropism is a major distinguishable feature between the two groups, as Rickettsiales generally invade the vascular epithelium, while *C. burnetii* invades macrophages, though they both replicate within a phagosome vacuole within the host cell. Rickettsiales, however, can only be transmitted by tick vectors, while *C. burnetii* can also be aerosolized (19).

Bacterial internalization and the parasitophorous vacuole

C. burnetii is internalized by activation of the phagocytic receptor CR3 through αvβ3 integrin and CD47. Virulent bacteria with the full LPS are poorly internalized due to interference with the αvβ3 integrin and CR3 interaction (20). *C. burnetii* has adapted to survive in host macrophages by residing and replicating via binary fission in a parasitophorous vacuole (PV), which is a harsh, low pH environment containing lysosomal characteristics (21). The bacterium exploits the host cell by preventing apoptosis and trafficking nutrients for bacterial replication in the PV (22,23). The highly-fusogenic PV maintains a pH of 5.2 and promotes lysosomal biogenesis and clearance of *C. burnetii* by decreasing the PV acidity to pH 4.8 (24). The acidity allows for *C. burnetii* to become metabolically active, switching from the environmentally resistant small cell variant to the replicative large cell variant (25). Upon internalization, the early phagosome is decorated with early endosome auto-antigen-1 (EEA1). Over time, the early phagosome matures and acquires

markers LAMP-1, CD63, V-H+ATPase, and an acidic pH. Phagosomes containing the virulent form of *C. burnetii* do not acquire small GTPase Rab7, a hallmark marker of late endosomes (20). Virulent *C. burnetii* is also notable in evading host recognition in that it does not activate host cell TLR4 or TLR2 (26). Addition of IFNγ *in vitro* to THP-1 monocytes stimulates the acquisition of cathepsin D, a lysosomal enzyme associated with phagosome-lysosome fusion (27). LAMP-1 and LAMP-2, which make up 50% of the proteins present on lysosomal membrane, delay the maturation and acidification of the PV (28).

Like *Legionella pneumophila* and *Rickettsiella grylli*, *C. burnetii* utilizes the type IV secretion system (T4SS), known as the Icm/Dot system, to deliver effector proteins into the host cell cytoplasm (29,30). These effectors play crucial roles in manipulating host cell processes and modulating the intracellular environment to benefit the bacterium, such as interfering with vesicular trafficking pathways, subverting immune responses, and modifying the host cell cytoskeleton. *C. burnetii* also modifies the PV membrane by incorporating host lipids, thereby shielding itself from host cell detection and immune surveillance (31,32). The T4SS is activated upon maturation of the *Coxiella*-containing PV with remodeling and massive expansion until it encompasses most of the host cell space (33). T4SS effectors primarily target factors that control autophagosome maturation and clathrin-mediated traffic, which assist in the providing nutrients and materials to the expanding vacuole (34,35).

Coxiella burnetii lipopolysaccharaide (LPS)

Coxiella burnetii exhibits phase variation, a phenomenon in which the bacterium switches between different LPS phase variants due to culture history. The sole difference in the virulent and avirulent form of *C. burnetii* lies in the O-antigen; the virulent form, smooth phase I, contains unusual sugars

and the avirulent form, rough phase II, lacks an O-antigen entirely due to high passage number (20,36). Virulent phase I *C. burnetii*, with its LPS, is able to subvert receptor-mediated endocytosis by inhibiting the interactions between integrins including CR3 (37). Studies have demonstrated that *C. burnetii* LPS can interfere with host immune responses by inhibiting pro-inflammatory cytokine production, impairing phagosome maturation, and suppressing activation of immune cells by promoting the host cell to produce anti-inflammatory cytokine IL-10 (38).

Select agent status and bioweapon potential

Due to its global distribution and endemic status in many parts of the world, Q fever is recognized as a significant public health concern (1,39). Those at greatest risk include workers in the livestock industry, such as farmers, veterinarians, and abattoir workers. Q fever can also have significant impacts on the operational readiness of military units, particularly those that are deployed to areas where the disease is endemic. Examples of regions that have dealt with recent outbreaks include parts of Australia, the Netherlands, and certain regions in Africa, where Q fever has been reported as an ongoing or recurring public health concern (40,41). A Q fever outbreak among military personnel can have significant impacts on operational readiness, as infected individuals may require hospitalization and prolonged treatment, which can reduce the number of available personnel for critical tasks.

Coxiella burnetii has the potential to be used as a bioweapon due to its ability to cause severe illness, its stability in the environment, and its potential for aerosol transmission (39,42). It has a low infectious dose of one organism and was investigated for its bioweapon potential during the Cold War by various countries, including the United States and the former Soviet Union (43).

Q fever can be difficult to diagnose, as it can present with a wide range of clinical manifestations, from mild flu-like symptoms to severe pneumonia or hepatitis. In addition, the bacterium can be difficult to culture, which can complicate laboratory diagnosis (44,45). This can result in underreporting of the disease and may contribute to the global burden of Q fever. Despite the global health implications of Q fever, there is currently no licensed vaccine available for human use in the US. Developing a vaccine for Q fever that is safe and effective will help to reduce the risk of outbreaks among military personnel and minimize the impact on operational readiness in addition to protecting at-risk groups that endure constant endemic exposure to ruminants.

Whole cell vaccine Q-VAX

Q-VAX is a whole-cell formalin-inactivated vaccine (WCV) against Q fever caused by *Coxiella burnetii*, has been developed and used in some countries, namely Australia, as a preventive measure (46,47). While Q-VAX has shown life-long efficacy in reducing the risk of Q fever, the major challenge it faces is that it been associated with various adverse reactions, including local pain, redness, and swelling at the injection site, as well as systemic reactions such as fever, headache, and muscle pain. These reactions are generally mild and self-limiting, but they can still affect vaccine acceptance and compliance, especially in individuals who have experienced adverse reactions in the past and contributes to the FDA's reluctance to approve for use in the United States.

Delayed-type hypersensitivity (DTH) is an immune response characterized by a localized inflammatory reaction that occurs 24 to 72 hours after exposure to an antigen (48). In the context of Q-VAX, DTH may be observed as a response to the vaccine components. In some individuals, administration of Q-VAX can elicit a DTH response at the injection site, especially if they have

had prior exposure to *C. burnetii* antigens such as in a prior infection (49–51). The DTH response involves the recruitment and activation of immune cells, particularly T cells, which recognize the vaccine antigens and initiate an inflammatory reaction. It manifests as redness, swelling, and induration at the site of vaccine injection. Even though Q-VAX has demonstrated efficacy in reducing the risk of Q fever, these challenges still need to be addressed and opens an avenue for the development of alternative vaccines.

Immune response to *C. burnetii*

The immune response to *C. burnetii* infection is complex and involves both innate and adaptive immune mechanisms. The bacterium has evolved to evade host immune surveillance and replicate within host cells, including macrophages and dendritic cells (52). During the early stages of infection, the bacterium can suppress the production of pro-inflammatory cytokines and chemokines, which can help it evade detection by the host immune system. Innate immune responses play a critical role in controlling *C. burnetii* infection (53). Recognition of the bacterium by pattern recognition receptors (PRRs) on macrophages and dendritic cells, such as TLR4 (toll-like receptor 4) and NOD2 (nucleotide-binding oligomerization domain-containing protein 2), leads to the production of pro-inflammatory cytokines, such as IL-1, IL-6, and TNFα, which recruit and activate other immune cells to the site of infection (54,55). This process is critical for the activation of adaptive immune responses, including T cell and B cell responses.

T cell responses are critical for the clearance of *C. burnetii* infection. $CD4^+$ T cells are essential for the activation of macrophages, which can phagocytose and kill the bacterium. $CD8^+$ T cells can directly kill infected cells, including macrophages and dendritic cells, and are important for controlling bacterial replication within host cells. B cell responses are important for producing

antibodies that can play a role in opsonization and phagocytosis, increasing macrophage engulfment and elimination of *C. burnetii*. Antibody-dependent cell-mediated cytotoxicity (ADCC) can also recruit natural killer (NK) cells that recognize the Fc region of antibodies bound to *C. burnetii* and release cytotoxic molecules, leading to the destruction of infected cells (56). Though important, overall antibody-mediated immunity plays a smaller role in direct bacterial clearance compared to T cell responses (57,58).

Antigen presentation

To effectively detect and respond to diverse foreign antigens, antigen-presenting cells (APCs) such as dendritic cells and macrophages engage in cross-talk and antigen presentation by interacting with B cells and $CD4^+$ and $CD8^+$ T lymphocytes. The recognition of antigens by lymphocytes triggers adaptive immune responses, leading to the generation of antigen-specific effector cells and the establishment of immunological memory (59,60).

APCs internalize antigens by phagocytosis, endocytosis, and receptor-mediated uptake, which then undergo proteolytic degradation in endosomes or lysosomes. This process generates antigenic peptide fragments that associate with major histocompatibility complex (MHC) molecules (61,62). Processed antigenic peptides are loaded onto MHC molecules, forming MHC-peptide complexes. MHC class I molecules present peptides to $CD8^+$ T cells, while MHC class II molecules present peptides to $CD4^+$ T cells that initiate helper T cell responses regulating immune reactions and facilitating B cell antibody production. MHC class I molecules primarily sample intracellular antigens, whereas MHC class II molecules predominantly sample extracellular antigens.

Interferon gamma (IFNγ)

Interferon gamma (IFNγ) is a cytokine that plays a critical role in the immune system's response to viral and bacterial infections, as well as in the regulation of immune cell function. IFNγ is mainly produced by T cells and natural killer (NK) cells, but it can also be produced by other immune cells such as macrophages and dendritic cells. Its main function is to activate immune cells and enhance their effector functions against infected cells and pathogens. IFNγ is also responsible for stimulating the production of nitric oxide (NO) and other reactive oxygen and nitrogen species (ROS and RNS) in macrophages, which can kill susceptible intracellular pathogens including *C. burnetii* (63). During the early stages of infection, *C. burnetii* can actively suppress the production of pro-inflammatory cytokines and chemokines, including IFNγ (52).

IFNγ promotes the differentiation of $CD4^+$ T cells into Th1 cells and enhances the expression of major histocompatibility complex (MHC) molecules on the surface of infected cells, facilitating the presentation of antigens to T cells and enhancing the activation of adaptive immune responses (64). Studies have shown that IFNγ is critical for the control of *C. burnetii* infection, and mice deficient in IFNγ or its receptor are more susceptible to infection (27,65–67). In addition, IFNγ production has been correlated with protective immunity in animal models of *C. burnetii* infection.

Nuclear Factor-Kappa B (NF-κB)

Toll-like receptors (TLRs) play a pivotal role in innate immune responses by recognizing pathogen-associated molecular patterns (PAMPs) and initiating a cascade of signaling events that lead to the activation of nuclear factor-kappa B (NF-κB) (68). NF-κB is a transcription factor that regulates the expression of numerous genes involved in immune responses, inflammation, and the adaptive immune system. Upon recognition of PAMPs, TLRs undergo conformational changes that enable the recruitment of intracellular adapter proteins, such as MyD88 (myeloid

differentiation primary response 88), leading to the activation of downstream signaling pathways (69). This activation results in the phosphorylation and subsequent degradation of inhibitor of κB (IκB) proteins, allowing NF-κB to translocate into the nucleus and initiate gene transcription. The pro-inflammatory cytokines and chemokines induced by NF-κB activation attract and activate immune cells, promoting antigen presentation, T cell priming, and antibody production (70–72). Following pathogen recognition receptor (PRR) and NF-κB activation, antigen presenting cells, including dendritic cells, upregulate MHC and costimulatory molecules and migrate to the draining lymph nodes to interact with naive T cells that are specific to the antigens (73,74). A simplified schematic is depicted in **FIG. 1.1**.

Figure 1.1

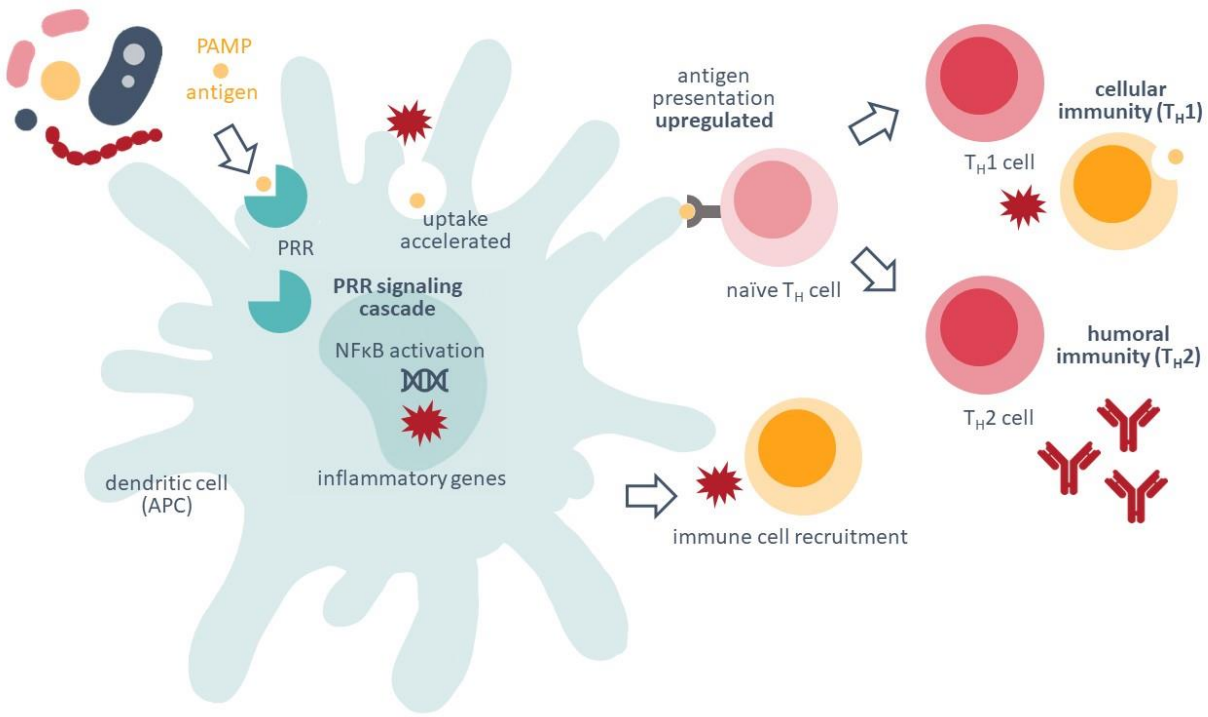

Figure 1.1 PAMP activation of NF-κB in antigen presenting cells (APC) result in immune cell recruitment and upregulation of cellular and humoral responses. When PAMPs are detected by antigen-presenting cells, the appropriate PRR signaling cascade results in NF-κB activation and immune cell recruitment via production of cytokines and chemokines. Antigen uptake is also accelerated, which allows for more efficient antigen presentation via MHC II to T helper cells that are differentiating to Th, Th2, Th17, or T regulatory cells based on the APC's secreted cytokines.

T helper cell differentiation

T helper (Th) cells are a heterogeneous subset of $CD4^+$ T cells that play a crucial role in orchestrating and regulating immune responses. These cells differentiate into distinct subsets characterized by their cytokine profiles and functions, namely Th1, Th2, Th17, regulatory T cells (Treg), and T follicular helper cells (Tfh) (75,76). Th1 cells orchestrate immune responses through the secretion of pro-inflammatory cytokines and play a crucial role in defense against intracellular pathogens and cell-mediated immunity. Key cytokines produced by Th1 cells include IFNγ, TNFα, and IL-2. TNFα contributes to inflammation, apoptosis, and activation of endothelial cells. IL-2 promotes T cell proliferation and enhances cytotoxic T cell responses. The Th1 response combats intracellular pathogens by promoting the activation and differentiation of cytotoxic T cells and macrophages (77).

Th2 cells are characterized by their secretion of cytokines such as IL-4, IL-5, IL-10, and IL-13. IL-4 is a key driver of B cell activation, class-switching to IgE and IgG1 isotypes, and induction of allergic responses. IL-5 is critical for the recruitment, activation, and survival of eosinophils, which play a role in defense against parasites (78). IL-10 exhibits immunomodulatory properties, suppressing pro-inflammatory responses and antigen presentation (79). IL-13 contributes to mucus production, tissue remodeling, and IgE production. Th2 responses are particularly important for immunity against extracellular pathogens, allergens, and parasitic infections.

Th17 cells play a role in immune responses against extracellular bacteria and fungi, as well as in autoimmune diseases. They are generally limited to the gastrointestinal tract in the absence of pathology, though expand upon infection. They produce IL-17A, IL-17F, IL-22, and TNFα, which recruit neutrophils and promote tissue inflammation and barrier defense (80,81). The primary

functions of Tregs are to suppress immune activation and maintain immune homeostasis. Tregs express the transcription factor Foxp3, which is crucial for their development and function (82). They exert their suppressive effects by inhibiting the activation and proliferation of other immune cells, such as effector T cells and antigen-presenting cells. Tregs are crucial for preventing autoimmune diseases, controlling inflammation, and regulating immune responses to self-antigens and harmless environmental substances through the expression of IL-10, transforming growth factor-beta (TGF-β), and IL-35. Expression of other contributors including cell surface receptors CTLA-4, CD39, and CD73 aid in directly targeting T cells or antigen presenting cells (83,84). Meanwhile, Tfh cells specialize in providing help to B cells in germinal centers during the generation of high-affinity antibodies. They express the chemokine receptor CXCR5, which promotes migration into B-cell follicles, and produce cytokines like IL-21, which aid in B cell proliferation, antibody class switching, and affinity maturation (85).

The differentiation of these Th cell subsets is regulated by various cytokines and transcription factors. Differentiation of Th1 cells is driven by IL-12 and the transcription factor T-bet, while Th2 cell differentiation is promoted by IL-4 and the transcription factor GATA-3 (80). Th17 cell differentiation is induced by TGF-β and IL-6, along with the transcription factors RORγt and STAT3 (86). Treg differentiation occurs in the thymus or peripheral tissues and is driven by interactions between the T cell receptor and MHC complexes on antigen-presenting cells. Other contributing factors include TGF-β, IL-2, and IL-10 (87,88). Tfh cell differentiation is influenced by IL-6, IL-21, and ICOS signaling, and the transcription factors Bcl-6 and c-Maf (85,89). The differentiation of Th cell subsets is a dynamic process influenced by the antigenic context, cytokine milieu, and interactions with antigen-presenting cells. These distinct Th cell subsets provide

specialized help to different arms of the immune system and contribute to the maintenance of immune homeostasis and effective immune responses against various pathogens and antigens.

Macrophages and bacterial clearance

Macrophages play a critical role in the immune response to *C. burnetii* infection and are one of the primary cell types for which *C. burnetii* exhibits tropism. Activated macrophages can phagocytose and kill *C. burnetii*, and the bacterium has evolved to resist this process. *C. burnetii* evades recognition by host macrophages and can prevent the fusion of phagosomes with lysosomes (52).

Two different activation states of macrophages, M1 and M2, have been described following the Th1/Th2 nomenclature and are just part of a wide spectrum of macrophage activation (90,91). For our purposes to simplify the concept, we will be referring to these generalized states as a dichotomy, though in reality it is far more complex. M1 macrophages are classically activated by proinflammatory molecules IFNγ and LPS. Interaction via the CD40 ligand from Th1 cells also promotes the M1 phenotype (92). They have a higher capacity of antigen presentation and microbicide via activation of the iNOS pathway and production of destructive molecules. The M2 macrophage phenotype is characterized by increased production of arginase-1, which blocks the iNOS pathway (93). Chronic Q fever is associated with the overabundance of arginase-1 and anti-inflammatory cytokine IL-10. *C. burnetii* is also known to stimulate an M2 macrophage polarization for survival in human macrophages, which causes them to become highly permissive to *C. burnetii* replication (66). M2 macrophages are an abundant source of IL-10, and treatment with anti-IL-10 antibodies has been demonstrated to reduce *C. burnetii* replication and persistence in the host (94). A simplified schematic depicting M1 and M2 macrophages is represented in **FIG. 1.2**.

To increase bactericidal activity against intracellular *C. burnetii*, the affected macrophages need to skew away from the resting M2 phenotype and toward an effector M1 phenotype to initiate an effective immune response. IFNγ and TNFα are two of the proinflammatory cytokines commonly associated with activation of the M1 macrophage phenotype and are strongly associated with cell mediated immunity (95,96). The importance of cell mediated immunity (CMI) against *C. burnetii* and other intracellular pathogens is well established (97–99). Activation of Ag-specific T cells is required for the control of *C. burnetii* infection as SCID, T cell deficient, and IFNγ k/o mice demonstrated greater susceptibility to infection (100,101). As IFNγ and TNFα are the prime candidates for increased bacterial clearance, noting the effects of the vaccine-induced proinflammatory cytokines is vital to understanding immunity and protection. Notably, pre-treatment of macrophages with IFNγ prior to infection *in vitro* induces the alkalization of *C. burnetii* vacuoles, implying bactericidal action (65). Reactive oxygen and nitrogen intermediates derived from iNOS, a hallmark of the M1 macrophage phenotype, are suspected to partially control *C. burnetii* infection (102). Interestingly, the phase 1 WCV is able to confer protection to mice deficient in either $CD4^+$ or $CD8^+$ T cells. Upon depletion of both populations, the mice are no longer protected (103). Both MHC I and MHC II-deficient mice exhibit more severe disease, though MHC I deficient mice developed a more severe infection and were unable to control bacterial replication (74). On a similar note, the cytotoxic $CD8^+$ cells involved are responsible for producing perforin, which is required to control *C. burnetii* infection. MHC II and $CD4^+$ cells, on the other hand, are responsible for secondary immune responses and help generate a protective antibody response. The culminations of these studies indicate that a strong cellular-mediated Th1 response is required for protection (57).

We have demonstrated the importance of $CD4^+$ T cells and macrophages in *C. burnetii* infection (**FIG. 1.3**). In a study with C57BL/6 mice, animals that have been immunized with WCV Q-VAX have significantly higher $CD4^+$ T cells than sham-vaccinated animals ($p<0.0001$), hinting at their role in inducing protective responses. In *in vitro* studies, avirulent phase II *C. burnetii* is significantly more permissible in M2 macrophages compared to M1 macrophages ($p=0.0006$ at MOI 25), which are also responsible for measurable iNOS production ($p<0.0001$ at MOI 100, $p=0.0005$ at MOI 25).

Figure 1.2

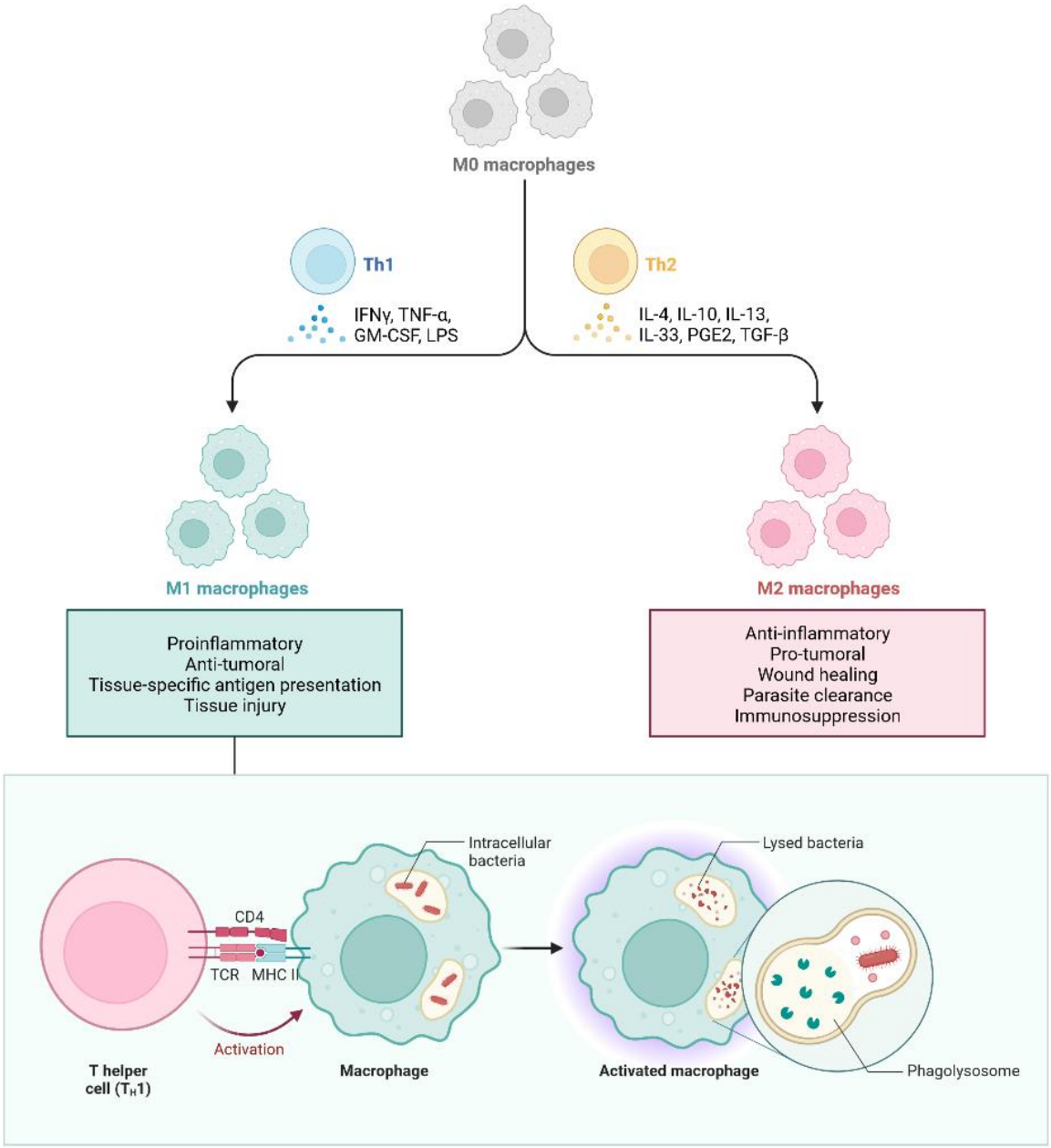

Figure 1.2. Antigen-specific T cells induced by antigen presentation activate macrophages. Following the Th1/Th2 paradigm, macrophages can exhibit M1 and M2 phenotypes upon activation via cytokines and interaction with Th1 cells. While M2 macrophages are anti-

inflammatory and allow for intracellular bacterial growth, M1 macrophages are proinflammatory and promote microbicidal activity, such as fusion of the phagosome in which intracellular bacteria reside with the acidic lysosome. Created in Biorender.

Figure 1.3

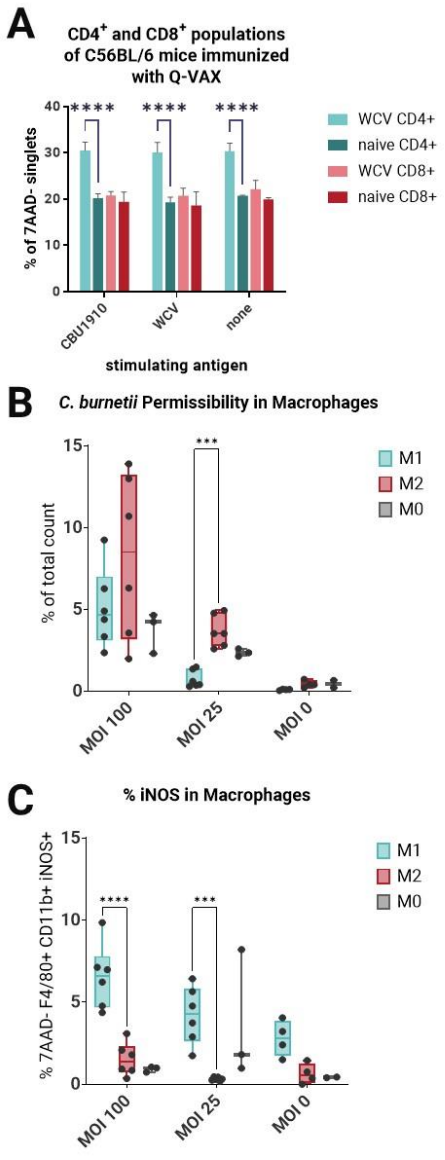

Figure 1.3. CD4$^+$ T cells and macrophages are important in controlling *C. burnetii* infection. (A) C57BL/6 mice were immunized with model C. burnetii antigen CBU1910, WCV Q-VAX, or PBS, boosted 14 days later, then terminated 10 days later (n=4). Splenocytes were extricated and assessed for their CD4$^+$ and CD8$^+$ cell populations. Statistics were performed with two-way ANOVA and Tukey's multiple comparisons test. **(B)** Bone marrow-derived macrophages (BMDM) were differentiated into M1 and M2 macrophages via the addition of IFNγ/LPS and IL-4, respectively. The BMDM were infected with avirulent phase II *C. burnetii* and incubated for 5 days (n=3-6). Statistics were performed with two-way ANOVA and Tukey's multiple comparisons test. **(C)** Infected BMDMs were assessed for iNOS production (n=4-5). Statistics were performed with two-way ANOVA and Tukey's multiple comparisons test.

Adjuvants

Adjuvants are compounds that are included in vaccines to enhance and modulate the immune response elicited by the vaccine antigens. The studies described here focus primarily on TLR agonists. TLRs are expressed on various immune cells, including dendritic cells, macrophages, and B cells. Upon recognition of PAMPs, TLRs initiate intracellular signaling pathways that lead to the activation of immune cells and the production of pro-inflammatory cytokines and other immune mediators. TLR agonist adjuvants are designed to mimic the effects of PAMPs, thus activating TLRs and promoting immune responses (**FIG. 1.4**). Common TLR agonists used as adjuvants include LPS to activate TLR4, CpG oligodeoxynucleotides (CpG ODN) to activate TLR9, and imidazoquinolines to activate TLR7 and TLR8 (104).

The top synergistic candidates used in these studies include a combination of synthetic TLR4 agonist monophosphoryl lipid A (MPLA), TLR9 agonist CpG ODN 1018, and AddaVAX, a squalene oil-in-water emulsion. MPLA is a significantly less toxic synthetic derivative of *Salmonella minnesota* lipopolysaccharide (LPS) due to the removal of the one or more acyl chain and phosphate groups, but is able to retain its immunogenicity and has been approved for use in the commercial SHNGRIX vaccine (105). Unmethylated CG dinucleotide motifs are TLR9 agonists commonly featured in prokaryotes, but rare in eukaryotes. Synthetic oligodeoxynucleotides (ODNs) are designed to mimic these bacterial nucleic acids and strongly promotes development of Th1 cells. CpG 1018 is a CpG-B class oligonucleotide, which demonstrates strong B cell activation, dendritic cell activation, but weak IFN-α induction (106). As a squalene oil-in-water emulsion, AddaVAX is capable of eliciting a mixed Th1/Th2 response. The mechanism is still poorly understood, but the efficacy is undisputed as equivalents have been

used in many commercially approved vaccines. The emulsion is a biphasic system of a hydrophilic and hydrophobic phase and requires a surfactant to stabilize the oil-water interface. AddaVAX and related emulsion adjuvants are capable of improving antigen presentation, facilitating transport of antigens, activating immune cells, and inducting cytokine production (107).

Summary

My thesis work aimed to contribute to *C. burnetii* vaccine development by constructing a chemically-programmable biologically-derived nanoparticle in the bacterial PGN sacculus and downselecting immunogenic protein antigens for subunit vaccine design. Here, we show that we were able to maximize the proteins' immunogenicity by combining them with an adjuvant cocktail of our lab's invention, which successfully conferred protection to challenged animals.

Figure 1.4

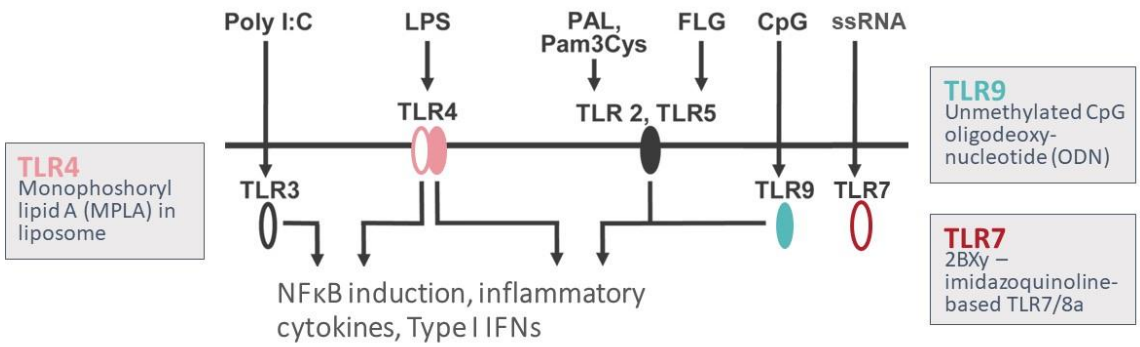

Figure 1.4. Simplified overview of examples of toll-like receptors and agonists. Agonists used in this study are highlighted. TLR4, TLR2, and TLR5 reside on the host cell plasma membrane while TLR3, TLR9, and TLR7 are endosomal.

CHAPTER 2:

Bacteria-like particle bead complexes as an immunostimulatory platform for high-throughput vaccine antigen capture and delivery

Sharon Jan, Jiin Felgner, Rafael Ramiro de Assis, Jenny E. Hernandez-Davies, Tyler Albin, Rie Nakajima, Algimantas Jasinskas, D. Huw Davies, and Philip L. Felgner

Abstract

Virus-like particles (VLPs) are a subclass of subunit vaccines that mimic virus structure without containing harmful genetic material, improving immunogenicity of recombinant protein and making them promising for vaccine development. The authentic conformation of VLPs allow for optimal antigen presentation has generated many VLP-based vaccines that have been proven safe and effective against viral pathogens. Nanoparticle vaccines with potent adjuvants can be designed to mimic VLPs, therefore optimize delivery and enhance immunogenicity. In this study, we explore polystyrene beads as potential antigen scaffolds using poly-His-tagged proteins and tris-NTA linkers to enable efficient antigen capture. The surface of the beads simulates the surface of the viral capsid, allowing for multivalent presentation and increased cross-linking with B and T cell receptors. We also explore the bacterial peptidoglycan (PGN) sacculus, a biological construct consisting of the intact peptidoglycan network, as a potential scaffold and adjuvant. We successfully demonstrate high-throughput protein production, efficient antigen capture, and chemical modification of the sacculus for protein bioconjugation. are demonstrated. Overall, programmable scaffolds including beads and the modified bacterial sacculus hold potential for safe and effective vaccines against diverse diseases, including *Coxiella burnetii*.

Introduction

Subunit vaccines, though less potent than whole-cell vaccines, are widely considered to be safer as they contain the minimal components necessary to elicit an effective immune response (108,109). Adjuvants are a crucial part of subunit vaccine development due to their ability to prime the innate immune response and shape adaptive immunity (110,111). Other studies have demonstrated that direct linking of antigen and adjuvantic scaffold encourages antigen internalization via phagocytosis and enhances cross-presentation when compared to unlinked antigen and adjuvant (112–114). The goal is to explore the properties of different scaffolds used in delivering candidate vaccine antigens to stimulate a protective and safe immune response.

Virus-like particles (VLPs) have emerged as a promising platform for vaccine development due to their ability to mimic the structure and antigenicity of viruses without the infectious genetic material (115–117). VLPs are composed of viral structural proteins that can self-assemble into particles that resemble intact viruses, but lack the genetic material required for replication. This makes VLPs a safe and effective alternative to live attenuated or inactivated virus vaccines. VLPs have been shown to induce strong and durable immune responses against a wide range of viral pathogens, including human papillomavirus, hepatitis B virus, and influenza virus (118–123). Moreover, the ability to engineer VLPs with foreign antigens has expanded their potential utility beyond viral vaccines, making them an attractive platform for the development of vaccines against other infectious diseases. Nanoparticle vaccine designs based on VLPs saw a rise in popularity as they were shown to be safer than traditional whole-cell vaccines and allowed for fine-tuning of aspects such as delivery and release. These nano-scaffolds can be combined with potent adjuvant formulations to effectively optimize delivery and increase immunogenicity (124,125).

Direct linking of antigen and scaffold encourages antigen internalization via phagocytosis and enhances cross-presentation when compared to unlinked antigen and adjuvant (126,127). Direct conjugation of antigens onto the surface of nanoparticles and other delivery vehicles can allow for antigen presentation to mimic that of a pathogen and induce a similar immune response (128). To couple a wide variety of protein antigens to different molecules and particles, we developed a self-assembly approach utilizing the poly-His-tag incorporated to our proteins expressed by *in vitro* transcription-translation (IVTT). Although the tris-NTA molecule is available commercially, it is prohibitively expensive. Thus, our collaborators were able to synthesize large quantities of tris-NTA-molecules containing a variety of chemical handles for conjugation (129,130). These compounds allow us to conjugate functionalized TLR agonists to the tris-NTA, followed by complexation with His-tagged antigens. Tris-NTA-biotin has been particularly useful in generating high-throughput vaccine tests and for diagnostic assays through streptavidin polystyrene bead capture. The other functionalized tris-NTAs have allowed us to generate conjugates with TLR agonists and nanoparticles for 'plug-and-play' antigen coupling (126,131). The binding of poly-His tagged protein to tris-NTA is high affinity, irreversible, and enables this "plug-and-play" approach for capturing antigens in a vaccine ready formulation.

Pathogen-associated molecular patterns (PAMPs) are potential vaccine adjuvants that can help steer the polarization of the immune response. One such candidate is bacterial peptidoglycan (PGN). The general structure of PGN, barring bacteria-specific modifications, is universal throughout the Eubacteria domain and easily recognized as an agonist for NOD-like receptors (NLR) (132–134). Upon recognition, the cascade induces downstream MAPK and NF-κB signaling to activate proinflammatory genes. Muramyl dipeptide (MDP) is a small molecule found in the peptidoglycan layer and has been extensively studied for its ability to stimulate a potent and

durable immune response, making it an attractive target for vaccine development (135). The sacculus is the entirety of the PGN network complex forming a sturdy framework that surrounds the cytoplasmic membrane of bacteria (136). We hypothesize that we can develop a vaccine antigen capture and *in vivo* delivery platform using the native bacterial PGN sacculus, which acts as a bacteria-like particle in priming the immune response.

Materials and Methods

Reagents and biologics

AddaVAX™ (squalene oil-in-water emulsion) was purchased from InvivoGen Inc. (San Diego, CA), CpG ODN 1018 (TLR9 agonists) were purchased from InvivoGen and Integrated DNA Technologies (Coralville, Iowa), respectively. CpG-ODN were dissolved in sterile water at 1 mM as stock. Monophosphoryl lipid A (MPLA, a TLR4 agonist) was purchased from Avanti Polar Lipids Inc. (Alabaster, AL). Recombinant proteins were expressed in *Escherichia coli* BL21 cells and purified by multiple column chromatography and endotoxin removal procedure by Genscript (Piscataway, NJ).

Animals

C57BL/6 female mice (6-12 weeks) were obtained from Charles River Laboratories (Wilmington, MA). Animal experiments were approved by the Institutional Animal Care and Use Committee of the University of California, Irvine and the Animal Care and Use Review Office (ACURO) of the U.S. Army Medical Research and Materiel Command (USAMRMC). Mice were housed in standard cages with enrichment at ABSL2 and guinea pigs were housed in approved animal biosafety level 3 (ABSL-3) facilities. For immunogenicity studies, mice were anesthetized in induction chambers with inhaled isoflurane/O_2 and passive scavenging with F/air canisters. Where

indicated, mice were immunized either subcutaneously at the base of the tail or intraperitoneally in the right abdominal quadrant. Blood was collected from submandibular vein with 25 g hypodermic needles (Medline, Northfield, IL), Microvette CB 300 lithium heparin (Sarstedt, Newton, NC), and BD Microtainer PST tubes with lithium heparin (BD, Franklin Lakes, NJ).

In vitro transcription translation (IVTT) of downselected C. burnetii proteins

Downselected *C. burnetii* ORFs were cloned into pXI vector using a high-throughput PCR cloning method previously described. Downselected *C. burnetii* proteins were expressed in an *E. coli*-based *in vitro* transcription translation system according to the manufacturer's instructions (biotechrabbit GmbH, Berlin, Germany). Briefly, plasmid templates were prepared using QIAprep Spin Miniprep kits (Qiagen, Venlo, Netherlands). Plasmid concentrations were confirmed using Nanodrop (Thermo Fisher Scientific, Waltham, MA) and analyzed using gel electrophoresis. 40 µL of 100 ng/µL DNA template was added to 200 µL reactions and resulting proteins were quantified and validated by western blot using a monoclonal anti-polyHistidine antibody produced in mouse (MilliporeSigma, Burlington, MA).

Protein purification of GFP and CBU1910

The protein of interest (GFP or CBU1910) was expressed in *Escherichia coli* DH5α cells (New England Biolabs, Ipswich, MA) using a pXI expression vector containing a T7 promoter and a 6x polyhistidine (His) tag sequence. The cells were grown in Terrific Broth (TB) medium containing 100 µg/mL of kanamycin at 37°C until the OD600 reached 0.6-0.8. Protein expression was induced by adding 1 mM isopropyl β-D-thiogalactopyranoside (IPTG) and the cells were incubated for an additional 3-4 hours at 37°C. The bacterial cells were harvested by centrifugation at 10,000 x g for 10 min at 4°C and the cell pellet was lysed in BugBuster protein extraction reagent per the

manufacturer's instructions (MilliporeSigma, Burlington, MA). The cell suspension was incubated on a rotating rocker for 10 min and then centrifuged at 16,000 x g for 20 min at 4°C to remove insoluble cell debris. The His-tagged protein present in the remaining supernatant was purified using a column loaded with HisPur Ni-NTA Resin (Thermo Fisher Scientific, Waltham, MA). The column was equilibrated with wash buffer (20 mM imidazole, 2x PBS) and the cleared lysate was loaded onto the column. The column was washed with wash buffer to remove any non-specifically bound proteins. The His-tagged protein was then eluted with elution buffer (250 mM imidazole, 2x PBS). The purified protein was analyzed by SDS-PAG to confirm purity and size.

Coupling of proteins onto polystyrene beads

Streptavidin 1 µm or 0.2 µm polystyrene beads were purchased from Bangs Laboratories (Fishers, IN). Beads were diluted 10-fold with buffer containing PBS and 0.02% Tween20 and washed by centrifuging at 5500 x g for 5 min. Biotin-Tris-NTA at a stock of 1 mg/mL was added in 2.5x molar excess to the streptavidin beads, incubated for 1 hour on a rotating rocker, and washed with PBS and 0.02% Tween20. 100x molar excess of $NiSO_4$ was added in the streptavidin-Tris-NTA beads, incubated for 2 hours on a rotating rocker, and washed with PBS and 0.02% Tween20. For protein conjugation, 1x molar equivalent of protein expressed with His-tags from either IVTT or purified was incubated with Ni-charged streptavidin-Tris-NTA beads and incubated for 2 hours on a rotating rocker. Beads were washed 4 times with PBS and 0.02% Tween and evaluated by SDS-PAGE to confirm conjugation.

SDS PAGE, silver stain, and western blot

Proteins were separated by precast NuPAGE 4-12% Bis-Tris protein gels (Invitrogen, Waltham, MA). Silver stains were prepared with the Pierce Silver Stain kit according to the manufacturer's

instructions (Thermo Fisher Scientific, Waltham, MA). For western blot, gels were transferred to a nitrocellulose membrane using the iBlot transfer system (Invitrogen, Waltham, MA). The membrane was blocked with 5% milk for 1 hr at room temperature. Primary monoclonal anti-His antibody produced in mouse (MilliporeSigma, Burlington, MA) was diluted according to the manufacturer's instructions and incubated with the membrane for 1 hr. The membrane was washed with PBS containing 0.02% Tween-20 and incubated with a horseradish peroxidase (HRP)-conjugated secondary antibody specific to the murine host (Bethyl Laboratories, Montgomery, TX) for 1 hr. Band intensity was quantified with ImageJ software.

Serological profiling by protein microarrays

C. burnetii proteome microarrays were produced as described previously (137–139). Briefly, proteins from the *C. burnetii* Nine Mile I strain RSA 493 proteome were expressed from purified plasmids in an *Escherichia coli*-based cell-free, *in vitro* transcription translation system (IVTT) (Biotechrabbit GmbH, Hennigsdorf, Germany). IVTT reactions were printed onto nitrocellulose-coated glass AVID slides (Grace Bio-Labs Inc., Bend, OR) using an Omni Grid 100 microarray printer (Genomic Solutions). Plasma was diluted 1:100 in protein array blocking buffer (GVS, Sanford, ME) and incubated with 0.1 mg/mL of a His-tag-containing peptide (HHHHHHHHHHGGGG) (Biomatik, Wilmington, DE) at room temperature for 30 min to block anti-His antibodies generated by the immunizations. Afterwards, the arrays were incubated overnight at 4ºC with gentle rocking. Arrays were washed three times with TBS-0.05% Tween 20 (T-TBS) and then incubated with goat anti-mouse IgG-biotin, IgG1-biotin, or IgG2c-biotin (1:200 in array blocking buffer) (Jackson ImmunoResearch, West Grove, PA) for 1 hour at room temperature with gentle rocking. Following another set of T-TBS washes, bound antibodies were detected with streptavidin-conjugated Qdot®655 or Qdot®800 (1:250 in array blocking buffer;

Thermo Fisher Scientific, Waltham, MA) for 1 hour at room temperature with gentle rocking. Arrays were washed three times with T-TBS, the slides rinsed thoroughly with water, and then air dried by centrifugation at 500 g for 10 min. Images were acquired and spot fluorescence intensities quantified using the ArrayCAM™ Imaging System (Grace Bio-Labs, Bend, OR). Signal intensities (SI) for each antigen on the array were background corrected by subtracting sample-specific T-PBS buffer signals from purified protein spot signals.

RAW-Blue NF-κB reporter cell line

RAW-Blue cells derived from RAW 264.7 murine macrophages were cultured according to the manufacturer's instructions (InvivoGen, San Diego, CA). Briefly, the cells were propagated in DMEM, high glucose, GlutaMAX with HEPES and 10% FBS (Gibco, Waltham, MA). Media was supplemented with 100 µg/mL penicillin/streptomycin (Thermo Fisher Scientific, Waltham, MA) and 100 µg/mL Normocin (InvivoGen, San Diego, CA). Cells were detached by cell scraper and plated into flat bottom 96-well plates with 100,000 cells in 180 µL of cell suspension. 20 µL of adjuvant at differing concentrations was added to the wells and the plate was incubated at 37°C with 5% CO_2 for 18 hr. QUANTI-Blue reagent, a secreted embryonic alkaline phosphatase (SEAP) detection medium, was used to visualize the plate according to the manufacturer's instructions (InvivoGen, San Diego, CA). 50 µL of the culture supernatants was added to 150 µL of QUANTI-Blue solution and incubated at 37°C for 2 hr. The plate was quantified by measuring absorbance OD at 620-655 nm.

T cell recall assays

Spleens were harvested from mice 10 days after they were boosted via the i.p. route and erythrocyte-depleted splenocyte suspensions prepared for T cell recall assay (IFNγ ELISpot) as

previously described (140). Purified antigens were titrated in the assay (final concentrations of 10, 5, 2.5, and 0 μg/mL). Spleen cells from naïve mice were assayed in parallel as a control for potential mitogenic activity of the recall antigens. Assays were performed in T cell medium (TCM) comprising Iscove's Modified Dulbecco's Medium (IMDM), containing 5×10^{-5} M β-mercaptoethanol, 100 IU/mL penicillin, 100 μg/mL streptomycin, and 10% heat-inactivated fetal calf serum. After 18 h of incubation, the assay supernatants were collected for multiplex cytokine screening using the LEGENDplex kit (BioLegend Inc., San Diego, CA) according to the manufacturer's instructions before the ELISpot was processed. Spots were quantified in an ImmunoSPOT® ELISpot plate reader (Cellular Technology Limited, Cleveland, OH).

Bacterial labeling

DH5α *E. coli* was grown overnight at 37°C in 5 mL of Terrific Broth on a shaker. A new 5 mL Terrific Broth culture with a 1:50 inoculation of the overnight growth also at 37°C was monitored until exponential growth phase at OD_{600} 0.3. 50 μL of 1 M R-propargylglycine (Thermo Fisher Scientific, Waltham, MA) was added to the culture and incubated at 37°C with agitation. The culture was centrifuged at 2000 x g for 15 min to pellet. The pellet was washed and resuspended with PBS then centrifuged again at 4000 x g for 10 min. Cells were fixed by adding ice-cold 100% methanol, incubated for 5 min on a rotating rocker, then pelleted and washed with PBS. Cells were labeled with AFDye 488 Azide and Click-&-Go Cell Reaction Buffer kit according to the manufacturer's instructions (Click Chemistry Tools, Scottsdale, AZ). The cells were washed and resuspended with ddH_2O for imaging.

Sacculus preparation

DH5α *E. coli* was grown overnight at 37°C in 5 mL of Terrific Broth on a shaker. A new 200 mL Terrific Broth culture with a 1:50 inoculation of the overnight growth also at 37°C was monitored until exponential growth phase at OD_{600} 0.3. 1 mL of 1 M R-propargylglycine (Thermo Fisher Scientific, Waltham, MA) was added to the culture and incubated at 37°C with agitation for 20 min. The culture was chilled on ice for 10 min and centrifuged at 2000 x g for 15 min to pellet. The pellet resuspended with 100 mM NaCl and the suspension was slowly added to boiling SDS on a hotplate at a rate of 0.5 mL/min over a period of 30 min. 8% wt/vol of SDS was added to the slurry and stirred at 80-90°C for 1 hour. The suspension was ultracentrifuged 3x at 45,000 x g for 30 min at room temperature and resuspended in ddH_2O after each round to remove the SDS. The final suspension was resuspended in 10 mM sodium phosphate buffer (pH 7.0) or ddH_2O for imaging.

Particle sizing of bacterial sacculus

Particle size analysis was performed with the Malvern Zetasizer ZS Nano DLS (Malvern, Worcestershire, UK). The sacculus sample was suspended in ddH_2O and mixed prior to loading in a cuvette. Multiple measurements were taken for each sample to ensure reproducibility.

Confocal imaging of labeled bacteria and polystyrene beads

Labeled bacteria preparations were immobilized on glass slides containing a thin layer of 0.5% agarose with a coverslip and imaged with a Zeiss LSM 780 (Oberkochen, Germany). Samples had an excitation of 494 nm and emission of 517 nm.

10 µL of the mixture containing 4.5 x 10^6 beads/µL with a density of 200,000 GFP per 1 µm bead was added to a 35 mm glass bottom chamber and immobilized with a coverslip. Images were obtained with an Olympus Fluoview FV3000i confocal laser scanning microscope (Tokyo, Japan).

The APC-Flash Red bead (Bangs Laboratories, Fishers, IN) was excited at 660 nm with an emission at 690 nm. The GFP containing a 6x His tag used was excited at 470 nm with an emission at 509 nm.

Transmission electron microscopy of polystyrene beads and sacculus

Carbon film on 300 mesh copper support grids (Ted Pella, Redding, CA) were prepared for hydrophilic sample deposition by glow discharge using the Leica EM ACE200 coating system (Leica Microsystems, Wetzlar, Germany). 10 µL of sample (4.4 mg/mL for sacculus diluted 1:100 with ddH_2O, and 4.5 x 10^6 polystyrene beads/µL) was stained with uranyl acetate and imaged using a JEM-2100F (JEOL, Tokyo, Japan) with Gatan OneView camera (Pleasanton, CA).

Statistical analyses

Statistical analyses were performed with GraphPad Prism v9.4.0 (GraphPad Software, La Jolla, CA, USA) and R Statistical Software v4.1.1 (Vienna, Austria). Results were compared using paired T test, one-way or two-way ANOVA with Dunnett's or Tukey's correction for multiple comparisons, and Wilcoxon signed-rank test. Differences were considered significant if p-value ≤ 0.05 (*), ≤ 0.01 (**), ≤ 0.001 (***), or ≤ 0.0001 (****).

R packages used in statistical analyses and visualization include:

- limma (https://rdocumentation.org/packages/limma/versions/3.28.14)
- ggplot2 (https://ggplot2.tidyverse.org)
- scales (https://rdocumentation.org/packages/scales/versions/1.2.1)

Results

In vitro transcription translation is used for high-throughput protein production

To work around the prohibitively expensive commercialized biotin and amino-functionalized tris-NTA, our collaborators developed an in-house synthetic strategy to generate tris-NTA with new chemical handles (130). Tris-NTA-biotin was used as the chemical handle for conjugation to polystyrene beads containing streptavidin due to the high affinity between the tetrameric streptavidin and biotin. Ni(II)-chelated nitrilotriacetic acid (NTA) demonstrates high binding affinity for proteins containing a polyhistidine tag, which allowed for coupling between the tris-NTA-charged beads and His-tagged protein (**FIG. 2.1**). In order to validate the use of tris-NTA as a linker between scaffold and antigen, we demonstrated proof-of-concept by conjugating fluorescently-labeled 1 μm polystyrene beads to purified GFP protein containing a 6x His tag (**FIG. 2.2A-C**).

To validate vaccine antigen capture and delivery via the high-throughput *in vitro* transcription-translation expression system, we expressed candidate downselected His-tagged *C. burnetii* proteins in the cell-free system and successfully demonstrated purity in the capture with silver stain and immunoblots implementing anti-His antibodies for visualization (**FIG. 2.2D-F**). The silver stain was used as an encompassing, sensitive, and high-contrast detection method of biomolecules including proteins and nucleic acids. IVTT-expressed protein capture with model *C. burnetii* antigen CBU1910 was antigen-specific and easily scalable.

C57BL/6 mice were then immunized subcutaneously with 3 μg of captured protein antigen on polystyrene beads, boosted 14 days post-prime with the same formulations, and assessed for immunogenicity over time. Plasma from the animals were obtained for days 0, 14, and 28 post-immunization and assessed on a *C. burnetii* whole-proteome microarray for antigen-specific IgG antibody production. Responses increased over time and specific with minimal nonspecific signals

and cross-reactivity (**FIG. 2.2G-H**). Overall, expressing proteins in a high-throughput fashion using a cell-free system and capturing them from the complex mixture with polystyrene beads containing tris-NTA linkers demonstrated robust and specific IgG response after immunization.

Figure 2.1

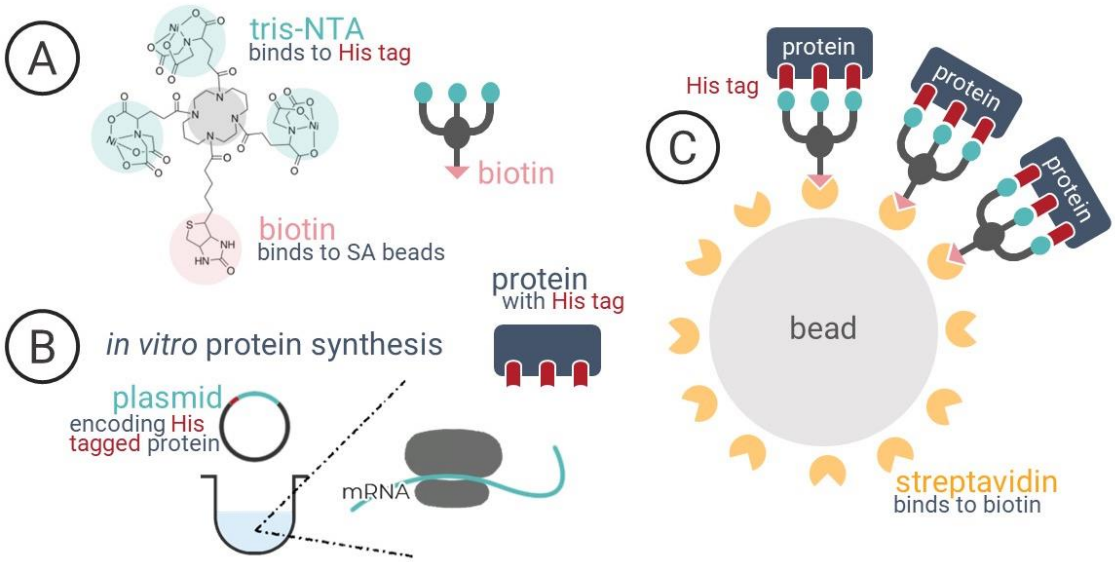

Figure 2.1. Schematic for antigen capture system capturing His-tagged proteins from in vitro protein synthesis via IVTT. (A) Chemical structure of tris-NTA-biotin. The His tag binds to the metal of metal chelator complexes, which in this case is nickel. **(B)** The plasmid encoding the His-tagged protein is expressed in an IVTT reaction, resulting in a protein residing within a complex mixture. **(C)** Capture onto a streptavidin-coated bead relies on the high binding affinity of biotin and streptavidin. Beads can be washed to extract the protein from the IVTT mixture.

Figure 2.2

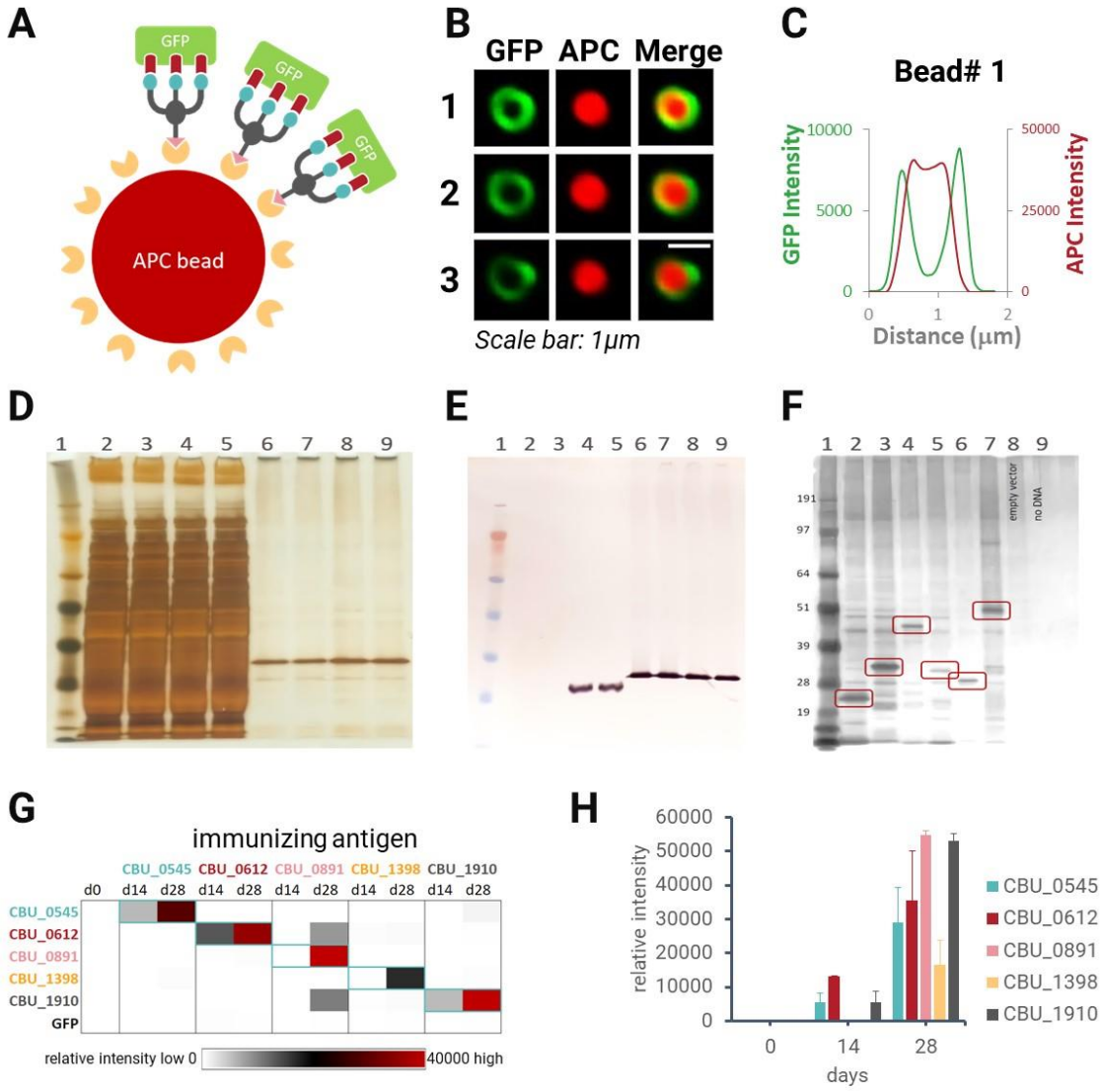

Figure 2.2. Efficient and high-throughput extraction of purified His-tagged proteins expressed in the cell-free system demonstrates immunogenicity. (A) Representative schematic of GFP (green fluorescent protein) conjugated to polystyrene APC streptavidin bead with tris-NTA linkers. **(B)** Confocal images of GFP conjugated to APC streptavidin beads using tris NTA-biotin linkers. **(C)** Relative intensities of GFP (ex. 488 nm, em. 510 nm) and APC (ex.

650 nm, em. 660 nm) colors across the distance of a 1 µm polystyrene bead. **(D)** Silver stain of the capture of CBU1910 on 1 µm bead. Lanes are ordered as follows: (1) marker, (2-3) IVTT with no DNA, (4-5) IVTT with model antigen, (6-9) bead capture. **(E)** Western blot following lane order of D. **(F)** Silver stain of all antigens captured. Highlighted in lanes 2-7 are bands containing target antigen. **G.** Heat map showing antigen-specific IgG response of the plasma of mice immunized with antigens captured on beads at days 14 and 28. Highlighted are regions in which an antibody response corresponded to the immunized antigen. **(H)** Relative intensities of antigen-specific antibody response in mice to immunized antigen captured on beads plotted over time. N=3 in each group.

Adjuvants enhance immunogenicity of multivalent bead formulations

Having demonstrated that individual antigens were able to be purified from complex IVTT mixtures, our next step was to mix the bead antigens together to deliver a multivalent vaccine formulation. Based on previous and concurrent studies, we had determined the adjuvant combination coined as IVAX-1 containing TLR4 agonist monophosphoryl lipid A (MPLA), TLR9 agonist CpG oligodeoxynucleotide (ODN) 1018, and squalene oil-in-water emulsion AddaVAX elicited the most balanced IgG1 and IgG2c responses, corresponding to the Th2 and Th1 response, respectively (141,142). In the context of *Coxiella burnetii*, eliciting a Th1 response to combat an infection is more desirable due to its microbicidal effect on intracellular pathogens. Using a NF-κB Raw 264.7 mouse macrophage reporter cell line, RAW-Blue, we evaluated the activity of the combination and individual components of IVAX-1 compared to known NF-κB activator *E. coli* LPS (**FIG. 2.3A**). As MPLA is a less endotoxic variation of LPS, it was not surprising that it was able to elicit a robust NF-κB response ($p=0.6181$). The majority of IVAX-1's NF-κB-inducing activity is attributed to MPLA ($p=0.9586$), though it should be noted that when CpG was formulated with a liposome for better endosomal delivery, it was able to demonstrate a more robust response (data not shown).

0.2 μm polystyrene beads were used to better enter the draining lymph nodes and elicit a stronger immune response. By using the same methodology in generating IVTT proteins captured on polystyrene beads, C57BL/6 mice were immunized with a cocktail of 3 μg each of 6 *C. burnetii* antigens, CBU0612, CBU1910, CBU0891, CBU0307, CBU0545, and CBU1398. These antigens were separately captured on beads as previously described and the beads were mixed for immunization. To validate the efficacy of the IVAX-1 adjuvant, another cocktail also containing

3 µg of the 6 *C. burnetii* antigens was combined with IVAX-1 and administered to mice on the same timeline. Animals were boosted 14 days post-prime, and plasma was collected at days 0, 14, and 28. The multiplex formulations of multiple antigens were able to induce robust antigen-specific IgG responses, though the difference between the unadjuvanted and adjuvanted groups was not significant for all antigens (CBU0612 p=0.1209, CBU1910 p=0.1763, CBU0891 p=0.1133, CBU0307 p=0.1070, CBU0545 p=0.1078, CBU1398 p=0.0978) (**FIG. 2.3B**). The signal intensities for the adjuvanted group did trend higher at earlier time points than the unadjuvanted group.

Plasma from day 28 was assessed for antigen-specific IgG1 and IgG2c signal intensities with a downselected proteome *C. burnetii* microarray. P values were calculated by comparing IgG1 and IgG2c signal intensities via Wilcoxon signed-rank test. A great majority of responses to the immunizing antigens skewed more heavily toward an IgG1 response in the unadjuvanted group (**FIG. 2.3C, 2.3E**), while this skewing is lost with the addition of IVAX-1 (**FIG. 2.3D, 2.3E**). Based on the data, we can confirm that the presence of the IVAX-1 adjuvant skews the IgG response from an IgG1-based to a IgG1/IgG2c balanced response.

The same animals were boosted again with IVTT antigens on beads on day 60 intraperitoneally and rested for 10 days before termination. A T cell recall assay was performed on the pooled splenocytes with stimulation using purified antigen. In the unadjuvanted group, only CBU1910 elicited a robust T cell recall response. With the addition of adjuvant, all immunizing antigens were above the limit of detection and formed more spot forming units. From this, we can conclude that the addition of adjuvant increases the immunogenicity of the antigens on beads *C. burnetii* vaccine formulation.

Figure 2.3

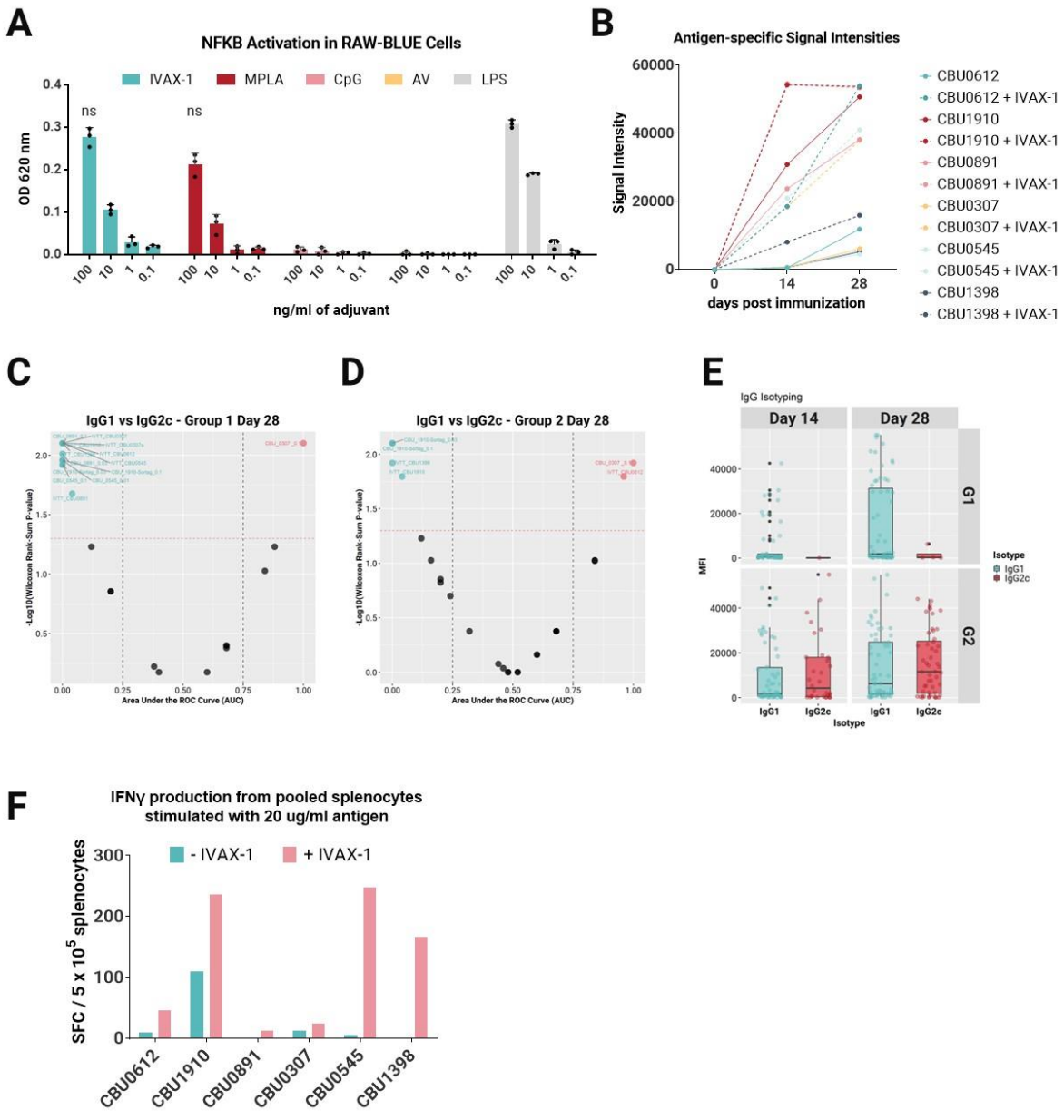

Figure 2.3. IVAX-1 (MPLA, CpG1018, AddaVAX) increases immunogenicity of multiplex bead formulation. (A) Individual components of IVAX-1 with different concentrations were assessed for NF-κB activity. *E. coli* LPS served as the positive control. Statistics were performed with one-way ANOVA and Dunnett's multiple comparisons test. **(B)** The multiplex formulations

consisted of a mixture of six individually-captured antigens on 0.2 μm beads with and without adjuvant cocktail IVAX-1. The individual antigens were captured onto tris-NTA-coated polystyrene beads, which were subsequently mixed together and administered to groups of n=5 C57BL/6 mice. Signal intensities of antigen-specific IgG titers of the group that received the antigens on beads only (solid) and adjuvanted (dashed). Animals were monitored over 28 days. Statistics were performed with paired T-test. **(C)** Volcano plot of mice immunized with multiplex beads, comparing IgG1 and IgG2c responses assessed on protein microarrays. The red line indicates the significance threshold. Proteins in blue indicate a higher response in IgG1 and proteins in red indicate a higher response in IgG2c. Statistics were performed with Wilcoxon signed-rank test. **(D)** Volcano plot of mice immunized with multiplex beads and IVAX-1. **(E)** Box plot summary of the demonstrated IgG isotyping. Signals with an MFI < 100 were excluded. Colored dots represent the signals of individual proteins. **(F)** Animals were primed and terminated 10 days later and their pooled splenocytes subjected to stimulation for 18 hours with immunizing antigen. Anti-IFNγ capture antibodies were used to determine spot counts in an IFNγ ELISPOT.

The bacterial sacculus can be modified to have chemical handles

With the knowledge that antigens can be purified from a complex mixture and bioconjugated to a bead scaffold, we proceeded with developing a chemically programmable bacteria-like particle using bacterial peptidoglycan, reminiscent of self-assembling virus-like particles. Bacterial peptidoglycan is a PAMP and can activate a signal cascade through the NOD-like receptors present on phagocytes and epithelial cells to activate downstream proinflammatory cytokines and chemokines (143,144). The sacculus, or the rigid peptidoglycan bacterial cell wall, can be modified for bioconjugation and extracted from bacteria by boiling in SDS (**FIG. 2.4A**) (145–147). Proof-of-concept was demonstrated with *E. coli* peptidoglycan sacculus due to its significantly faster doubling time of 20 min compared to *C. burnetii*'s 2 days. The inclusion of (R)-propargylglycine, or D-alanine-alkyne, during one bacterial doubling time allows for the incorporation of the amino acid alanine within the peptidoglycan with an alkyne chemical handle poised for bioconjugation (148,149). After boiling in SDS and ultracentrifugation to separate peptidoglycan sacculus from the contents of the cells, the sacculus was subjected to particle size analysis and transmission electron microscopy for visual confirmation of isolation and purity (**FIG. 2.4B-D**). The resulting purified *E. coli* sacculus was then bioconjugated to a fluorophore with an azide handle via click chemistry and visualized with confocal microscopy (**FIG. 2.4E**). Overall, we were able to demonstrate that modification of bacterial cell walls allows for future conjugation of appropriate tris-NTA linkers and that the sacculus can be isolated and used as a potential antigen scaffold.

Figure 2.4

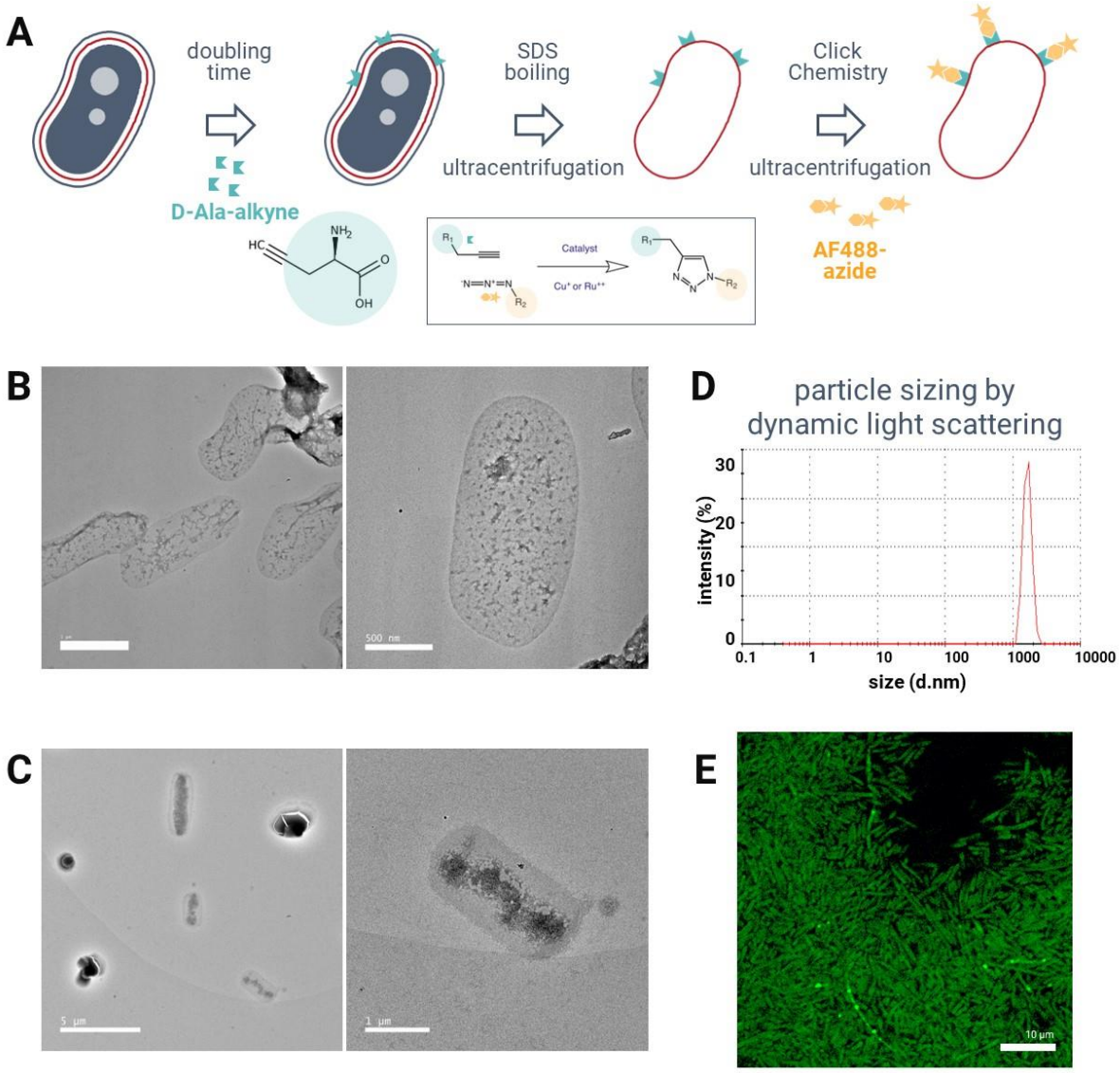

Figure 2.4. Feasibility of modification, isolation, and purification of the bacterial sacculus. **(A)** Schematic for incorporation of D-alanine amino acid containing an alkyne chemical handle for bioconjugation and isolation method of the bacterial PGN sacculus. **(B)** Representative transmission electron microscopy images of the isolated *E. coli* sacculus prior to modification. **(C)**

Representative transmission electron microscopy images of the *E. coli* PGN sacculus post modification and conjugation. **(D)** Particle sizing by dynamic light scattering of the isolated *E. coli* sacculus. **(E)** Representative confocal image of the *E. coli* sacculus bioconjugated to a AF488 fluorophore with an azide chemical handle.

Determining immunogenicity of the sacculus

To determine the immunogenicity of the sacculus and evaluate its use in vaccine development, we included the *E. coli* sacculus in vaccine formulations to act as an adjuvant and determine its efficacy. 3 purified *C. burnetii* antigens of the original 6 were selected for simplification: CBU1910, CBU0891, and CBU0545. 3 μg of each purified soluble antigen was formulated with different combinations of AddaVAX and *E. coli* sacculus and administered to C57BL/6 mice. Plasma was collected from the animals at days 0, 14, and 28, and assessed for antigen-specific IgG production (**FIG. 2.5A-B**). The animals were boosted intraperitoneally at day 60 and terminated 10 days later for splenocyte harvest to assess IFNγ production with T cell recall memory (**FIG 2.5C**). When compared to soluble antigen alone, the *E. coli* sacculus as an adjuvant performed better at generating antigen-specific antibodies, especially in the cases of CBU1910 and CBU0545-specific IgG ($p=0.0002$ at day 14, $p=0.0327$ at day 28). However, the addition of sacculus did not elicit more IFNγ in splenocytes when compared to soluble antigen alone (CBU 1910 $p>0.9999$, CBU0891 $p=0.8695$, CBU0545 $p=0.9997$). Especially in the case of CBU1910 stimulation, we see a significant increase in IFNγ when the antigens were combined with both the sacculus and AddaVAX ($p=0.0256$), indicating a synergistic effect in the adjuvant combination in regard to cell-mediated immunity and T cell effector functions.

Figure 2.5

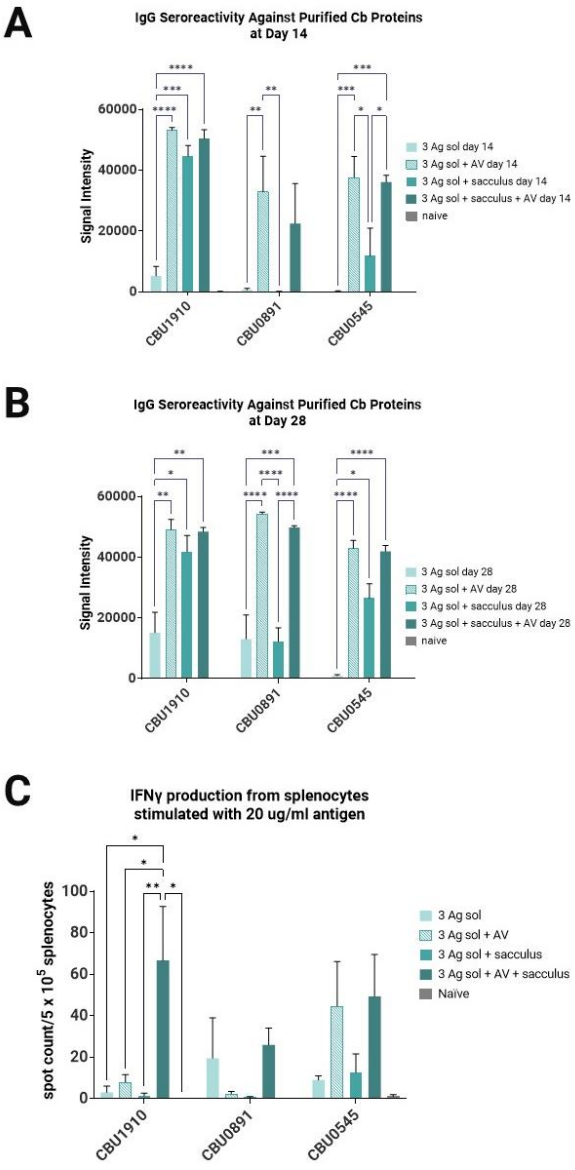

Figure 2.5. The sacculus increases immunogenicity of subunit vaccine formulations and demonstrates synergy with AddaVAX. C57BL/6 mice were immunized with purified protein antigen and a combination of purified *E. coli* sacculus and AddaVAX. N=3 or 4. **(A)** Plasma from day 14 post immunization assessed on a C. burnetii protein microarray looking at antigen-specific IgG responses to immunizing antigens. **(B)** Plasma from day 28 post immunization. **(C)** IFNγ spot-forming cells were quantified after antigen recall on *ex vivo* splenocytes. Statistics were performed with two-way ANOVA and Tukey's multiple comparisons test.

Discussion

The development of chemically programmable scaffolds using nanoparticles as a versatile platform for bead design holds great promise for vaccine development. This study demonstrated the successful utilization of polystyrene beads as building blocks to create programmable scaffolds, allowing precise control over the composition and functionality of the resulting vaccine (**FIG. 2.1 and 2.2**). We were able to demonstrate proof-of-concept of linking scaffold to protein produced in a high-throughput fashion by utilizing the high-affinity binding of streptavidin present on polystyrene beads and biotin on a tris-NTA-biotin linker. With different methods of bioconjugation, biolinkers with different chemical handles can be applied to scaffolds with different surface properties. The ability to precisely control the surface chemistry of nanoparticles facilitates the attachment of functional groups or ligands, further expanding the scope of applications.

The size and shape of nanoparticles also can be precisely engineered, resulting in beads with tunable dimensions and morphologies. This control over bead size and shape is crucial, as it directly impacts the performance, functionality, and delivery. The lymph nodes are critical sites for immune cell activation and immune response initiation and the lymphatic system acts as a natural transport system for drug delivery and distribution (150). By delivering vaccines or therapeutic agents directly to the lymph nodes, it is possible to target dendritic cells and lymphocytes, leading to improved immune system modulation and enhanced immune responses. To efficiently access the draining lymph nodes, nanoparticles should ideally be small enough to traverse the lymphatic vessels and avoid entrapment in the peripheral tissues (151). Subcutaneously administered nanoparticles typically need to be smaller than approximately 100

nm to facilitate efficient transport to the draining lymph nodes (150). On the other hand, nanoparticles administered through mucosal routes, such as intranasal or oral, may need to be smaller than 50 nm to effectively access the lymphatic system (152). In this study, we demonstrated conjugation with 1 μm and 0.2 μm beads and were still able to generate robust immune responses from both T and B cell arms in IFNγ production and IgG antibody readouts, but smaller beads and assessment of delivery to the draining lymph node warrant further investigation.

Multivalency is another aspect to consider in rational vaccine design, as immunogenicity can be increased by leveraging the principles of antigen presentation and immune cell activation. By presenting multiple copies of relevant antigens or epitopes, multivalent vaccines can stimulate a more robust and diverse immune response compared to monovalent or single-component vaccines (153,154). The repetitive presentation of antigens or epitopes on the vaccine surface enhances their recognition by immune receptors such as B cell receptors (BCRs) or T cell receptors (TCRs) (155). This can lead to crosslinking and signaling cascades that promote B cell activation, proliferation, and differentiation into antibody-secreting plasma cells. Multivalency also promotes generation of robust T cell responses, including $CD8^+$ cytotoxic T lymphocytes (CTLs) and $CD4^+$ helper T cells, which are crucial for cell-mediated immunity and pathogen clearance.

In our multivalent polystyrene bead formulation, we also include the IVAX-1 adjuvant combination and validate its efficacy in activating the NF-κB pathway in vitro (**FIG. 2.3A**). IVAX-1's efficacy proved to be as potent as *E. coli* LPS, and we proceeded to formulate two multivalent bead vaccines, one with IVAX-1 and one without. Antigen-specific IgG response increased across the board with the inclusion of IVAX-1, and the IgG subtyping skewed away from a IgG1/Th2

response toward a IgG2c/Th1 response (**FIG. 2.3B-E**). As *C. burnetii* is an intracellular pathogen, an enhanced Th1 response is desirable in pathogen elimination, as activated $CD4^+$ T cells in the Th1 response produce proinflammatory cytokines including IFNγ and IL-2. IFNγ activates macrophages, promoting their antimicrobial functions, such as increased phagocytosis and production of microbicidal molecules. IL-2 supports the proliferation and activation of cytotoxic T cells and natural killer (NK) cells, which target and eliminate infected cells. We were able to demonstrate that our multivalent vaccine formulation with IVAX-1 was able to produce more IFNγ when stimulated with each of the immunizing antigens (**FIG. 2.3F**). With that, we were able to confirm that inclusion of the adjuvant combination of MPLA, CpG 1018, and AddVAX fine-tunes the immune response to promote IFNγ production and contended protection against *C. burnetii*.

In a similar vein, muramyl dipeptide (MDP) is a small molecule PAMP that is commonly found in the peptidoglycan layer of bacterial cell walls. MDP is recognized by the innate immune system through the nucleotide-binding oligomerization domain-containing protein 2 (NOD2) receptor, which is primarily expressed on monocytes, macrophages, and dendritic cells (132,144). Upon recognition of MDP by NOD2, a signaling cascade is initiated that leads to the activation of multiple downstream pathways, including the NF-κB pathway, the mitogen-activated protein kinase (MAPK) pathway, and the type I interferon (IFN) pathway. Activation of these pathways results in the production and release of proinflammatory cytokines, such as TNFα, IL-1β, and IL-6, as well as type I IFNs, which play a critical role in antimicrobial defense. The NF-κB pathway is one of the major downstream signaling pathways activated by MDP. Upon activation, NF-κB translocates into the nucleus and binds to specific target genes, resulting in the expression of proinflammatory cytokines, chemokines, and adhesion molecules (156,157). These molecules

recruit and activate immune cells, leading to the elimination of the pathogen and the resolution of infection.

The ability to engineer the sacculus scaffold with foreign antigens provides a powerful tool for the development of novel vaccines that can efficiently target and activate the immune system. Here, we show that the structurally stable bacterial sacculus containing MDP within the PGN can be homogenously isolated and modified to include chemical handles ready for bioconjugation (**FIG. 2.4**). By including an alkyne handle on an essential amino acid during growth, the sacculus can be coupled to the tris-NTA-amine linker, as demonstrated by the conjugation to a fluorophore with an amine handle for visualization. The approach of chemically modifying bacterial PGN has been successfully used to develop vaccines against a variety of bacterial pathogens, including enterococci and staphylococci (158–160). These vaccines have been shown to elicit a strong immune response and provide protection against subsequent challenge with the respective pathogens. Another vaccine development approach involves the use of sacculus-derived particles, such as outer membrane vesicles (OMVs), as a vaccine platform (161–163). OMVs are naturally occurring membrane-bound particles that are shed from the bacterial cell surface. These particles can be isolated and purified from bacterial cultures and can be used to deliver antigens or other immunostimulatory molecules to the immune system. This approach has been used to develop vaccines against a variety of bacterial pathogens, including *Neisseria meningitidis* and *Vibrio cholerae* (164,165).

We evaluated the immunogenic activity of the generated *E. coli* PGN sacculus as an adjuvant by combining it with soluble protein antigen and anticipating the increase in immune response readouts, namely antigen-specific IgG production and IFNγ production upon recall (**FIG. 2.5**).

Addition of the sacculus significantly enhanced the antigen-specific antibodies produced against two of the three immunizing antigens by day 28, CBU1910 and CBU0545. Simultaneous inclusion of AddaVAX also synergistically increased IFNγ production when immune cells were stimulated with recall antigen, specifically CBU1910, *ex-vivo*.

Despite the potential advantages of using the sacculus as a vaccine scaffold, there are also several challenges that must be overcome. In the context of *C. burnetii*, isolation of the PGN sacculus faces logistical challenges due to its status as a tier 2 select agent and difficulty in accessing and growing large quantities due to its long doubling time, making it unfortunately impractical for scaling up. These include the need for standardized methods for sacculus isolation and purification, the potential for immunogenicity against self-antigens present in the sacculus, and the potential for cross-reactivity with other bacterial species that share similar sacculus structures.

In conclusion, we have demonstrated the feasibility of chemically programmable bacteria-like particles first with polystyrene beads and then with modifiable bacterial PGN sacculus. The sacculus is a promising scaffold for vaccine development, with the potential to elicit a strong and protective immune response. However, further research is needed to overcome the challenges associated with its use and to develop effective sacculus-based vaccines against a range of bacterial pathogens. Optimization related to synthesis, stability, and biocompatibility warrants further investigation and would ultimately pave the way for the widespread utilization of these programmable nanoparticle systems in vaccine development and the biomedical field.

CHAPTER 3:

Multivalent vaccines demonstrate immunogenicity and protect against *Coxiella burnetii* aerosol challenge

Sharon Jan, Alycia P. Fratzke, Jiin Felgner, Jenny E. Hernandez-Davies, Li Liang, Rie Nakajima, Algimantas Jasinskas, Medalyn Supnet, Aarti Jain, Philip L. Felgner, D. Huw Davies, and Anthony E. Gregory

Abstract

Vaccines are among the most cost-effective public health measures for controlling infectious diseases. *Coxiella burnetii* is the etiological agent of Q fever, a disease with a wide clinical spectrum that ranges from mild symptoms, such as fever and fatigue, to more severe disease such as pneumonia and hepatitis. The formalin-inactivated whole cell vaccine Q-VAX® contains hundreds of antigens from the organisms and confers lifelong protection in humans, but prior sensitization from infection or vaccination can result in deleterious reactogenic responses to vaccination. Consequently, there is great interest in developing non-reactogenic alternatives based on adjuvanted recombinant proteins. In this study, we aimed to develop a multivalent vaccine that conferred protection with reduced reactogenicity. We hypothesized that a multivalent vaccine consisting of multiple antigens would be more immunogenic and protective than a monovalent vaccine owing to the large number of potential protective antigens in the *C. burnetii* proteome. To address this, we identify immunogenic T and B cell antigens, and selected proteins were purified and evaluated with a novel combination adjuvant (IVAX-1), with or without *C. burnetii* LPS in immunogenicity and efficacy studies *in vivo* in mice and in a Hartley guinea pig intratracheal aerosol challenge model using *C. burnetii* strain NMI RSA493. The data showed that multivalent vaccines are more immunogenic and efficacious than monovalent vaccines, and more closely emulate the protection achieved by Q-VAX. Although 6 antigens were the most immunogenic, we also discovered that multiplexing beyond 4 antigens introduces detectable reactogenicity, indicating there is an upper limit to the number of antigens that can be safely included in a multivalent Q-fever vaccine.

Introduction

Coxiella burnetii causes Q fever, which in many cases results in an acute, febrile illness but may also manifest chronically and lead to pneumonia and endocarditis, which can be fatal. Owing to its very high infectivity (ID50=1), high stability in the environment, and aerosol transmissibility, *C. burnetii* is considered a potential biological weapon and classified by the Centers for Disease Control as a tier 2 select agent (166,167). Q-VAX is a purified suspension of formalin-inactivated, *Coxiella burnetii* Phase I Henzerling strain (RSA 331) grown in the yolk sacs of embryonated eggs and provides robust protection of humans against Q fever (168,169). However, the vaccine can be reactogenic in individuals that have been previously exposed to *C. burnetii*. Prior exposure must be ascertained by serological screening and intradermal skin testing before immunization, which creates added costs and delays to the vaccination process. Understanding the mechanisms of vaccine-induced protective immunity and minimizing components that can elicit reactogenicities are necessary to rationally design a safe and effective vaccine.

Subunit vaccines, though less immunogenic than the whole cell vaccines, are safer due to having fewer unknown components. However, they must be delivered with potent adjuvants that enhancing antigen recognition, uptake, and processing by antigen-presenting cells (170). Toll-like receptor (TLR) agonists represent the next generation of adjuvants, and several have recently been licensed for clinical use (123,171,172). The TLRs themselves are a class of pattern recognition receptor (PRR) commonly found either on the surface or on endosomal membranes of innate immune cells, fibroblasts, and epithelial cells. TLR agonists can engage in downstream signaling to induce activity of transcription factor NFκB and production of cytokines, chemokines, and type I interferons. In this study, we have used a previously described combinatorial adjuvant, IVAX-1, a combination adjuvant which comprises TLR4 agonist MPLA (monophosphoryl lipid A), TLR9

agonist CpG oligodeoxynucleotide (ODN) 1018, and a squalene-in-water emulsion, AddaVAX (141). MPLA, a TLR4 agonist, is significantly less toxic synthetic derivative of *Salmonella minnesota* lipopolysaccharide (LPS) due to the removal of the one or more acyl chains and phosphate groups (173). MPLA primes adaptive immunity and has been approved for use in humans in the commercial SHNGRIX vaccine (174). CpG ODNs are TLR9 agonists designed to mimic bacterial nucleic acids and strongly promotes development of Th1 cells. AddaVAX is a squalene oil-in-water emulsion that elicits a mixed Th1/Th2 response by antigen presentation, facilitating transport of antigens, activating immune cells, and inducing cytokine production (175,176).

Due to the high-risk factor and labor-intensive process of producing whole-cell vaccine (WCV), *C. burnetii* is an ideal candidate for the development of subunit vaccines. Unlike viruses with small genomes comprising of a few proteins, *C. burnetii* Nine Mile Phase I (RSA 493) has a large proteome of 1815 annotated proteins to select from covering a wide variety of antigens in its unconventional life cycle and aiding in host evasion (177,178). We hypothesize that a multivalent vaccine combining several immunogenic antigens would be the optimal course of action and offer better protection than a monovalent vaccine. Multiple proteins containing multiple epitopes can induce different populations of immune cells for breadth and more closely simulates Q-VAX, which is well-documented to provide life-long protection (179). These epitopes are recognized by T cells and B cells and are presented on the surface of antigen-presenting cells after internalization and digestion (180). Single-epitope peptides have consistently demonstrated low efficacy, so there has been a push for multivalent constructs. Multiple epitopes allow for binding at multiple sites, which increases downstream effects including simultaneous activation of cellular and humoral responses (181). Antigen selection must fulfill multiple criteria, including expression on the

bacterial surface for antibody recognition, availability of processed peptides by MHC molecules, and structural properties compatible with efficient protein production (182). In this study, we have taken the whole-antigen approach to activate both B and T cell compartments of the adaptive immune response (183). We first identified immunogenic *C. burnetii* antigens for use in a multivalent vaccine by using a literature search and published and unpublished protein microarray data. These were then tested by administration with IVAX-1 and other TLR agonists for immunogenicity studies in C57BL/6 mice and validated in an aerosol challenge model using mice and Hartley guinea pigs. We show that several vaccine candidates containing the most immunogenic antigens provide protection against challenge comparable to Q-VAX. Our data from these studies show our multivalent vaccines induces potent humoral and cellular immune responses in animal models.

Materials and Methods

Reagents and biologics

Q-VAX® was purchased from Seqirus (bioCSL, Melbourne, Australia). Equivalent *C. burnetii* whole cell vaccine (WCV) was generously provided by the Dr. James Samuel lab at Texas A&M University. *C. burnetii* Nine Mile phase I (NMI) clone 7 (RSA493) was grown in selective ACCM-2 media and inactivated with 2% formalin for 48 hours for the whole cell vaccine. Recombinant proteins were expressed in *Escherichia coli* BL21 cells and purified by multiple column chromatography and endotoxin removal procedure by Genscript (Piscataway, NJ). *C. burnetii* NMI RSA493 was purchased from BEI Resources (Manassas, VA) and quantified via qPCR with genomic DNA extraction via High Pure PCR Template Preparation Kit (Roche, Basel, Switzerland) and PowerUp SYBR Green Master Mix (Thermo Fisher Scientific, Waltham, MA) for infection. Primers amplify a 74 base pair fragment in *C. burnetii* com1 [FAF216: 5’

GCACTATTTTTAGCCGGAACCTT 3', RAF290: 5' TTGAGGAGAAAAACTGGATTGAGA 3'] (184). AddaVAX™ (squalene oil-in-water emulsion) was purchased from InvivoGen Inc. (San Diego, CA), CpG ODN 1018 (TLR9 agonists) were purchased from InvivoGen and Integrated DNA Technologies (Coralville, Iowa), respectively. CpG-ODN were dissolved in sterile water at 1mM as stock. Monophosphoryl lipid A (MPLA, a TLR4 agonist) was purchased from Avanti Polar Lipids Inc. (Alabaster, AL).

Animals

C57BL/6 female mice (6-12 weeks) and Hartley guinea pigs (300-400 g) were obtained from Charles River Laboratories (Wilmington, MA). Animal experiments were approved by the Institutional Animal Care and Use Committee of the University of California, Irvine and the Animal Care and Use Review Office (ACURO) of the U.S. Army Medical Research and Materiel Command (USAMRMC). Mice were housed in standard cages with enrichment at ABSL2 and guinea pigs were housed in approved animal biosafety level 3 (ABSL-3) facilities. For immunogenicity studies, mice were anesthetized in induction chambers with inhaled isoflurane/O_2 and passive scavenging with F/air canisters. Guinea pigs were anesthetized with an intraperitoneal (IP) injection of 100 mg/kg ketamine and 10 mg/kg xylazine in PBS. Where indicated, mice were immunized either subcutaneously at the base of the tail or intramuscularly in the semitendinosus and semimembranosus muscles of the hind limb. Guinea pigs were immunized intramuscularly in the semitendinosus and semimembranosus muscles. Blood was collected from submandibular vein in mice and the lateral saphenous vein in guinea pigs with 25 g hypodermic needles (Medline, Northfield, IL), Microvette CB 300 lithium heparin (Sarstedt, Newton, NC), and BD Microtainer PST tubes with lithium heparin (BD, Franklin Lakes, NJ).

Serological profiling by protein microarrays

Gene identification and nomenclature is based throughout this study on the complete genome sequence published by Seshadri and colleagues (185). *C. burnetii* proteome microarrays were produced as described previously (137–139). Briefly, proteins from the *C. burnetii* Nine Mile I strain RSA 493 proteome were expressed from purified plasmids in an *Escherichia coli*-based cell-free, *in vitro* transcription translation system (IVTT) (Biotechrabbit GmbH, Hennigsdorf, Germany). IVTT reactions were printed onto nitrocellulose-coated glass AVID slides (Grace Bio-Labs Inc., Bend, OR) using an Omni Grid 100 microarray printer (Genomic Solutions). Plasma was diluted 1:100 in protein array blocking buffer (GVS, Sanford, ME) and incubated with 0.1 mg/mL of a His-tag-containing peptide (HHHHHHHHHHGGGG) (Biomatik, Wilmington, DE) at room temperature for 30 min to block anti-His antibodies generated by the immunizations. Afterwards, the arrays were incubated overnight at 4ºC with gentle rocking. Arrays were washed three times with TBS-0.05% Tween 20 (T-TBS) and then incubated with goat anti-mouse IgG-biotin, IgG1-biotin, or IgG2c-biotin (1:200 in array blocking buffer) (Jackson ImmunoResearch, West Grove, PA) for 1 hour at room temperature with gentle rocking. Following another set of T-TBS washes, bound antibodies were detected with streptavidin-conjugated Qdot®655 or Qdot®800 (1:250 in array blocking buffer; Thermo Fisher Scientific, Waltham, MA) for 1 hour at room temperature with gentle rocking. Arrays were washed three times with T-TBS, the slides rinsed thoroughly with water, and then air dried by centrifugation at 500 g for 10 min. Images were acquired and spot fluorescence intensities quantified using the ArrayCAM™ Imaging System (Grace Bio-Labs, Bend, OR). Signal intensities (SI) for each antigen on the array were background corrected by subtracting sample-specific T-PBS buffer signals from purified protein spot signals.

IVTT expression and capture on polystyrene beads

Down-selected proteins were expressed *in vitro* in 200 µl IVTT reactions as described above. Each protein is expressed with an N-terminal 10x poly-histidine and C-terminal HA epitope tags. After 16h reaction at 21ºC, proteins were captured via x10 His tags by adding 100 µl to nickel charged His-TrapSpin resin (GE Healthcare Life Sciences). The resin consists of ~ 34 µm-diameter Sepharose beads with a binding capacity of 750 µg of His-tagged protein per mL. Flow-through was reapplied to columns and then washed to remove non-bound IVTT material. Successful capture of proteins to the beads was monitored by printing microarrays of IVTT, flow-though and bead wash on nitrocellulose-coated slides **(SUPPLEMENTAL FIG S3.1**).

T cell recall assays

Spleens were harvested from mice 10 days after they were boosted via the i.p. route and erythrocyte-depleted splenocyte suspensions prepared for T cell recall assay (IFNγ ELISpot) as previously described (140). Purified antigens were titrated in the assay (final concentrations of 10, 5, 2.5, and 0 µg/mL). Spleen cells from naïve mice were assayed in parallel as a control for potential mitogenic activity of the recall antigens. Assays were performed in T cell medium (TCM) comprising Iscove's Modified Dulbecco's Medium (IMDM), containing 5×10^{-5} M β-mercaptoethanol, 100 IU/mL penicillin, 100 µg/mL streptomycin, and 10% heat-inactivated fetal calf serum. After 18 h of incubation, the assay supernatants were collected for multiplex cytokine screening using the LEGENDplex kit (BioLegend Inc., San Diego, CA) according to the manufacturer's instructions before the ELISpot was processed. Spots were quantified in an ImmunoSPOT® ELISpot plate reader (Cellular Technology Limited, Cleveland, OH).

Guinea pig hypersensitivity experiments

Guinea pigs were sensitized with a subcutaneous administration of Q-VAX and rested for two weeks. Transponders were delivered SC for identification and to monitor weight and temperature change. To elicit hypersensitivity responses, four or six approximately 2-3 cm areas were shaved using electric clippers on the right and left flanks. Vaccine candidates, WCV, or PBS sham was then injected intradermally at each of the shaved sites. Temperature, weight, and reaction sites were monitored daily for two weeks. Each vaccine candidate was evaluated in 4 guinea pigs.

Histopathology

Skin sites from guinea pigs were fixed in 10% neutral buffered formalin for at least 72 hours at room temperature. For the hypersensitivity experiments, three sections were cut from the shaved areas containing the epidermis to the underlying abdominal or intercostal muscle. Tissues were submitted to AML Laboratories (Jacksonville, FL, USA) for processing, embedding, and sectioning at 5 μm before staining with hematoxylin and eosin (HE). Histopathology slides were deidentified and evaluated by an ACVP boarded pathologist. Histopathologic scoring was performed on a 0-5 scale.

Guinea pig challenge experiments

Guinea pigs were subcutaneously administered RFID microchip transponders (BMDS Avidity Science, Waterford, WI) in the back of the neck for identification purposes and to monitor weight and temperature for the duration of the experiment. They were then administered candidate vaccines, WCV or PBS (sham) in 100 μL sterile PBS by intramuscular injection in the semitendinosus and semimembranosus muscles. A boost vaccine was given in the opposite hindlimb two weeks later. Blood and plasma were collected from the lateral saphenous vein on days 10, 21, 28, 35, and 42 post-prime. Guinea pigs were intratracheally infected with 5×10^5

genomic equivalents (GE) of *C. burnetii* NMI RSA493 after resting for 7 weeks post-prime. Animals were anesthetized with an IP injection of 100 mg/kg ketamine and 10 mg/kg xylazine in PBS. A MADgic pediatric laryngo-tracheal mucosal atomizer device (Teleflex, Morrisville, NC) was inserted to administer the bacteria intratracheally in 100 μL of PBS. Guinea pigs were monitored daily, and weight and temperature measurements were taken. Four to five guinea pigs were utilized for each experimental group.

Statistical analyses

Statistical analyses were performed with GraphPad Prism v9.4.0 (GraphPad Software, La Jolla, CA, USA). Results were compared using one-way or two-way ANOVA with Dunnett's or Tukey's correction for multiple comparisons. Differences were considered significant if p-value ≤ 0.05 (*), ≤ 0.01 (**), ≤ 0.001 (***), or ≤ 0.0001 (****).

Results

Identification of target antigens in the response to Q-VAX®

It was of considerable interest to first profile antibodies (Abs) and T cells in response to Q-VAX to identify recognized antigens as subunit vaccine candidates. Ab (IgG) profiling was performed in C57BL/6 mice administered a single dose via subcutaneous or intramuscular routes using proteome microarrays (**FIG. 3.1A**). Only one protein, CBU1910, was consistently recognized, with other reactive proteins giving a scattered, more stochastic recognition pattern. The breadth of the Q-VAX Ab profile was unexpectedly narrow, given that there are 1,815 different proteins in the proteome. There were no obvious differences in Ab profiles between the intramuscular and subcutaneous routes of immunization.

Figure 3.1

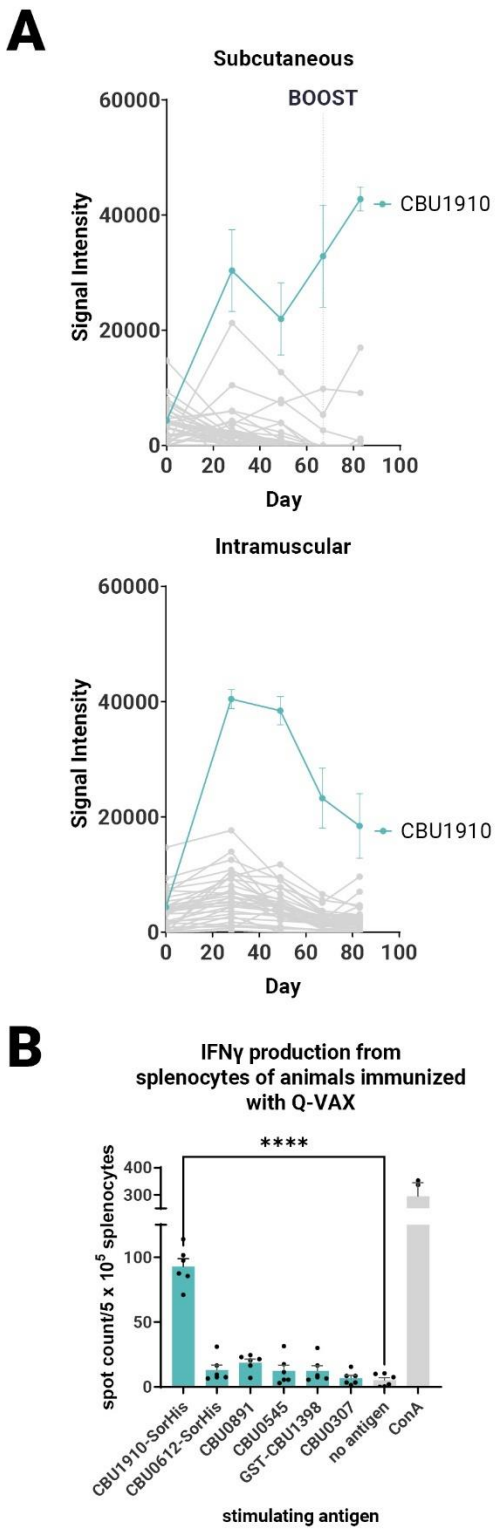

Figure 3.1. Antibody and T cell profiling after administration of Q-VAX®. (A) Time course IgG profiles from plasma of C57BL/6 mice administered Q-VAX via subcutaneous and intramuscular routes (n=5 mice per group). The top 5 tier 1 antigens and the top 30 reactive antigens on d28 are included. The hashed line in panel A indicates when the boost was administered (d69); mice in the intramuscular group were not boosted. **(B)** In T cell recall experiments, C57BL/6 mice (n=5) were immunized with Q-VAX® intraperitoneally and their splenocytes were harvested 10 days after the prime. The splenocytes were stimulated by purified protein from the downselected panel of lead antigens. Significance is compared to the no antigen group. Statistics were performed with one-way ANOVA and Dunnett's multiple comparisons test.

To attempt to broaden the Ab profile and identify additional candidate vaccine targets, mice primed via the s.c. route were boosted with Q-VAX, weighed and carefully observed daily for changes in behavior. No adverse events were seen, and animals were bled at the end point 14 days later (day 83). After boosting, IgG signals increased only to existing reactive antigens, with no increase in breadth of response. These data show the antibody breadth in response to administration of Q-VAX is remarkably narrow, even after boosting.

Given the limited serological breadth induced by Q-VAX, we broadened the search to include serological profiling in cases of natural infection. For this, we used published and unpublished in-house protein microarray studies from human and animal Q-fever studies as well as mass spectrometry identification of seroreactive proteins from *C. burnetii*, as reviewed in 2013 by Vranakis and colleagues (137,138,186–191). Antigens were ranked based on reactivity on the protein microarrays and a total score was assigned based on these two metrics (**TABLE 3.1**). Higher priorities were given to those antigens with a predicted transmembrane domain, as these are more likely to be surface proteins and have easily-accessible epitopes for antigen presentation. This list initially comprised CBU0612, CBU1910, CBU0891, CBU0307 and CBU0664 as “Tier 1” antigens.

Table 3.1. Literature, proteomics, and protein microarray selection of *Coxiella burnetii* protein antigen candidates.

Tier	ORF	Gene ID	Description	MWt (kDa)	Array studies (n=13)	2D gel/MS (n=10)	Overall score	Immuno 2D gel/MS	TM HMM	Literature	Immunogenicity	Final subset	Tags and mods
1	CBU1910	com1	Outer membrane protein	27.7	8	9	17	yes	yes	yes	yes	yes	SorHis, Truncated
1	CBU0612	skp	Outer membrane chaperone OmpH	18.2	9	9	18	yes	yes	yes	yes	yes	SorHis, Truncated
1	CBU0891		hypothetical exported membrane associated protein	34.3	8	4	12	no	(yes)	yes	yes	yes	Truncated
1	CBU0307		OmpA-like transmembrane domain-containing protein	25.4	2	6	8	yes	no	yes	yes	yes	Truncated
1	CBU0664		ISAs1 family transposase	41.9	1	0	1	no	yes	no	no	no	
2	CBU0092	ybgF	tol-pal system protein YbgF	33.5	6	9	15	yes	no	yes	no	no	
2	CBU0545	lemA	LemA family	23.6	5	8	13	no	yes	yes	yes	yes	Full length
2	CBU1398	sucB	2-oxoglutarate dehydrogenase E2	44.5	6	6	12	yes	no	yes	yes	yes	GST
2	CBU0630	mip	peptidyl-prolyl cis-trans isomerase	25.3	3	8	11	yes	no	yes	yes	no	GST
2	CBU1143	yajC	preprotein translocase subunit	12.8	5	6	11	yes	(yes)	yes	no	no	
2	CBU0718		Hypothetical membrane associated protein	10.3	3	7	10	no	no	no	yes	no	GST
2	CBU1627	IcmE	Type IV (Icm/Dot) secretion system protein	114.3	5	4	9	no	yes	yes	no	no	
2	CBU1094		Membrane fusion protein, multidrug efflux system	41.8	3	4	7	no	yes	no	yes	no	His-GST
2	CBU1513		short chain dehydrogenase/ reductase oxidoreductase	28.4	5	1	6	no	no	no	yes	no	GST
2	CBU0611		Hypothetical Outer Membrane Protein insertion porin family	88.3	0	4	4	no	yes	yes	yes	no	His-GST
2	CBU1260	ompA	OmpA-like transmembrane domain-containing protein	27.3	0	4	4	yes	yes	yes	no	no	
2	CBU0198		Hypothetical Outer Membrane Protein insertion porin family	63.6	0	3	3	no	yes	yes	no	no	

Properties of the identified proteins from publicly available datasets and databases are noted. Includes columns indicating use and modifications in experiments. “Immunogenicity” indicates the protein’s use in early T cell screens.

Where possible, we attempted to produce 'tag-less' protein to minimize incorporation of off-target epitopes. Thus, CBU0891, CBU0307 and CBU0664 proteins were expressed with the SUMO-His tag which was cleaved from the protein before use (192). However, CBU0612 and CBU1910 were expressed with Sortase recognition motifs (either C-terminal LPXTG Sortag or an N-terminal GGG tag) with the intention of using the Sortase tag to couple proteins to TLR agonists (193). Expression and solubility of CBU0891 and CBU0307 were initially low but improved by subsequently expressing truncated versions lacking transmembrane domain and signal peptide, and signal peptide, respectively. CBU0612-Sortag and CBU1910-Sortag were subsequently modified with a C-terminal polyhistidine (termed CBU0612-SorHis and CBU1910-SorHis) to evaluate the utility of tris-NTA for coupling proteins to TLRs in place of Sortase (194). Overall, proteins expressed with His-SUMO (CBU0891, CBU0307) showed only modest solubility. Protein CBU0664 showed poor solubility and was not pursued further.

An additional 12 antigens (tier 2) were selected and tested in pilot experiments for *E. coli* expression and solubility. All 12 tier 2 proteins were expressed as GST-GG fusion proteins separated by a TEV protease cleavage site to improve solubility. The GG motif was included so cleavage of His-GST-GG-TEV yields protein with an N-terminal GGG tag available for downstream coupling reactions. Pilot studies showed only HisGST-CBU0545 remained soluble after GST cleavage. Of the 12 tier 2 proteins, 7 were suitable for scale up (CBU0545, GST-CBU1398, GST-CBU0630, GST-CBU0718, HisGST-CBU1094, GST-CBU1513, HisGST-CBU0611), whereas 5 proteins remained either poorly expressed or insoluble (CBU0902, CBU1143, CBU1627, CBU1260, CBU0198) and were not investigated further. The final list of purified tier 1 and tier 2 proteins used for immunogenicity studies are indicated in **TABLE 3.1**.

To determine if Q-VAX induced a T cell response against any of the purified tier 1 and tier 2 proteins, we performed a T cell recall assay on splenocytes of mice that were immunized intraperitoneally (i.p.) with Q-VAX. Splenocytes were harvested 10 days after immunization, pooled from n=3 mice, and incubated with purified recall protein for 18 hr (**SUPPLEMENTAL FIG. S3.1**). Antigen-specific IFNγ responses were seen to GST-CBU1398, CBU0891, CBU0545, and CBU1910-SorHis, with CBU1910-SorHis being dominant. Antigens that induced low levels of IFNγ in the T cell recall response and were difficult to purify were excluded from further experiments. The T cell recall experiment was repeated with a subset of 6 lead candidate antigens (**TABLE 3.1**), with a representative experiment shown in **FIG. 3.1B**. Overall, the data indicates CBU1910 is dominant in the antibody response to Q-VAX, which is accompanied by a robust IFNγ-positive Th1 T cell response in the recall assay ($p < 0.0001$).

Individual antigens are immunogenic when administered to mice

In parallel with protein purification described above, immunogenicity studies were also performed with antigens expressed from pXi plasmids in transcription/translation (IVTT) reactions (as used for custom protein microarrays) and captured onto Ni-Sepharose beads. This method, which exploits the ability of IVTT to express virtually any protein in soluble form and obviates the need for traditional protein purification, allows many potential targets antigens to be screened directly for immunogenicity *in vivo*. Loading of protein to the beads was confirmed by probing arrays with anti-epitope tag antibodies (**SUPPLEMENTAL FIG. S3.2**). We then administered each individually to mice (n=3 per group) via the s.c. route. One group of animals was administered purified CBU1910 protein for comparison. Plasma was collected at days 0, 10, and 28 and analyzed for antigen-specific IgG responses on protein microarrays displaying both IVTT-expressed and purified proteins, as shown in **FIG. 3.2A and B**. Robust antibody responses were evident in 3 of

the proteins tested – CBU1910, CBU0612, and CBU0891. The Abs produced against the IVTT expression products were both IgG1 and IgG2c, while those engendered by purified protein (CBU1910-SorHis) were IgG1 (Th2) only. Increased IgG2c responses correspond to the Th1 T cell response, which is defined by proinflammatory cytokine production and macrophage activation promoting intracellular bacterial killing(195). IgG1 corresponds to a Th2 response, which is appropriate for extracellular pathogens and upregulating granule release in basophils and other granulocytes. Previous studies have demonstrated protective immunity against *C. burnetii* is driven by a Th1 response, as evident by elevated IFNγ, TNFα, and IgG2c antibodies (196–198). We attribute this to the purified proteins lacking immunostimulatory adjuvants when compared to the IVTT expression products. The increase in IgG signals over time are show in **FIG. 3.2B**.

A T cell recall assay were performed with the same mice boosted with the corresponding adjuvanted purified antigens via the i.p. route on day 28 and spleens harvested 10 days later (**FIG. 3.2C**). Minor non-specific or mitogenic background activity was noticed against purified CBU0545 in splenocytes from mice immunized with no DNA beads; the remaining proteins elicited no response. Antigen-specific IFNγ responses were seen to all the priming antigens except for CBU0891. In the case of CBU0545, the recall response remained high at all antigen concentrations tested, revealing a robust antigen-specific response above any non-specific effects. The weakest IFNγ response was seen against CBU0891. T cell cross-reactivities were noted, for example mice immunized with CBU0612-SorHis showed measurable cross-reactivity for CBU0545 and CBU0307. These were non-reciprocal, appeared independent of shared tags, and sequence alignments did not reveal any obvious reasons for these patterns. Nevertheless, the serology and T cell data were consistent with the immunogenicity of all 8 proteins when

administered individually. Overall, the data indicate the candidate vaccine antigens can engender Ab and/or T cell responses in C57BL/6 mice.

Figure 3.2

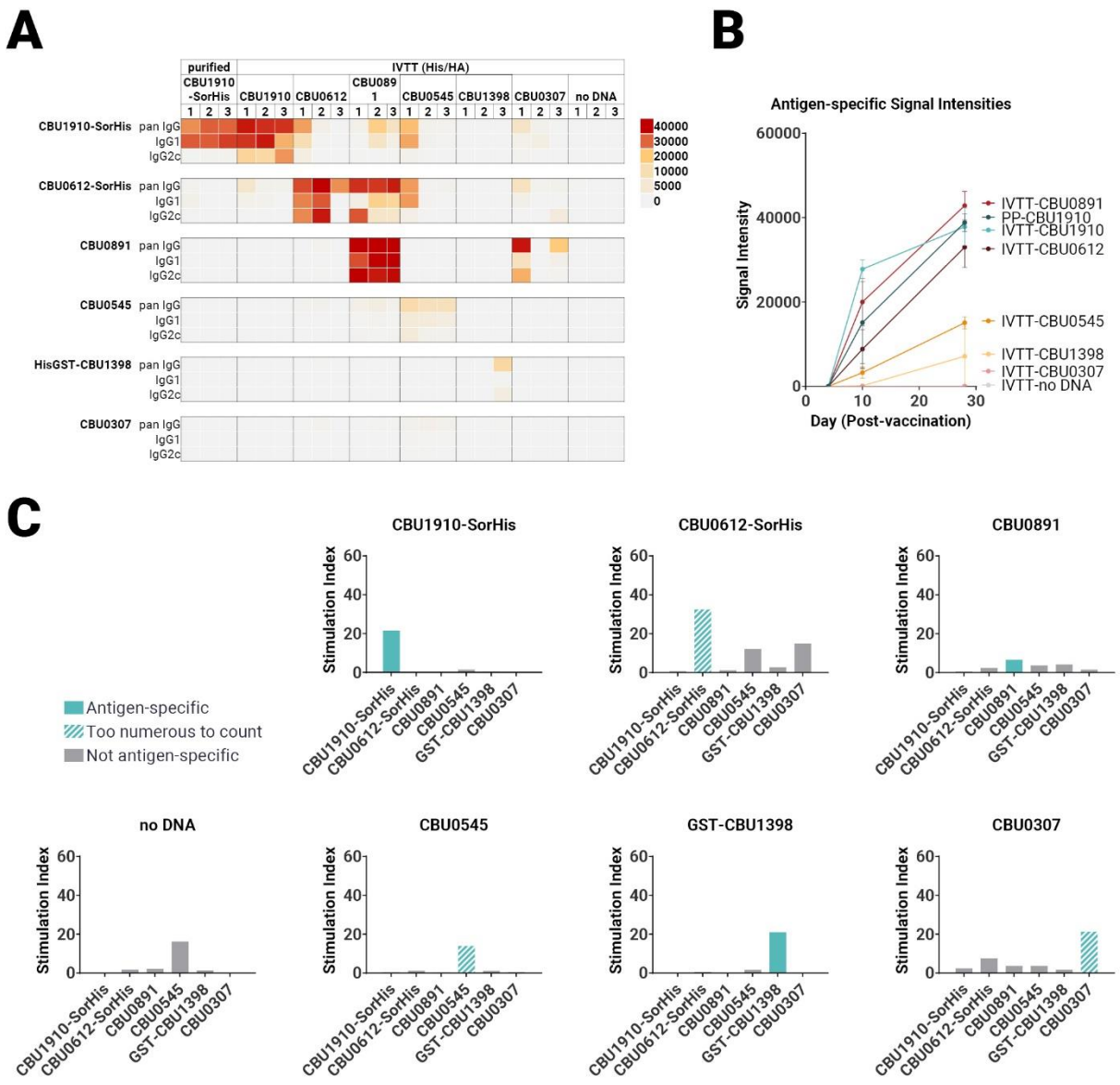

Figure 3.2. Immunogenicity screen of candidate *C. burnetii* antigens. Groups of C57BL/6 mice (n=3 per group) were immunized with purified CBU1910-SorHis protein (pp1910) or His-Trap resin to which different *C. burnetii* proteins expressed in IVTT reactions were bound via polyhistidine tags and formulated in AddaVAX™ for immunization. **(A)** Plasma were probed on microarrays displaying purified *C. burnetii* proteins, and bound Abs visualized with secondary Abs against IgG, IgG1 and IgG2c. Heat map shows of signals on d28; red=high,

yellow=intermediate, white=low; arrayed proteins lifted left and immunizing antigens listed at the top. **(B)** Array signals (group mean +/- SD) at different time points post-immunization. **(C)** T cell immunogenicity screen of candidate *C. burnetii* antigens. Groups of mice (n=3) were immunized with IVTT-expressed proteins and boosted 8 weeks later with purified proteins indicated in each panel for recall assay (IFNγ ELISPOT). Numbers of spot forming cells at different concentrations of antigen are expressed as a fold-over the number of spots at 0mg/ml antigen. Colored bars = assay recall antigen corresponding to immunizing antigen.

IVAX-1 is a potent adjuvant and increases Th1 and IgG2c responses

We next evaluated the immunogenicity-enhancing effects of including TLR agonists and the squalene oil-in-water emulsion AddaVAX. For this, we formulated purified CBU1910 in a combination adjuvant, IVAX-1, which comprises TLR4 agonist monophosphoryl lipid A (MPLA), TLR9 agonist CpG oligodeoxynucleotide (ODN) 1018, and AddaVAX (141,142). Formulations containing purified CBU1910 and IVAX-1 were administered to C57BL/6 mice as a single dose and compared to control groups Q-VAX and PBS (**TABLE 3.2** and **FIG. 3.3A**). One group was given two doses 14 days apart to observe the benefits of a prime/boost model versus a single dose. Another experimental group contained Nine Mile I (NMI) LPS to more closely emulate Q-VAX.

Plasma was collected at days 9, 14, 28, and 42 and evaluated on protein microarray for antibodies against CBU1910 (**FIG. 3.3B**). Interestingly, IgG signals had lower intensities in the group containing the NMI LPS. Plasma from day 42 was analyzed for IgG1 and IgG2c to determine Th2 vs. Th1 responses, respectively (**FIG. 3.3C**). Mice immunized with CBU1910 without adjuvant skewed very heavily toward an IgG1/Th2 response, while the Q-VAX group polarized towards IgG2c/Th1. Experimental groups comprising of CBU1910 with adjuvants IVAX-1, IVAX-1 prime/boost, or IVAX-1 + NMI LPS exhibited a balanced IgG1/IgG2c response and higher overall responses when compared to the unadjuvanted group ($p= 0.0151$, $p=0.0008$, $p=0.7565$ for IgG1, $p<0.0001$, $p<0.0001$, $p=0.4710$ for IgG2). We observed a significant dampening response with lower IgG2c signal intensities in the group containing the NMI LPS when compared to the CBU1910 + IVAX-1 group ($p<0.0001$).

In the T cell immunogenicity screen, animals were primed with a single dose and euthanized 9 days later. One group was administered a boost 14 post-prime for comparison (**FIG. 3.3A**). Splenocytes were stimulated for 18 hours with CBU1910 antigen and IFNγ produced from the

stimulation was captured and quantified by both ELISpot (**FIG. 3.3D**) and cytokine bead assay (**FIG. 3.3E**). The prime/boost group with CBU1910 and IVAX-1 generated more IFNγ spot-forming cells than the other groups ($p=0.0380$), and the group given only the protein antigen by itself generated 0 spots. The addition of IVAX-1 to antigens increased IFNγ production when compared to antigen alone ($p= 0.9806$), though the addition of NMI LPS dampened the response, similar to the IgG response. The response of the adjuvanted group with NMI LPS is weaker than that of Q-VAX ($p= 0.8776$). The cytokine bead assay results also reflected the IFNγ T cell recall results in that the group that received a prime/boost of CBU1910 and IVAX-1 adjuvant induced the highest IFNγ and IL-2 response, corresponding to a Th1 response (**FIG. 3.3E**). IFNγ and IL-2 production was significantly higher in the prime/boost group compared with the single dose immunization ($p<0.0001$ and $p=0.0186$, respectively). The Th2 cytokine levels generated in response to recall antigen stimulation in all cases were low. Overall, these data show the addition of the IVAX-1 adjuvant enhanced the IgG, T cell recall, and cytokine response when compared to soluble antigen alone and sham-vaccinated groups.

Table 3.2. Vaccine formulations including adjuvants for immunogenicity studies in C57BL/6 mice.

Group	Name	Antigen	Adjuvants
1	CBU1910	Purified SorHis-tagged truncated CBU1910 protein	-
2	CBU1910 + IVAX-1	Purified SorHis-tagged truncated CBU1910 protein	MPLA, CpG1018, AddaVAX
3	CBU1910 + IVAX-1 (2 doses)	Purified SorHis-tagged truncated CBU1910 protein	MPLA, CpG1018, AddaVAX
4	CBU1910 + LPS + IVAX-1	Purified SorHis-tagged truncated CBU1910 protein	NMI LPS, MPLA, CpG1018, AddaVAX
5	Q-VAX	Formalin-inactivated whole cell vaccine positive control	-
6	PBS	PBS negative control	-

Candidate vaccines contained 3 μg of antigen per vaccine dose. For adjuvants, AddaVax was dosed at 50% v/v, 3 nmol MPLA and 1 nmol CpG-1018. Q-VAX was dosed at 2.5 μg of antigen per vaccine dose.

Figure 3.3

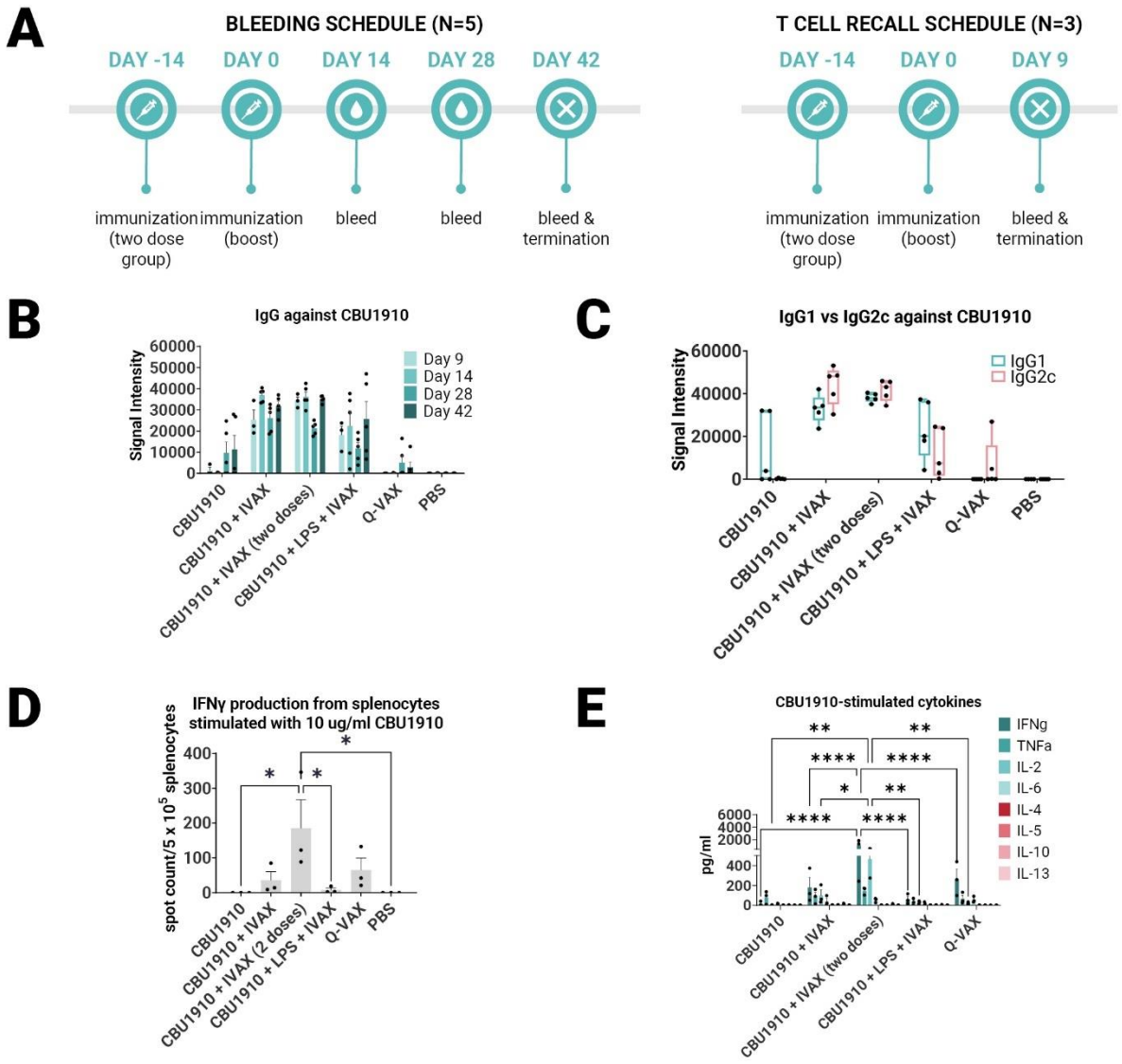

Figure 3.3. IVAX-1 (MPLA, CpG1018, AddaVAX) is a potent combination adjuvant for enhancing IgG2c responses and increasing proinflammatory cytokine production. (A) Timeline of events. Two groups with the same immunizations comprised of immunodominant protein CBU1910 and adjuvant combinations were run simultaneously. One group (n=5) was used to study the longevity of the IgG response, and another (n=3) was used for T cell assays. **(B)** Plasma from both experimental groups were probed on a *C. burnetii* protein microarray looking at

response to immunizing antigen CBU1910. Q-VAX and PBS were used as positive and negative controls. **(C)** Plasma from day 42 was used to assess IgG1 and IgG2c responses on the protein microarray. **(D)** Animals from the T cell recall group were terminated at day 9 and their splenocytes subjected to stimulation for 18 hours with CBU1910. Anti-IFNγ capture antibodies were used to determine spot counts in an IFNγ ELISPOT. Statistics were performed with one-way ANOVA and Dunnett's multiple comparisons test. **(E)** Supernatants from the 18-hour stimulation were assessed for Th1/Th2 cytokines using a cytokine bead assay. Extrapolated values for the PBS control group were subtracted from the other groups. Statistics were performed with two-way ANOVA and Tukey's multiple comparisons test.

Guinea pig hypersensitivity model establishes reactogenicity threshold with multivalency

The Hartley guinea pig is considered a more relevant animal model than the mouse for development of Q-fever vaccines due to their high susceptibility to respiratory pathogens with their ability to develop fever and other visible pathological changes (43,199,200). The formulations used in the guinea pig immunogenicity studies are indicated in **TABLE 3.3**. Group 1 contains TLR7 agonist 2Bxy and was a formulation from on a previous study (139). 2Bxy is an imidazoquinoline derivative that promotes $CD8^+$ T cell activity (201). We evaluated reactogenic responses to the vaccine candidates using an intradermal assay in guinea pigs. For this, guinea pigs were sensitized to Q-VAX via subcutaneous injection followed by resting for 2 weeks (49,202). Animals were shaved in their flanks and vaccine formations were then administered to the exposed skin. Experimental animals (n=4) received intradermal immunizations of the 6 candidate vaccines, and control animals (n=7) received WCV and PBS immunizations. Weights and temperatures were monitored for 14 days (**SUPPLEMENTAL FIG. S3.3A**). There was no significant difference between experimental and control groups, and all animals steadily gained weight over time.

Table 3.3. Vaccine formulations used in Hartley guinea pig challenge and reactogenicity studies.

Group	Name	Antigen	Adjuvants
1	6 Ag + TLR7 + IVAX-1	CBU1910, CBU0612, CBU0891, CBU0545, CBU0307, CBU1398	2Bxy, MPLA, CpG1018, AddaVAX
2	6 Ag + IVAX-1	CBU1910, CBU0612, CBU0891, CBU0545, CBU0307, CBU1398	MPLA, CpG1018, AddaVAX
3	4 Ag + IVAX-1	CBU1910, CBU0612, CBU0891, CBU0545	MPLA, CpG1018, AddaVAX
4	4 Ag + IVAX-1 + NMI LPS	CBU1910, CBU0612, CBU0891, CBU0545	MPLA, CpG1018, AddaVAX, NMI LPS
5	CBU1910 + IVAX-1	CBU1910	MPLA, CpG1018, AddaVAX
6	CBU1910 + IVAX-1 + NMI LPS	CBU1910	MPLA, CpG1018, AddaVAX, NMI LPS
7	Q-VAX/WCV	Formalin-inactivated whole cell vaccine positive control	-
8	PBS	PBS negative control	-

Candidate vaccines contained 0.25 nmol per antigen in each vaccine dose. AddaVax was dosed at 50% v/v, MPLA at 2 nmol CpG-1018 at 2 nmol. Q-VAX was dosed at 5 µg of antigen per vaccine dose.

Figure 3.4

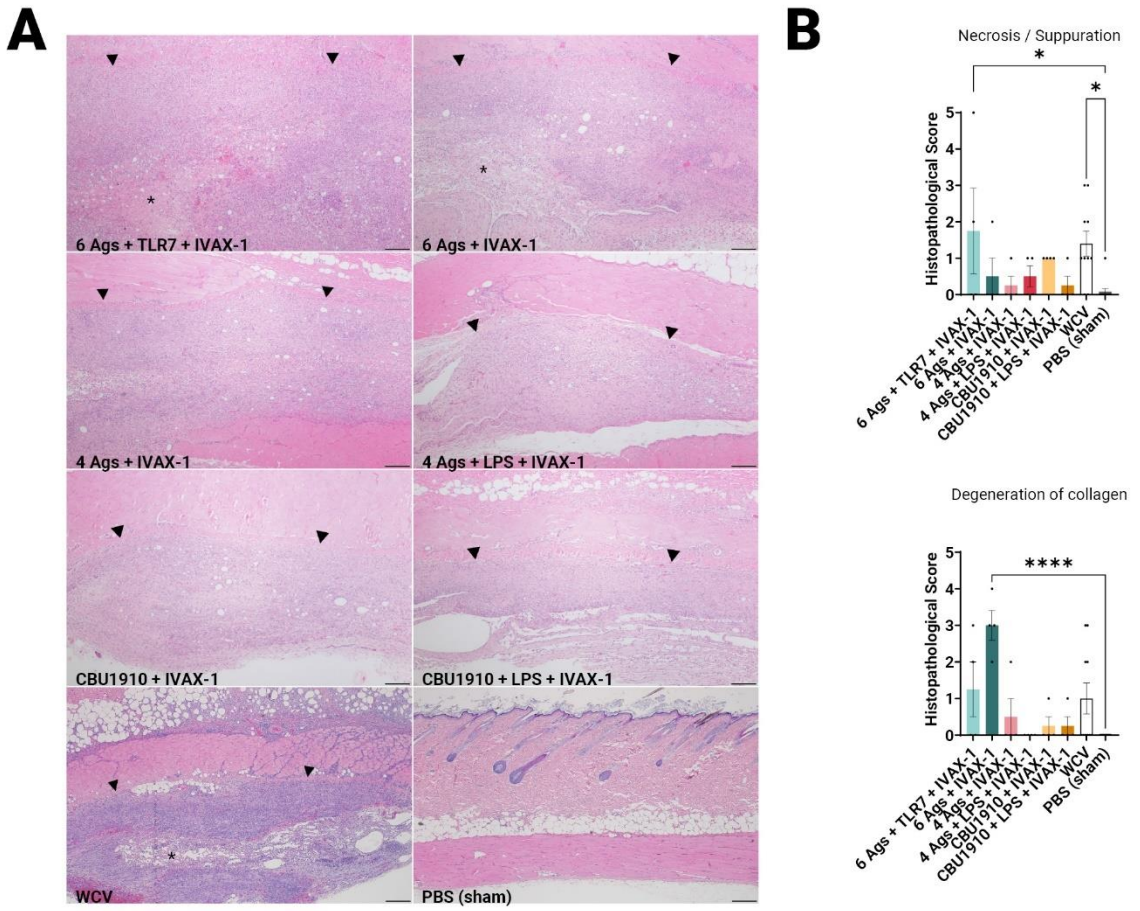

Figure 3.4. Guinea pig vaccine formulations were evaluated for reactogenicity. All animals were sensitized with Q-VAX and rested for 14 days, then intradermally administered either the 6 vaccine candidates (n=4) or Q-VAX and PBS intradermally (n=7) on shaved skin sections. **(A)** Representative histopathological H&E-stained skin sections of experimental groups at 4x magnification with a 200 um scale bar. Arrowheads border areas of immune cell infiltrate/inflammation and asterisks indicate areas of degenerate neutrophils/abscess formation. **(B)** Mean histopathological scores for experimental groups separated into different morphologic

categories. Significance is compared to the PBS group. Statistics were performed with one-way ANOVA and Dunnett's multiple comparisons test.

At the end of the 14-day period, the animals were euthanized and the injection sites were sectioned for hematoxylin and eosin (H&E) staining (**FIG. 3.4A**). Pathology in each section was scored on a scale from 0-5, with 5 being the most severe. Histopathology evaluation was parsed into 4 morphological categories: necrosis/suppuration, degeneration of collagen, fibrosis/granulation tissue, and mononuclear cell infiltration (**FIG. 3.4B** and **SUPPLEMENTAL FIG. 3.3B**). Necrosis and suppuration are weighted the most heavily in the parsed scores, with Group 1 and WCV demonstrating the most ($p=0.0253$ and $p= 0.0149$). Group 1, containing 6 antigens, TLR7 agonist, and IVAX-1, showed marked cellular inflammation composed primarily of macrophages with occasional central foci of necrosis and cellular debris (abscesses) or collagen degeneration. There is a moderate amount of fibrosis surrounding the inflammation and foci of hemorrhage are present within the lesions. Multifocally, adjacent skeletal muscle myofibers are degenerate. These observations are comparable with findings in the WCV sites. The presence and severity of foci of necrosis in the remaining experimental groups was not significantly greater than in the PBS group. Group 2 exhibited noticeable degeneration of collagen ($p<0.0001$) compared to the PBS control group, while all the remaining experimental groups were comparable to the WCV group. In all experimental groups, there was moderate fibrosis within the subcutis as well as mononuclear cell infiltration (**SUPPLEMENTAL FIG. 3.3B**). By giving more scoring weight to the necrosis/suppuration and degeneration of collagen categories due to severity, we determine that the 6-antigen vaccine groups are implied to be more reactogenic than groups with fewer antigens.

IgG response in plasma is antigen-specific and durable in multivalently-immunized Hartley guinea pigs

We also wanted to confirm whether the antigens identified as immunogenic in the mouse model were similarly immunogenic in the guinea pig. Animals were administered multivalent protein

vaccines with the IVAX-1 adjuvant, boosted 14 days later, and rested for 7 weeks. Plasma was collected from vaccinated guinea pigs at regular intervals and assessed on the protein microarray platform for antigen-specific antibody responses (**FIG. 3.5A**). Consistent with mouse studies, Q-VAX generated antibodies to CBU1910 only, which increased over time. All 6 experimental groups elicited durable CBU1910-specific IgG responses that persisted to day 42 post-immunization ($p<0.0001$, $p<0.0001$, $p=0.0027$, $p=0.0012$ $p<0.0001$, $p=0.3828$). Interestingly, the introduction of NMI LPS dampened the IgG response to antigens CBU0891, CBU0612, and CBU0545. IgG responses against CBU0307 were not detectable in any of the groups despite being an antigen in 2 of the 6 experimental groups. This corroborated with **FIG. 3.2** when mice were immunized with individual antigens. The vaccine formulation group containing only CBU1910 and IVAX-1 exhibited mild cross-reactivity with CBU0612, but this is likely due to the purified proteins containing the same Sortag tag used in the purification process.

IgG1 and IgG2 responses were also measured on a protein microarray to assess Th1/Th2 biases (**FIG. 3.5B**). Based on the subtyping data, all experimental vaccine formulations generated stronger CBU1910-specific IgG2 responses than Q-VAX ($p= 0.0692$, $p=0.0043$, $p=0.0057$, $p=0.0070$, $p=0.0068$, $p=0.0445$). Generally, signal intensities for IgG2 were higher than IgG1, indicating that the formulations all skewed more toward Th1 than Th2 response. Again, introducing the NMI LPS dampened the response for both IgG1 and IgG2 against CBU0612 and CBU0891.

Figure 3.5

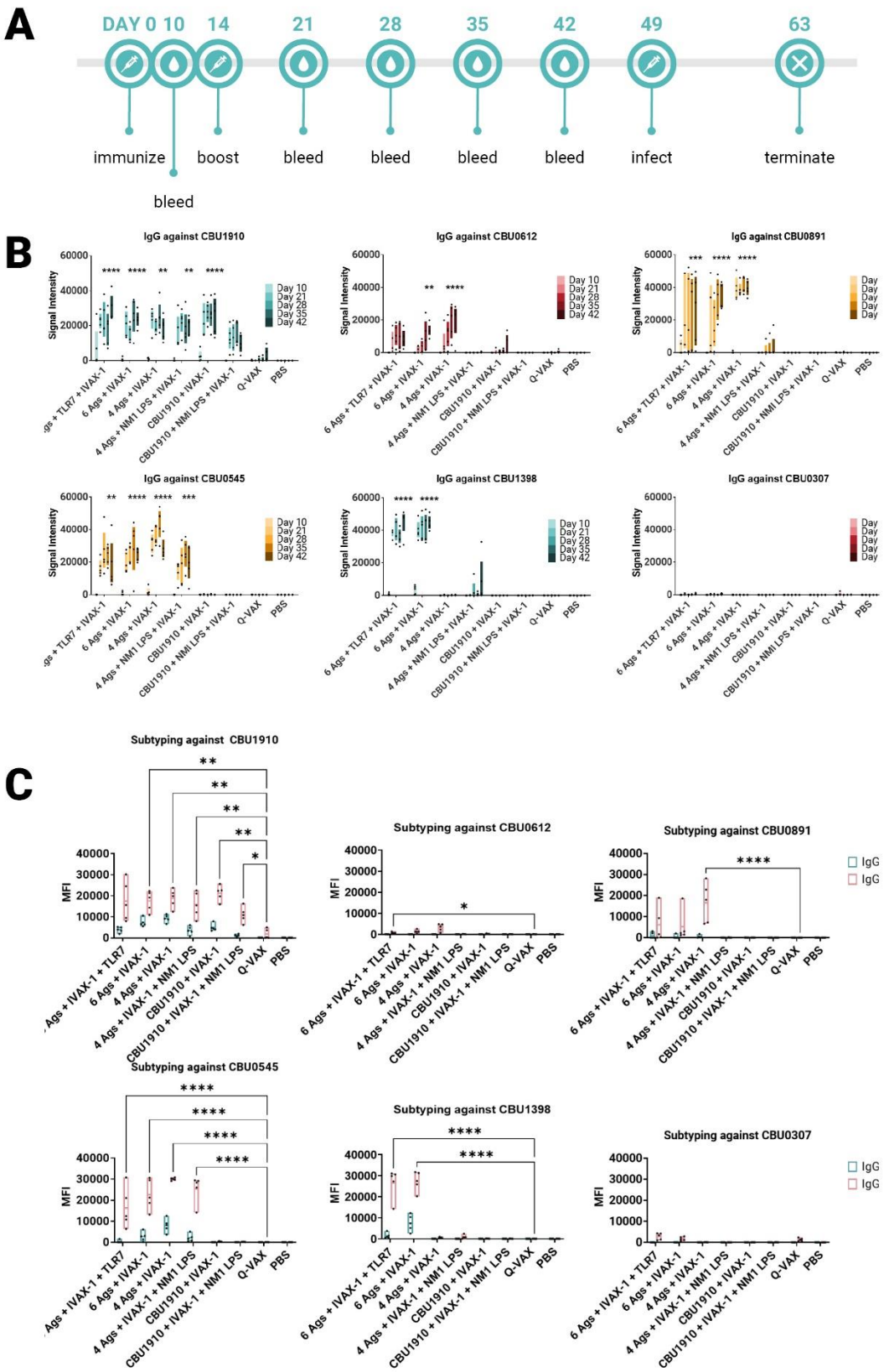
A
DAY 0 10 14 21 28 35 42 49 63
immunize
boost
bleed
bleed
bleed
bleed
infect
terminate
bleed
B
IgG against CBU1910
IgG against CBU0612
IgG against CBU0891
IgG against CBU0545
IgG against CBU1398
IgG against CBU0307
Signal Intensity
Day 10
Day 21
Day 28
Day 35
Day 42
6 Ags + TLR7 + IVAX-1
6 Ags + IVAX-1
4 Ags + IVAX-1
4 Ags + NM1 LPS + IVAX-1
CBU1910 + IVAX-1
CBU1910 + NMI LPS + IVAX-1
Q-VAX
PBS
C
Subtyping against CBU1910
Subtyping against CBU0612
Subtyping against CBU0891
Subtyping against CBU0545
Subtyping against CBU1398
Subtyping against CBU0307
MFI
IgG
IgG
6 Ags + IVAX-1 + TLR7
6 Ags + IVAX-1
4 Ags + IVAX-1
4 Ags + IVAX-1 + NM1 LPS
CBU1910 + IVAX-1
CBU1910 + IVAX-1 + NM1 LPS
Q-VAX
PBS

Figure 3.5. Multiple antigens induce IgG responses in Hartley guinea pigs. (A) Timeline of events. Animals were rested for 7 weeks after initial immunization prior to challenge. A challenge study with *Coxiella burnetii* strain NMI RSA493 was performed in Hartley guinea pigs (n=5). Formulations with 4 antigens include CBU1910, CBU0891, CBU0612 and CBU0545. CBU1398 and CBU0307 were included in formulations involving 6 antigens. NMI LPS used as an immunogen in candidate formulations was extracted from formalin-inactivated *C. burnetii* NMI RSA493. TLR7 is 2Bxy and part of the top formulation from a previous challenge study serving as a baseline. IVAX-1 includes, MPLA, CpG1018, and AddaVAX. **(B)** Plasma was collected at intervals on days 10, 21, 28, 35, and 42 post prime and assessed for IgG production using the protein microarray platform containing *C. burnetii* antigens. Significance looks at plasma from day 42 compared to WCV and performed with one-way ANOVA and Dunnett's multiple comparisons test. **(C)** Plasma from day 42 was assessed for production of IgG1 and IgG2 on the *C. burnetii* protein microarray. Statistics were performed with two-way ANOVA and Dunnett's multiple comparisons test.

Multivalent vaccines demonstrate protection against intratracheal C. burnetii NMI challenge

Guinea pigs used for immunogenicity screening were challenged 7 weeks post-prime with 5 x 10^5 genomic equivalents of *C. burnetii* NMI RSA493. Animals were monitored for weight and temperature change over a 14-day period post-infection. Whole cell vaccine (WCV; an in-house produced vaccine equivalent to Q-VAX) and sham-PBS were used as positive and negative controls, respectively.

Sham-vaccinated animals exhibited a marked decrease in body weight between days 9 and 12, and increased body temperature between days 7 and 10, when compared to the other groups (**FIG. 3.6A and 3.6B**). WCV positive control animals showed steady increases in body weight and maintained consistent body temperature for the duration of the two-week challenge. When observing changes in body weight, the groups that performed most similarly to WCV include groups 2, 4, and 6 with no significant difference on any of the days (**FIG. 3.6A**). This includes both groups that include NMI LPS as an antigen. Change in temperature shows group 1, 4, and 6 with no marked significance on any of the days when compared to WCV (**FIG. 3.6B**). From this, we can conclude that the groups containing 6 antigens, groups 1 and 2, showed similar trends with little difference when compared to positive control WCV changes in body temperature and weight and the inclusion of NMI LPS provides some modest additional protection.

The animals were terminated after the 14-day observation period. Splenomegaly, a hallmark of Q fever, was significantly lower in 4 of the 6 vaccine candidate groups when compared to PBS sham (**FIG. 3.6C**) (p= 0.0013, p=0.0022, p=0.5071, p=0.0055, p=0.7927, p=0.0165). The top performers were groups 1, 2, and 4 and was determined by being the most comparable to WCV.

Figure 3.6

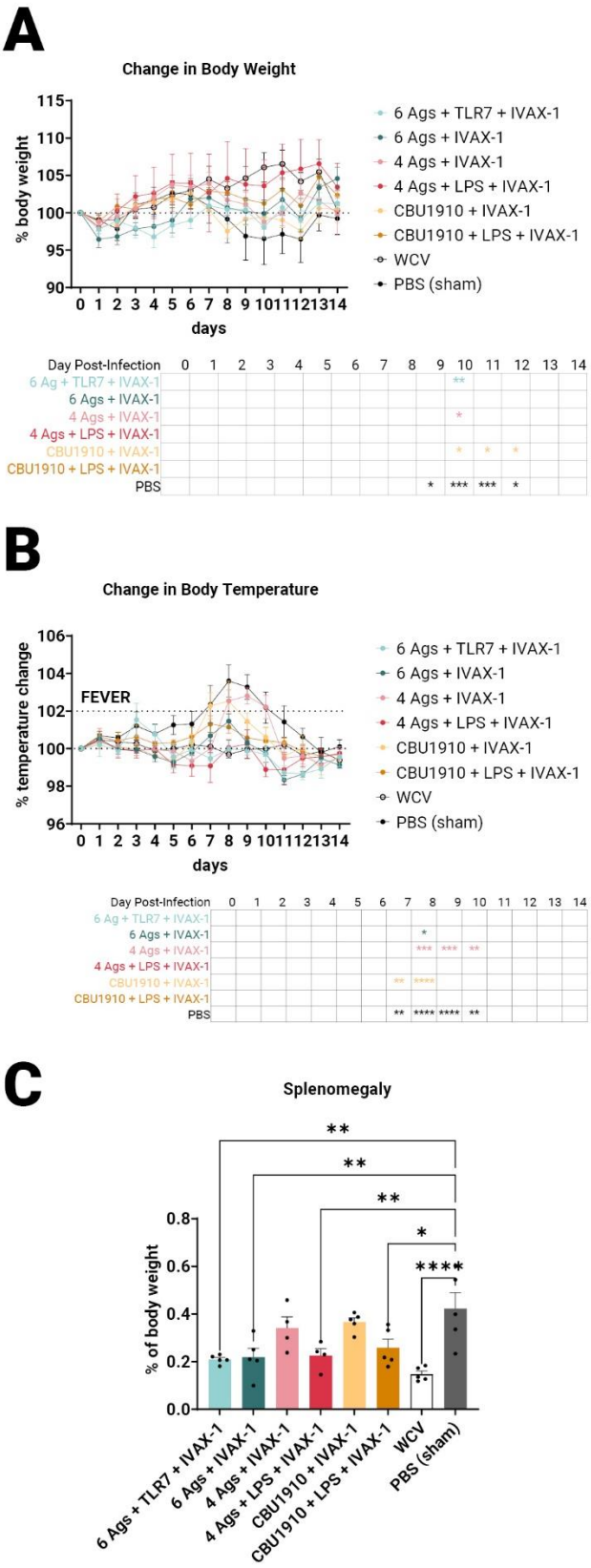

Figure 3. 6. An intratracheal aerosol challenge study with *Coxiella burnetii* strain NMI RSA493 was performed in Hartley guinea pigs (n=5). (A) Changes in body weight in calculated percentages were recorded for 14 days after infection. Significance is compared to the WCV group and performed with two-way ANOVA and Dunnett's multiple comparison tests. **(B)** Changes in temperature in calculated percentages were recorded for 14 days after infection. Fever is denoted as an increase in temperature greater than 2%. Significance is compared to the WCV group and performed with two-way ANOVA and Dunnett's multiple comparison tests. **(C)** Splenomegaly was determined after termination by comparing to the PBS group. Statistics were performed with one-way ANOVA and Dunnett's multiple comparisons test.

Discussion

In this study, we tested the hypothesis that immunogenicity and efficacy of a *C. burnetii* subunit vaccine formulations would increase with antigen multimerization. To address this, we first identified several lead candidate antigens using a proteomic screening approach for antibody and T cell target antigens (**FIG. 3.1**). After undergoing an extensive selection and purification process, we were able to show that a panel of X *C. burnetii* antigens were immunogenic individually, capable of eliciting antigen-specific antibody and/or T cell recall responses (**FIG. 3.2**). Use of IVAX-1 as an adjuvant enhanced the Th1 response, emulating that of protective WCVs such as Q-VAX (**FIG. 3.3**). We demonstrated efficacy in a Hartley guinea pig model and showed that a multivalent formulation provided the best protective response with some additional protection afforded by including NMI LPS (**FIG. 3.4**, **FIG. 3.5**, and **FIG. 3.6**).

The importance of antibody-mediated immunity (AMI) in *C. burnetii* infection has long been a topic of contention. Previous studies have shown that immunized patients seropositive for *C. burnetii* develop IgA and IgG specific antibody responses to phase I antigen (203,204). Acute Q fever patients generate IgM to phase I antigen, while chronic Q fever patients develop IgA and IgG to phase I antigen(205). Other *in vitro* studies demonstrated that incubating *C. burnetii* with immune sera increased their phagocytic uptake by macrophages (206). The consensus is that antibodies affect bacterial uptake by phagocytes in the early stages of infection but has no effect on the replication and growth of internalized *C. burnetii*. A study conducted by Zhang et al. showed that splenomegaly and bacterial burdens in SCID (T and B cell deficient) mice was not reduced with adoptive transfer of immune sera and B cells (207). In another study, Read et al. show that SCID mice that were reconstituted with T cells were able to control infection just as well as those that were rescued with both B and T cells (208). These studies show that even though antibodies,

especially those against phase I antigens, are useful diagnostic markers, they appear to play a smaller role in bacterial control and protection against infection. Despite Q-VAX's ability to provide lifelong protection with a single immunization, its antibody breadth is limited with CBU1910 being the only immunodominant antigen on a whole proteome microarray (**FIG. 3.1A**). Our immunizing antigens generated improved IgG responses when compared to Q-VAX (**FIG. 3.2**, **FIG. 3.3B**, **FIG. 3.5B**), and while not as critical to bacterial elimination, are still valid indicators of immunogenicity and the Th1/Th2 response.

Cell-mediated immunity (CMI), is essential for protection against *C. burnetii*. Studies by other groups have shown that IFNγ and TNFα are critical markers associated with reduced *C. burnetii* burden post-infection and that TNFα is required for IFNγ-mediated killing of *C. burnetii* (198,209,210). Reactive oxygen species is noted to have minimal effect on controlling the bacteria, but nitric oxide (NO) species, generated from upregulation of proinflammatory cytokines including IFNγ, has been shown to inhibit replication of *C. burnetii* by limiting the size of *Coxiella* containing vacuoles (CCVs) (27,210,211). NO is not the only contributor to bacterial clearance though, as bone marrow-derived macrophages from iNOS KO mice treated with IFNγ had reduced *C. burnetii* viability despite negligible NO presence (63). Cells pretreated with IFNγ exhibit increased microbicidal activity, while cells that have already been infected are less so. Stimulating the immune system with vaccination and increasing IFNγ production with adjuvants and immunogenic antigens helps to control bacterial replication and mitigate infection. We have shown that immunizing with immunogenic antigens identified in this study results in robust IFNγ responses after antigen recall (**FIG. 3.2**).

Adjuvants included in the subunit vaccine formulations tested here include squalene oil-in-water emulsion AddaVAX, TLR4 agonist MPLA, and TLR9 agonist CpG 1018. Q-VAX elicits a skewed

IgG2c/Th1 response, and these adjuvants are noted to help favor a more Th1-biased response. Formulations without adjuvant tend to be Th2-skewed (**FIG. 3.3C** and **3.3D**). As demonstrated in **FIG. 3.3**, the introduction of adjuvant to a single immunogenic antigen increases proinflammatory Th1 cytokine production (IFNγ, TNFα, IL-2, and IL-6) and downregulates Th2-associated cytokines (IL-4, IL-5, IL-10, IL-13). Q-VAX exhibits a robust Th1 response as shown in **FIG. 3.3B** and excluding the adjuvant results in a Th2-skewed response.

Immunization induces delayed type IV hypersensitivity (DTH), mediated by sensitized antigenic-specific T cells and can cause fever, malaise, and inoculation site granulomatous reactions (212). This differs from antibody-mediated hypersensitivities which may involve acute IgE antibodies (type I), IgG or IgM antibodies (type II), and immune complex formation (type III) (213). Cell-mediated inflammatory reactions may be $CD4^+$ or $CD8^+$ dependent and are usually limited to near the site of injection. Fratzke et al. demonstrated that sensitization of C57BL/6 mice with *C. burnetii* WCV results in reactogenicity that is $CD4^+$ T cell dependent rather than $CD8^+$ (49). Sensitization can be characterized by increased production of IFNγ and IL-17a to trigger cellular immunity. Improved *C. burnetii* vaccine design aims to define the antigens necessary to elicit a protective immune response while minimizing the reactogenic DTH response.

After demonstrating immunogenicity in mice, we moved onto the more biologically relevant guinea pig model with the top combination of protein antigens and adjuvants. We looked at dermal hypersensitivity and observed that including more antigens results in more severe reactogenicity (**FIG. 3.4**). We observe more early stage suppurative necrosis in the WCV group. In the group containing 6 antigens and IVAX-1, there is significantly more degeneration of collagen. The groups including NMI LPS developed the fewest mononuclear infiltrates when compared to WCV, indicating less reactogenicity with a reduced innate immune response (**SUPPLEMENTARY**

FIG. S3.3B). The increased responses when comparing groups with more antigens to those with fewer supports the hypothesis that including more antigens results in more overall immunogenicity. With this data, there is crossable threshold in the number of antigens in a multivalent vaccine and our candidates containing 4 antigens and fewer induce less severe reactogenic responses.

In the guinea pig challenge study, we concluded that the inclusion of more antigens and NMI *C. burnetii* LPS most closely emulates the protection from WCV (**FIG. 3.6**). The formulation containing 4 antigens and NMI LPS performs the closest to WCV with no significant difference in the body weight and temperature for the entire duration of the infection. The formulation containing a single antigen with NMI LPS also performs similarly with no significant differences when compared to WCV. The groups containing all 6 experimental antigens exhibit protection by showing no significant difference to Q-VAX in either weight loss or temperature change (**FIG. 3.6A** and **3.6B**). Splenomegaly is a major indicator of *C. burnetii* infection, and the best performers in that category when compared to PBS are the two groups that contain 6 antigens and the group that has 4 antigens and NMI LPS (**FIG. 3.6C**). It can be extrapolated from this dataset that vaccine formulations containing antigens in addition to LPS would confer better protection.

C. burnetii LPS is the only virulence factor identified in the infection of an immunocompetent animal model and has been acknowledged as a shielding molecule in allowing the pathogen to evade the host immune response (214). *C. burnetii* phase I LPS subverts host immunity by shielding the bacteria from compliment and antibody binding (215). Furthermore, NMI LPS disrupts mitogen-activated protein kinase (MAPK) signaling through disruption of TLR-2 and -4 and evades receptor-mediated phagocytosis by inhibiting and remodeling actin cytoskeleton organization (20,216,217). Addition of NMI phase I LPS as an immunogenic antigen in subunit

vaccine formulations corroborate this theory and demonstrate lower signal intensities of IgG antibodies to immunizing antigens when compared to groups that did not receive the LPS (**FIG. 3.5B** and **3.5C**). The overall cellular response is lower in groups containing NMI phase I LPS, as there are also lower levels of Th1 cytokines (IFNγ, TNFα, IL-2) (**FIG. 3.3**). Studies from other groups in the past have shown that patients suffering from Q fever endocarditis, a chronic manifestation of Q fever, exhibit higher levels of TNFα and IL-1β in PBMCs and monocytes from blood. Introducing anti-TNF antibodies decreases uptake efficiency of *C. burnetii* into monocytes but does not play a role in intracellular killing (218).

Avirulent phase II LPS easily activates phosphorylation of MAPK p38, while exposure to phase I LPS results in no activation. P38 is one of three MAPK signaling pathway subfamilies, and phase I LPS has been shown to activate the other two pathways, JNK and ERK (219). This is through the presumed mechanism of phase I LPS-induced cytoskeletal remodeling, preventing colocalization of TLR-2 and TLR-4(216). P38 is upstream of transcription factor NF-κB, which is critical for upregulating proinflammatory molecules (77,220). Inhibition of this pathway via *C. burnetii* LPS may be the explanation for why immunogenicity readouts are lower for vaccine groups containing LPS (**FIG. 3.3** and **3.6**).

Overall, a panel of immunogenic *C. burnetii* antigens administered with potent Th1-stimulating adjuvants and native *C. burnetii* LPS demonstrate immunogenicity in mice and protection in a Hartley guinea pig aerosol model. Based on the presented data, we conclude multivalency does result in a more protective vaccine as we observe better performance in 4 and 6-antigen formulations. There is an upper limit for the number of antigens consequentially causing reactogenicity, with 6-antigen formulations scoring higher in necrosis and collagen degeneration and 4-antigen formulations having such effects minimized. Despite dampening immunogenic

responses in both animal models, vaccines containing NMI LPS modestly improve protection. Further studies on our potential vaccine candidates need to investigate the durability in animal models to recapitulate Q-VAX's effectiveness as a single dose conferring lifelong protection. Another aspect to investigate is potential reactogenicity in substituting the additional two antigens present the 6-antigen formulations versus the 4-antigen ones. This will clarify if the reactogenicity is being caused by the addition of those specific antigens or from increasing multivalency in general. There is a balance that must be established in maximizing the number of immunogenic antigen and reducing the logistical difficulty in purifying NMI LPS that warrants further investigation. From a practical standpoint, the difficulty in protein purification serves as a major roadblock in subunit vaccine development. With the rise of mRNA technology, once immunogenic proteins are identified, we can begin to move away from the labor-intensive protein purification process and toward a high-throughput method of manufacturing mRNA and easily incorporating more antigens for effective, multivalent vaccines.

Supplementary Figure S3.1

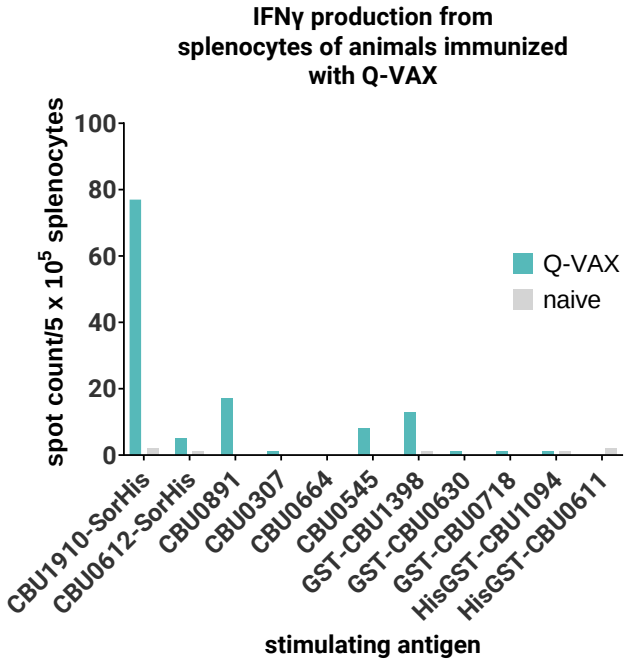

Supplementary Figure S3.1. Splenocytes from mice immunized with Q-VAX generate responses to purified protein. C57BL/6 mice (n=3) were immunized with Q-VAX intraperitoneally and their splenocytes were harvested 10 days after the prime. The pooled splenocytes were stimulated by purified protein from a downselected panel of lead antigens indicated in table 1 ("Immunogenicity" column).

Supplementary Figure S3.2

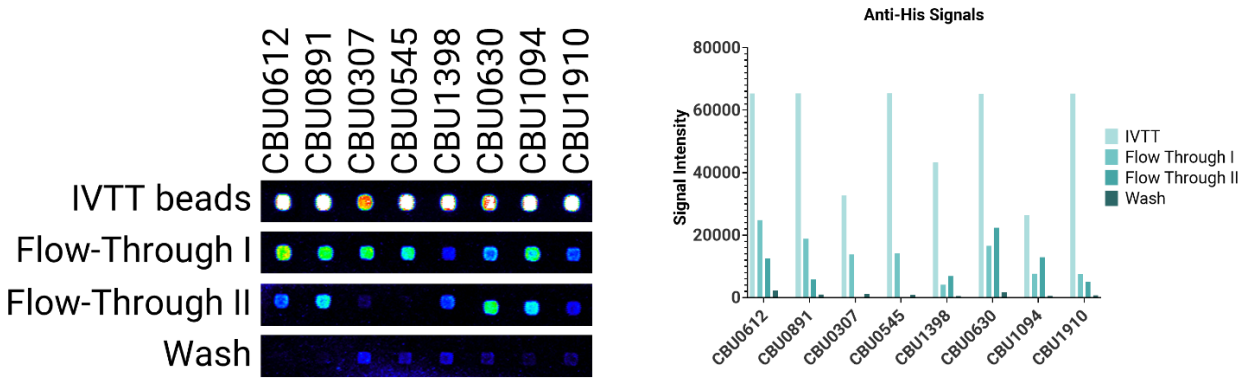

Supplementary Figure S3.2. *Coxiella* proteins expressed in IVTT were captured on Sepharose beads for mouse immunizations. IVTT reactions of CBU antigens were applied on GE His-TrapSpin columns. Flow-through fractions were collected and re-applied to the columns. Columns were washed to remove IVTT master mixture components. IVTT beads, flow-through, and washes were collected, printed on nitrocellulose slides, and probed against using anti-tag antibodies.

Supplementary Figure S3.3

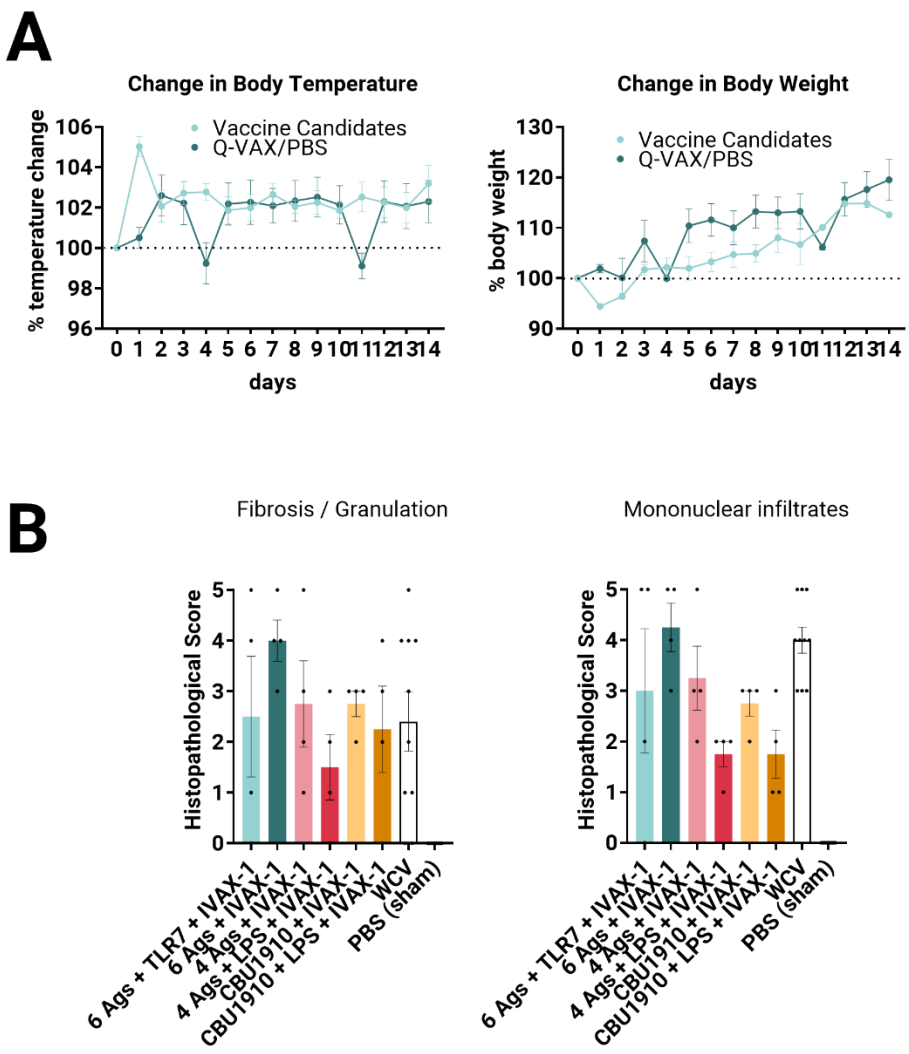

Supplementary figure S3.3. Guinea pig vaccine formulations were evaluated for reactogenicity. All animals were sensitized with Q-VAX and rested for 14 days, then intradermally administered either the 6 vaccine candidates (n=4) or Q-VAX and PBS intradermally (n=7) on shaved skin sections. **(A)** Changes in body temperature and weight in calculated percentages were recorded for 14 days after intradermal immunization. **(B)** Mean histopathological scores for experimental groups separated into different morphological categories.

CHAPTER 4:

CONCLUSIONS AND PERSPECTIVES

Conclusions and Future Directions

Coxiella burnetii is globally endemic, highly infectious pathogen with biothreat potential, indicating a need for an effective, non-reactogenic vaccine. Formalin-inactivated whole cell vaccine Q-VAX conveys life-long protection but has not been granted approval for use in the United States due to its reactogenicity, which comes with costly validation and skin testing screening. The studies in this thesis describe efforts to develop subunit vaccines for Q fever and incorporating immunogenic adjuvants and scaffolds for optimizing antigen presentation.

In order to effectively couple protein antigens to different molecules and nanoparticles, we developed a self-assembly approach reminiscent of a VLP with a poly-His tag incorporated in our protein constructs. Tris-NTA molecules can be synthesized containing a variety of chemical handles for flexible bioconjugation. These compounds allow us to functionalize His-tagged antigens with new functional groups which can be followed by direct conjugation to scaffolds. We successfully demonstrate antigen capture from a complex IVTT mixture onto 1 µ and 0.2 µm polystyrene beads, indicating high-throughput potential with accelerated protein production without the need for costly expression and purification.

Our studies have also demonstrated that the IVAX-1 adjuvant cocktail synergistically upregulated antibody breadth and elicited a balanced $CD4^+$ Th1/Th2 response in the *Coxiella* mouse model and guinea pig model, improving efficacy against pathogen infection upon challenge. We were able to demonstrate increased immunogenicity with both antigens captured on beads and mixtures of soluble, commercially purified protein.

Nanoparticles improve immunogenicity of antigens by multimeric antigen presentation on the surface. The greater the multivalency of antigen, the greater the extent and stability of BCR

crosslinking, resulting in more robust BCR signaling. This results in the activation and differentiation of B cells in the germinal center to ultimately give rise to class switched and high affinity memory B cells and plasma cells (221,222). In addition, incorporation of PAMPs in or on the nanoparticles would represent additional distinct mechanisms for enhanced multivalent/multimeric engagement of their corresponding PRRs.

In addition to the polystyrene beads we implemented in this thesis, we isolated and purified the bacterial PGN sacculus, which encompassed our defined nanoparticle parameters of innately displaying adjuvant activity by being recognizable by PRRs and also by being modifiable. We were able to successfully demonstrate the sacculus's flexibility in accommodating chemical conjugations and surface modifications in addition to confirming its adjuvant activity. The platform is very promising, as the scaffold itself is already immunogenic in successfully activating NK-κB and eliciting appropriate host immune responses (132,143). Further studies need to be performed to confirm its chemical programmability, scalability, and efficacy *in vivo*.

In an effort to develop a less reactogenic vaccine that exhibits the same protective capabilities as Q-VAX, we narrowed down our list of candidate antigens for a multivalent subunit vaccine formulation used in chapter 2 and 3. These antigens have been used in concurrently published works in collaboration with our group during my tenure, but the rationale behind the selection was not described until now (126,139). CBU1910 is the model *C. burnetii* antigen, exhibiting great immunogenicity and nearly overpowering all other antigens. However, we were able to show that multivalency and the incorporation of additional antigens augments the immune response.

C. burnetii LPS is also featured prominently as an effective antigen not in generating standard immune readouts, including antigen-specific antibody and IFNγ production, but exhibits moderate levels of protection in the guinea pig challenge model even when combined with a single antigen.

Many studies have been done by other groups looking at the function and structure of LPS, and further investigation into its antigen potential should be conducted. The ultimate goal of rational *C. burnetii* vaccine design is to achieve a single-dose vaccine that provides lifelong protection, and if a single immunogenic antigen combined with an adjuvant cocktail containing *C. burnetii* LPS is achieves adequate protection, then we would need to look no further.

Beyond the scope of this thesis, we have constructed a collection of nanoparticles that enter the antigen presentation pathway differently and release antigen at different rates with our collaborators. These nanoparticles are based on liposomes or emulsions (lipid-based nanoparticles), polymeric or protein nanoparticles, that can induce durable antibody and T cell responses after a single injection. These include liposomes, the E2 nanoparticle, an antigen-encapsulating ketal nanoparticle, and denpols (129,223,224). Future studies involve evaluating their immunogenicity and efficacy in conferring protection against *C. burnetii* challenge, and many of these are currently underway.

Overall, we were able to successfully contribute to the body of work surrounding *C. burnetti* vaccine development by focusing on whole protein subunit vaccines. The bead and sacculus scaffolds and IVAX-1 antigen cocktail described here have the flexibility to be widely applicable to other pathogens, such as influenza (141,142). To continue down the path toward a successful *C. burnetii* vaccine for the sake of public health, more studies need to be conducted to find optimal combinations of protein epitopes and immunogenic adjuvants promoting IFNγ production in lymphocytes and microbicidal action in infected macrophages.

Perspectives

Vaccinology is a vastly interdisciplinary field effectively incorporating chemistry, bioengineering, proteomics, structural biology, microbiology, molecular biology, and immunology just to name a few disciplines. I've had the great honor of working with excellent scientists knowledgeable in the field of preclinical vaccine design with skills ranging from antigen identification to rational delivery platform design and optimization.

Traditional approaches to vaccine development involved the use of attenuated or inactivated pathogens from Edward Jenner's days, subunit vaccines, or live vectors. While these approaches have been successful in many cases, they often rely on empirical methods and have limitations in terms of safety, efficacy, and scalability. Rational vaccine design takes a more targeted and evidence-based approach by leveraging our understanding of pathogen biology, immunology, and host-pathogen interactions. It aims to identify key antigens or immunogenic epitopes that can elicit protective immune responses. Advances in genomics, proteomics, and bioinformatics have greatly accelerated the identification and characterization of candidate antigens, allowing for more precise antigen selection. The development of novel adjuvants with improved safety and efficacy profiles has also evolved over the years, branching out from the use of aluminum salt solutions in the 1920s (225). Emulsions, such as AddaVAX, and lipid-based particles are other adjuvants that have been enjoying popularity and use in modern influenza vaccines due to their abilities to upregulate antigen-presenting cell migration to the site of injection and prime immune responses. Newer to the scene, combinations of TLR agonists can effectively take advantage of divergent signaling pathways to upregulate dendritic cell activation (226).

In addition, advancements in vaccine delivery systems have revolutionized the field. Novel platforms such as virus-like particles (VLPs), nanoparticles, and liposomes offer benefits such as improved antigen stability, controlled release, and targeted delivery to specific immune cells or

tissues. These platforms can enhance antigen uptake, promote antigen presentation, and stimulate immune responses in a more controlled and targeted manner.

Furthermore, rational vaccine design allows for the development of multi-component or multivalent vaccines, where multiple antigens or epitopes are incorporated to enhance the breadth and potency of the immune response. By targeting multiple components of a pathogen, these vaccines can provide broader protection and reduce the risk of immune evasion. With how dynamic *in vivo* biological systems are, every one of the delivery vehicles designed with collaborators address alternative solutions to different problems, ranging from antigen display, delivery, and encapsulation. Though my own nanoparticles in the polystyrene beads and the sacculus were not pursued further in challenge studies due to biodegradability and logistics in scaling up, similar concepts and technologies can be applied to other nanoparticle designs.

The landscape of *Coxiella burnetii* vaccine design is characterized by ongoing efforts to develop safe and effective vaccines against this intracellular bacterium. Several vaccine candidates have been explored, including whole cell inactivated vaccines, live attenuated vaccines, subunit vaccines, and DNA vaccines. As demonstrated by Q-VAX, whole cell inactivated vaccines are promising, but their safety considerations pose challenges. Live attenuated vaccines have demonstrated efficacy in animal studies, but safety concerns remain for human use.

Subunit vaccines, which utilize specific antigens of *Coxiella burnetii*, have been investigated extensively by us and other groups alike. Key antigens include the highly immunogenic outer membrane protein Com1 CBU1910, as well as other surface-exposed proteins including LPS. Recombinant protein-based subunit vaccines have shown varying degrees of success in preclinical studies, with some candidates inducing protective immune responses, as demonstrated in these works. Incorporation of effective adjuvants to improve the immunogenicity is a key area of

research right now, and the use of bioinformatics and genomic approaches has provided insights into potential vaccine targets and virulence factors.

While progress has been made in *C. burnetii* vaccine development, the challenges in designing an optimal vaccine, including balancing safety and efficacy, remain. Continued research efforts are needed to refine vaccine candidates, improve immunogenicity, assess long-term protection, and address issues related to vaccine production, storage, and distribution. By incorporating rational vaccine design strategies and integrating our knowledge of pathogen biology, immunology, and innovative technologies, we can move toward a more targeted and effective approach to developing vaccines that can confer long-lasting and robust protection. Collaborative efforts among researchers, industry partners, and public health agencies are crucial to advancing *C. burnetii* vaccine design and ultimately reducing the burden of Q fever.

References

1. Ullah Q, Jamil T, Saqib M, Iqbal M, Neubauer H. Q Fever—A Neglected Zoonosis. Microorganisms. 2022 Jul 28;10(8):1530.

2. Wegdam-Blans MCA, Kampschreur LM, Delsing CE, Bleeker-Rovers CP, Sprong T, van Kasteren MEE, et al. Chronic Q fever: Review of the literature and a proposal of new diagnostic criteria. Journal of Infection. 2012 Mar 1;64(3):247–59.

3. Miller JD, Shaw EI, Thompson HA. Coxiella burnetii, Q Fever, and Bioterrorism. In: Anderson B, Friedman H, Bendinelli M, editors. Microorganisms and Bioterrorism [Internet]. Boston, MA: Springer US; 2006 [cited 2023 May 18]. p. 181–208. (Infectious Agents and Pathogenesis). Available from: https://doi.org/10.1007/0-387-28159-2_10

4. Oren A, Garrity GM. Valid publication of the names of forty-two phyla of prokaryotes. International Journal of Systematic and Evolutionary Microbiology. 2021;71(10):005056.

5. Meir A, Macé K, Lukoyanova N, Chetrit D, Hospenthal MK, Redzej A, et al. Mechanism of effector capture and delivery by the type IV secretion system from Legionella pneumophila. Nat Commun. 2020 Jun 8;11(1):2864.

6. Maurin M, Raoult D. Q Fever. Clin Microbiol Rev. 1999 Oct;12(4):518–53.

7. Leclerque A. Whole genome-based assessment of the taxonomic position of the arthropod pathogenic bacterium Rickettsiella grylli. FEMS Microbiology Letters. 2008 Jun 1;283(1):117–27.

8. Cordaux R, Paces-Fessy M, Raimond M, Michel-Salzat A, Zimmer M, Bouchon D. Molecular Characterization and Evolution of Arthropod-Pathogenic Rickettsiella Bacteria. Appl Environ Microbiol. 2007 Aug;73(15):5045–7.

9. Roest HIJ, Bossers A, van Zijderveld FG, Rebel JML. Clinical microbiology of Coxiella burnetii and relevant aspects for the diagnosis and control of the zoonotic disease Q fever. Veterinary Quarterly. 2013 Sep 1;33(3):148–60.

10. Hirschmann JV. The Discovery of Q Fever and Its Cause. The American Journal of the Medical Sciences. 2019 Jul 1;358(1):3–10.

11. Dragan AL, Voth DE. Coxiella burnetii: international pathogen of mystery. Microbes and Infection. 2020 Apr 1;22(3):100–10.

12. Cox HR. Rickettsia Diaporica and American Q Fever. The American Journal of Tropical Medicine and Hygiene. 1940 Jul 1;s1-20(4):463–9.

13. Fournier PE, Raoult D. Current Knowledge on Phylogeny and Taxonomy of Rickettsia spp. Annals of the New York Academy of Sciences. 2009;1166(1):1–11.

14. Gray MW. Rickettsia, typhus and the mitochondrial connection. Nature. 1998 Nov;396(6707):109–10.

15. Emelyanov VV. Evolutionary relationship of Rickettsiae and mitochondria. FEBS Letters. 2001 Jul 13;501(1):11–8.

16. Plotz H, Smadel JE, Anderson TF, Chambers LA. MORPHOLOGICAL STRUCTURE OF RICKETTSIAE. Journal of Experimental Medicine. 1943 Apr 1;77(4):355–8.

17. Gillespie JJ, Salje J. Orientia and Rickettsia: different flowers from the same garden. Current Opinion in Microbiology. 2023 Aug 1;74:102318.

18. Baca OG, Paretsky D. Q fever and Coxiella burnetii: a model for host-parasite interactions. MICROBIOL REV. 1983;47.

19. Ganta RR. Rickettsiaceae and Coxiellaceae. In: Veterinary Microbiology [Internet]. John Wiley & Sons, Ltd; 2022 [cited 2023 Jun 5]. p. 377–80. Available from: https://onlinelibrary.wiley.com/doi/abs/10.1002/9781119650836.ch39

20. Abnave P, Muracciole X, Ghigo E. Coxiella burnetii Lipopolysaccharide: What Do We Know? Int J Mol Sci. 2017 Nov 23;18(12):2509.

21. Hackstadt T, Williams JC. Biochemical stratagem for obligate parasitism of eukaryotic cells by Coxiella burnetii. Proceedings of the National Academy of Sciences. 1981 May 1;78(5):3240–4.

22. Zamboni DS, McGrath S, Rabinovitch M, Roy CR. Coxiella burnetii express type IV secretion system proteins that function similarly to components of the Legionella pneumophila Dot/Icm system. Molecular Microbiology. 2003;49(4):965–76.

23. Lührmann A, Roy CR. Coxiella burnetii Inhibits Activation of Host Cell Apoptosis through a Mechanism That Involves Preventing Cytochrome c Release from Mitochondria. Infection and Immunity. 2007 Nov 1;75(11):5282–9.

24. Samanta D, Clemente TM, Schuler BE, Gilk SD. Coxiella burnetii Type 4B Secretion System-dependent manipulation of endolysosomal maturation is required for bacterial growth. PLOS Pathogens. 2019 Dec 23;15(12):e1007855.

25. Coleman SA, Fischer ER, Howe D, Mead DJ, Heinzen RA. Temporal Analysis of Coxiella burnetii Morphological Differentiation. Journal of Bacteriology. 2004 Nov;186(21):7344–52.

26. Waag DM. Coxiella burnetii: Host and bacterial responses to infection. Vaccine. 2007 Oct 16;25(42):7288–95.

27. Ghigo E, Capo C, Tung CH, Raoult D, Gorvel JP, Mege JL. Coxiella burnetii Survival in THP-1 Monocytes Involves the Impairment of Phagosome Maturation: IFN-γ Mediates its

Restoration and Bacterial Killing1. The Journal of Immunology. 2002 Oct 15;169(8):4488–95.

28. Schulze-Luehrmann J, Eckart RA, Ölke M, Saftig P, Liebler-Tenorio E, Lührmann A. LAMP proteins account for the maturation delay during the establishment of the Coxiella burnetii-containing vacuole. Cellular Microbiology. 2016;18(2):181–94.

29. Segal G, Feldman M, Zusman T. The Icm/Dot type-IV secretion systems of Legionella pneumophila and Coxiella burnetii. FEMS Microbiology Reviews. 2005 Jan 1;29(1):65–81.

30. Lührmann A, Newton HJ, Bonazzi M. Beginning to Understand the Role of the Type IV Secretion System Effector Proteins in Coxiella burnetii Pathogenesis. In: Backert S, Grohmann E, editors. Type IV Secretion in Gram-Negative and Gram-Positive Bacteria [Internet]. Cham: Springer International Publishing; 2017 [cited 2023 Jun 5]. p. 243–68. (Current Topics in Microbiology and Immunology). Available from: https://doi.org/10.1007/978-3-319-75241-9_10

31. Mansilla Pareja ME, Bongiovanni A, Lafont F, Colombo MI. Alterations of the Coxiella burnetii Replicative Vacuole Membrane Integrity and Interplay with the Autophagy Pathway. Frontiers in Cellular and Infection Microbiology [Internet]. 2017 [cited 2023 Jun 5];7. Available from: https://www.frontiersin.org/articles/10.3389/fcimb.2017.00112

32. Gilk SD, Cockrell DC, Luterbach C, Hansen B, Knodler LA, Ibarra JA, et al. Bacterial colonization of host cells in the absence of cholesterol. PLoS Pathog. 2013 Jan;9(1):e1003107.

33. Newton HJ, McDonough JA, Roy CR. Effector Protein Translocation by the Coxiella burnetii Dot/Icm Type IV Secretion System Requires Endocytic Maturation of the Pathogen-Occupied Vacuole. PLOS ONE. 2013 Jan 17;8(1):e54566.

34. Winchell CG, Graham JG, Kurten RC, Voth DE. Coxiella burnetii Type IV Secretion-Dependent Recruitment of Macrophage Autophagosomes. Infection and Immunity. 2014 May 12;82(6):2229–38.

35. Latomanski EA, Newton P, Khoo CA, Newton HJ. The Effector Cig57 Hijacks FCHO-Mediated Vesicular Trafficking to Facilitate Intracellular Replication of Coxiella burnetii. PLOS Pathogens. 2016 Dec 21;12(12):e1006101.

36. Toman R, Škultéty L. Structural study on a lipopolysaccharide from Coxiella burnetii strain Nine Mile in avirulent phase II. Carbohydrate Research. 1996 Mar 22;283:175–85.

37. Capo C, Lindberg FP, Meconi S, Zaffran Y, Tardei G, Brown EJ, et al. Subversion of monocyte functions by coxiella burnetii: impairment of the cross-talk between alphavbeta3 integrin and CR3. J Immunol. 1999 Dec 1;163(11):6078–85.

38. Ghigo E, Honstettre A, Capo C, Gorvel JP, Raoult D, Mege JL. Link between Impaired Maturation of Phagosomes and Defective Coxiella burnetii Killing in Patients with Chronic Q Fever. The Journal of Infectious Diseases. 2004 Nov 15;190(10):1767–72.

39. Madariaga MG, Rezai K, Trenholme GM, Weinstein RA. Q fever: a biological weapon in your backyard. The Lancet Infectious Diseases. 2003 Nov 1;3(11):709–21.

40. Tissot-Dupont H, Raoult D. Q Fever. Infectious Disease Clinics of North America. 2008 Sep 1;22(3):505–14.

41. Schimmer B, Morroy G, Dijkstra F, Schneeberger PM, Weers-Pothoff G, Timen A, et al. Large ongoing Q fever outbreak in the south of The Netherlands, 2008. Eurosurveillance. 2008 Jul 31;13(31):18939.

42. Jones RM, Nicas M, Hubbard AE, Reingold AL. The Infectious Dose of *Coxiella Burnetii* (Q Fever). Appl Biosaf. 2006 Mar;11(1):32–41.

43. Brooke RJ, Kretzschmar ME, Mutters NT, Teunis PF. Human dose response relation for airborne exposure to Coxiella burnetii. BMC Infectious Diseases. 2013 Oct 21;13(1):488.

44. Omsland A, Hackstadt T, Heinzen RA. Bringing Culture to the Uncultured: Coxiella burnetii and Lessons for Obligate Intracellular Bacterial Pathogens. PLOS Pathogens. 2013 Sep 5;9(9):e1003540.

45. Omsland A. Axenic Growth of Coxiella burnetii. In: Toman R, Heinzen RA, Samuel JE, Mege JL, editors. Coxiella burnetii: Recent Advances and New Perspectives in Research of the Q Fever Bacterium [Internet]. Dordrecht: Springer Netherlands; 2012 [cited 2023 May 18]. p. 215–29. (Advances in Experimental Medicine and Biology). Available from: https://doi.org/10.1007/978-94-007-4315-1_11

46. Gilroy N, Formica N, Beers M, Egan A, Conaty S, Marmion B. Abattoir-associated Q fever: a Q fever outbreak during a Q fever vaccination program. Australian and New Zealand Journal of Public Health. 2001;25(4):362–7.

47. Greig JE, Patel MS, Clements MS, Taylor NK. Control strategies for Q fever based on results of pre-vaccination screening in Victoria, 1988 to 2001. Australian and New Zealand Journal of Public Health. 2005;29(1):53–7.

48. Ahmed AR, Blose DA. Delayed-Type Hypersensitivity Skin Testing: A Review. Archives of Dermatology. 1983 Nov 1;119(11):934–45.

49. Fratzke AP, Gregory AE, van Schaik EJ, Samuel JE. Coxiella burnetii Whole Cell Vaccine Produces a Th1 Delayed-Type Hypersensitivity Response in a Novel Sensitized Mouse Model. Front Immunol. 2021 Sep 20;12:754712.

50. Jerrells TR, Mallavia LP, Hinrichs DJ. Detection of long-term cellular immunity to Coxiella burneti as assayed by lymphocyte transformation. Infection and Immunity. 1975 Feb;11(2):280–6.

51. Kazár J, Schramek S, Lisák V, Brezina R. Antigenicity of chloroform-methanol-treated Coxiella burnetii preparations. Acta Virol. 1987 Mar 1;31(2):158–67.

52. Amara AB, Bechah Y, Mege JL. Immune Response and Coxiella burnetii Invasion. In: Toman R, Heinzen RA, Samuel JE, Mege JL, editors. Coxiella burnetii: Recent Advances and New Perspectives in Research of the Q Fever Bacterium [Internet]. Dordrecht: Springer Netherlands; 2012 [cited 2020 Oct 14]. p. 287–98. (Advances in Experimental Medicine and Biology). Available from: https://doi.org/10.1007/978-94-007-4315-1_15

53. Sireci G, Badami GD, Di Liberto D, Blanda V, Grippi F, Di Paola L, et al. Recent Advances on the Innate Immune Response to Coxiella burnetii. Frontiers in Cellular and Infection Microbiology [Internet]. 2021 [cited 2023 May 18];11. Available from: https://www.frontiersin.org/articles/10.3389/fcimb.2021.754455

54. Benoit M, Bechah Y, Capo C, Murray PJ, Mege JL, Desnues B. Role of the cytoplasmic pattern recognition receptor Nod2 in Coxiella burnetii infection. Clinical Microbiology and Infection. 2009 Dec 1;15:154–5.

55. Fisher JR, Chroust ZD, Onyoni F, Soong L. Pattern Recognition Receptors in Innate Immunity to Obligate Intracellular Bacteria. Zoonoses (Burlingt). 2021;1(1):10.

56. Koster FT, Kirkpatrick TL, Rowatt JD, Baca OG. Antibody-dependent cellular cytotoxicity of Coxiella burnetii-infected J774 macrophage target cells. Infect Immun. 1984 Jan;43(1):253–6.

57. Zhang G, Russell-Lodrigue KE, Andoh M, Zhang Y, Hendrix LR, Samuel JE. Mechanisms of Vaccine-Induced Protective Immunity against Coxiella burnetii Infection in BALB/c Mice. The Journal of Immunology. 2007 Dec 15;179(12):8372–80.

58. Zhang G, Zhang Y, Samuel JE. Components of Protective Immunity. In: Toman R, Heinzen RA, Samuel JE, Mege JL, editors. Coxiella burnetii: Recent Advances and New Perspectives in Research of the Q Fever Bacterium [Internet]. Dordrecht: Springer Netherlands; 2012 [cited 2023 May 19]. p. 91–104. (Advances in Experimental Medicine and Biology). Available from: https://doi.org/10.1007/978-94-007-4315-1_5

59. Batista FD, Harwood NE. The who, how and where of antigen presentation to B cells. Nat Rev Immunol. 2009 Jan;9(1):15–27.

60. Guermonprez P, Valladeau J, Zitvogel L, Théry C, Amigorena S. Antigen Presentation and T Cell Stimulation by Dendritic Cells. Annual Review of Immunology. 2002;20(1):621–67.

61. Rock KL, Reits E, Neefjes J. Present Yourself! By MHC Class I and MHC Class II Molecules. Trends in Immunology. 2016 Nov 1;37(11):724–37.

62. Neefjes J, Jongsma MLM, Paul P, Bakke O. Towards a systems understanding of MHC class I and MHC class II antigen presentation. Nat Rev Immunol. 2011 Dec;11(12):823–36.

63. Zamboni DS, Rabinovitch M. Nitric Oxide Partially Controls Coxiella burnetii Phase II Infection in Mouse Primary Macrophages. Infect Immun. 2003 Mar;71(3):1225–33.

64. Ma J, Chen T, Mandelin J, Ceponis A, Miller NE, Hukkanen M, et al. Regulation of macrophage activation. Cell Mol Life Sci. 2003 Nov;60(11):2334–46.

65. Dellacasagrande J, Capo C, Raoult D, Mege JL. IFN-γ-Mediated Control of Coxiella burnetii Survival in Monocytes: The Role of Cell Apoptosis and TNF. The Journal of Immunology. 1999 Feb 15;162(4):2259–65.

66. Benoit M, Barbarat B, Bernard A, Olive D, Mege JL. Coxiella burnetii, the agent of Q fever, stimulates an atypical M2 activation program in human macrophages. European Journal of Immunology. 2008;38(4):1065–70.

67. Turco J, Thompson HA, Winkler HH. Interferon-gamma inhibits growth of Coxiella burnetii in mouse fibroblasts. Infection and Immunity. 1984 Sep;45(3):781–3.

68. Kumar H, Kawai T, Akira S. Pathogen Recognition by the Innate Immune System. International Reviews of Immunology. 2011 Jan 1;30(1):16–34.

69. Neumann M, Naumann M. Beyond IκBs: alternative regulation of NF-KB activity. The FASEB Journal. 2007;21(11):2642–54.

70. Watts C, West MA, Zaru R. TLR signalling regulated antigen presentation in dendritic cells. Current Opinion in Immunology. 2010 Feb 1;22(1):124–30.

71. Yoshimura S, Bondeson J, Foxwell BMJ, Brennan FM, Feldmann M. Effective antigen presentation by dendritic cells is NF-κB dependent: coordinate regulation of MHC, co-stimulatory molecules and cytokines. International Immunology. 2001 May 1;13(5):675–83.

72. Zinatizadeh MR, Schock B, Chalbatani GM, Zarandi PK, Jalali SA, Miri SR. The Nuclear Factor Kappa B (NF-kB) signaling in cancer development and immune diseases. Genes & Diseases. 2021 May 1;8(3):287–97.

73. Germain RN. MHC-dependent antigen processing and peptide presentation: Providing ligands for T lymphocyte activation. Cell. 1994 Jan 28;76(2):287–99.

74. Buttrum L, Ledbetter L, Cherla R, Zhang Y, Mitchell WJ, Zhang G. Both Major Histocompatibility Complex Class I (MHC-I) and MHC-II Molecules Are Required, while MHC-I Appears To Play a Critical Role in Host Defense against Primary *Coxiella burnetii* Infection. Roy CR, editor. Infect Immun. 2018 Jan 8;86(4):e00602-17, /iai/86/4/e00602-17.atom.

75. Romagnani S. The Th1/Th2 paradigm. Immunology Today. 1997 Jun 1;18(6):263–6.

76. Netea MG, Meer JWMV der, Sutmuller RP, Adema GJ, Kullberg BJ. From the Th1/Th2 Paradigm towards a Toll-Like Receptor/T-Helper Bias. Antimicrobial Agents and Chemotherapy. 2005 Oct 1;49(10):3991–6.

77. Shi JH, Sun SC. Tumor Necrosis Factor Receptor-Associated Factor Regulation of Nuclear Factor κB and Mitogen-Activated Protein Kinase Pathways. Frontiers in Immunology [Internet]. 2018 [cited 2023 Feb 22];9. Available from: https://www.frontiersin.org/articles/10.3389/fimmu.2018.01849

78. O'Byrne PM, Inman MD, Parameswaran K. The trials and tribulations of IL-5, eosinophils, and allergic asthma. Journal of Allergy and Clinical Immunology. 2001 Oct 1;108(4):503–8.

79. Mittal SK, Roche PA. Suppression of antigen presentation by IL-10. Current Opinion in Immunology. 2015 Jun 1;34:22–7.

80. Gagliani N, Huber S. Basic Aspects of T Helper Cell Differentiation. In: Lugli E, editor. T-Cell Differentiation: Methods and Protocols [Internet]. New York, NY: Springer; 2017 [cited 2023 Jun 5]. p. 19–30. (Methods in Molecular Biology). Available from: https://doi.org/10.1007/978-1-4939-6548-9_2

81. Zhu J. T Helper Cell Differentiation, Heterogeneity, and Plasticity. Cold Spring Harb Perspect Biol. 2018 Oct 1;10(10):a030338.

82. Shevyrev D, Tereshchenko V. Treg Heterogeneity, Function, and Homeostasis. Frontiers in Immunology [Internet]. 2020 [cited 2023 Jun 5];10. Available from: https://www.frontiersin.org/articles/10.3389/fimmu.2019.03100

83. Raffin C, Vo LT, Bluestone JA. Treg cell-based therapies: challenges and perspectives. Nat Rev Immunol. 2020 Mar;20(3):158–72.

84. Onishi Y, Fehervari Z, Yamaguchi T, Sakaguchi S. Foxp3+ natural regulatory T cells preferentially form aggregates on dendritic cells in vitro and actively inhibit their maturation. Proc Natl Acad Sci U S A. 2008 Jul 22;105(29):10113–8.

85. Hou Y, Cao Y, Dong L, Huang Y, Zhang Z, Bi Y, et al. Regulation of follicular T helper cell differentiation in antitumor immunity. International Journal of Cancer. 2023;153(2):265–77.

86. Zhang M, Zhou L, Xu Y, Yang M, Xu Y, Komaniecki GP, et al. A STAT3 palmitoylation cycle promotes TH17 differentiation and colitis. Nature. 2020 Oct;586(7829):434–9.

87. Klein L, Robey EA, Hsieh CS. Central CD4+ T cell tolerance: deletion versus regulatory T cell differentiation. Nat Rev Immunol. 2019 Jan;19(1):7–18.

88. Savage PA, Klawon DEJ, Miller CH. Regulatory T Cell Development. Annual Review of Immunology. 2020;38(1):421–53.

89. Andris F, Denanglaire S, Anciaux M, Hercor M, Hussein H, Leo O. The Transcription Factor c-Maf Promotes the Differentiation of Follicular Helper T Cells. Front Immunol. 2017 Apr 27;8:480.

90. Mills CD, Kincaid K, Alt JM, Heilman MJ, Hill AM. M-1/M-2 Macrophages and the Th1/Th2 Paradigm. J Immunol. 2000 Jun 15;164(12):6166–73.

91. Medzhitov R. The spectrum of inflammatory responses. Science. 2021 Nov 26;374(6571):1070–5.

92. Charles A Janeway J, Travers P, Walport M, Shlomchik MJ. Macrophage activation by armed CD4 TH1 cells. In: Immunobiology: The Immune System in Health and Disease 5th edition [Internet]. Garland Science; 2001 [cited 2023 May 19]. Available from: https://www.ncbi.nlm.nih.gov/books/NBK27153/

93. Bronte V, Zanovello P. Regulation of immune responses by L -arginine metabolism. Nature Reviews Immunology. 2005 Aug;5(8):641–54.

94. Ghigo E, Capo C, Raoult D, Mege JL. Interleukin-10 stimulates Coxiella burnetii replication in human monocytes through tumor necrosis factor down-modulation: role in microbicidal defect of Q fever. Infect Immun. 2001 Apr;69(4):2345–52.

95. Wolfs TGAM, Buurman WA, Schadewijk A van, Vries B de, Daemen MARC, Hiemstra PS, et al. In Vivo Expression of Toll-Like Receptor 2 and 4 by Renal Epithelial Cells: IFN-γ and TNF-α Mediated Up-Regulation During Inflammation. The Journal of Immunology. 2002 Feb 1;168(3):1286–93.

96. Yap GS, Sher A. Cell-mediated Immunity to Toxoplasma Gondii: Initiation, Regulation and Effector Function. Immunobiology. 1999 Dec 1;201(2):240–7.

97. Hahn H, Kaufmann SHE. The Role of Cell-Mediated Immunity in Bacterial Infections. Reviews of Infectious Diseases. 1981;3(6):1221–50.

98. Portnoy DA, Auerbuch V, Glomski IJ. The cell biology of Listeria monocytogenes infection the intersection of bacterial pathogenesis and cell-mediated immunity. J Cell Biol. 2002 Aug 5;158(3):409–14.

99. Stenger S, Modlin RL. T cell mediated immunity to Mycobacterium tuberculosis. Current Opinion in Microbiology. 1999 Feb 1;2(1):89–93.

100. Andoh M, Zhang G, Russell-Lodrigue KE, Shive HR, Weeks BR, Samuel JE. T cells are essential for bacterial clearance, and gamma interferon, tumor necrosis factor alpha, and B cells are crucial for disease development in Coxiella burnetii infection in mice. Infect Immun. 2007 Jul;75(7):3245–55.

101. Andoh M, Naganawa T, Hotta A, Yamaguchi T, Fukushi H, Masegi T, et al. SCID mouse model for lethal Q fever. Infect Immun. 2003 Aug;71(8):4717–23.

102. Ghigo E, Capo C, Tung CH, Raoult D, Gorvel JP, Mege JL. Coxiella burnetii Survival in THP-1 Monocytes Involves the Impairment of Phagosome Maturation: IFN-γ Mediates its Restoration and Bacterial Killing. The Journal of Immunology. 2002 Oct 15;169(8):4488–95.

103. Read AJ, Erickson S, Harmsen AG. Role of CD4+ and CD8+ T cells in clearance of primary pulmonary infection with Coxiella burnetii. Infect Immun. 2010/03/29 ed. 2010 Jul;78(7):3019–26.

104. Bagchi A, Herrup EA, Warren HS, Trigilio J, Shin HS, Valentine C, et al. MyD88-Dependent and MyD88-Independent Pathways in Synergy, Priming, and Tolerance between TLR Agonists1. The Journal of Immunology. 2007 Jan 15;178(2):1164–71.

105. Casella CR, Mitchell TC. Putting endotoxin to work for us: monophosphoryl lipid A as a safe and effective vaccine adjuvant. Cell Mol Life Sci. 2008 Oct;65(20):3231–40.

106. Campbell JD. Development of the CpG Adjuvant 1018: A Case Study. In: Fox CB, editor. Vaccine Adjuvants: Methods and Protocols [Internet]. New York, NY: Springer; 2017 [cited 2020 Oct 14]. p. 15–27. (Methods in Molecular Biology). Available from: https://doi.org/10.1007/978-1-4939-6445-1_2

107. Foged C, Rades T, Perrie Y, Hook S. Subunit vaccine delivery. Springer; 2015.

108. Vartak A, Sucheck SJ. Recent Advances in Subunit Vaccine Carriers. Vaccines. 2016 Jun;4(2):12.

109. Hansson M, Nygren PA, Sta˚hl S. Design and production of recombinant subunit vaccines. Biotechnology and Applied Biochemistry. 2000;32(2):95–107.

110. Cox JC, Coulter AR. Adjuvants—a classification and review of their modes of action. Vaccine. 1997 Feb 1;15(3):248–56.

111. Del Giudice G, Rappuoli R, Didierlaurent AM. Correlates of adjuvanticity: A review on adjuvants in licensed vaccines. Seminars in Immunology. 2018 Oct 1;39:14–21.

112. Huang P, Wang X, Liang X, Yang J, Zhang C, Kong D, et al. Nano-, micro-, and macroscale drug delivery systems for cancer immunotherapy. Acta Biomaterialia. 2019 Feb 1;85:1–26.

113. Bookstaver ML, Tsai SJ, Bromberg JS, Jewell CM. Improving Vaccine and Immunotherapy Design Using Biomaterials. Trends in Immunology. 2018 Feb 1;39(2):135–50.

114. Moyer TJ, Zmolek AC, Irvine DJ. Beyond antigens and adjuvants: formulating future vaccines. J Clin Invest. 2016 Mar 1;126(3):799–808.

115. Huang X, Wang X, Zhang J, Xia N, Zhao Q. Escherichia coli-derived virus-like particles in vaccine development. npj Vaccines. 2017 Feb 9;2(1):1–9.

116. Chackerian B. Virus-like particles: flexible platforms for vaccine development. Expert Review of Vaccines. 2007 Jun 1;6(3):381–90.

117. Mohsen MO, Augusto G, Bachmann MF. The 3Ds in virus-like particle based-vaccines: “Design, Delivery and Dynamics.” Immunological Reviews. 2020;296(1):155–68.

118. Kang SM, Kim MC, Compans RW. Virus-like particles as universal influenza vaccines. Expert Review of Vaccines. 2012 Aug 1;11(8):995–1007.

119. Quan FS, Lee YT, Kim KH, Kim MC, Kang SM. Progress in developing virus-like particle influenza vaccines. Expert Review of Vaccines. 2016 Oct 2;15(10):1281–93.

120. Joe CCD, Chatterjee S, Lovrecz G, Adams TE, Thaysen-Andersen M, Walsh R, et al. Glycoengineered hepatitis B virus-like particles with enhanced immunogenicity. Vaccine. 2020 May 8;38(22):3892–901.

121. Wang JW, Roden RB. Virus-like particles for the prevention of human papillomavirus-associated malignancies. Expert Review of Vaccines. 2013 Feb 1;12(2):129–41.

122. Schiller JT, Castellsagué X, Villa LL, Hildesheim A. An update of prophylactic human papillomavirus L1 virus-like particle vaccine clinical trial results. Vaccine. 2008 Aug 19;26:K53–61.

123. Hyer RN, Janssen RS. Immunogenicity and safety of a 2-dose hepatitis B vaccine, HBsAg/CpG 1018, in persons with diabetes mellitus aged 60–70 years. Vaccine. 2019 Sep 16;37(39):5854–61.

124. Singh M, Chakrapani A, O’Hagan D. Nanoparticles and microparticles as vaccine-delivery systems. Expert Review of Vaccines. 2007 Oct 1;6(5):797–808.

125. Gregory A, Williamson D, Titball R. Vaccine delivery using nanoparticles. Frontiers in Cellular and Infection Microbiology [Internet]. 2013 [cited 2023 May 18];3. Available from: https://www.frontiersin.org/articles/10.3389/fcimb.2013.00013

126. Gilkes AP, Albin TJ, Manna S, Supnet M, Ruiz S, Tom J, et al. Tuning Subunit Vaccines with Novel TLR Triagonist Adjuvants to Generate Protective Immune Responses against Coxiella burnetii. J Immunol. 2019 Dec 23;ji1900991.

127. Dong X, Liang J, Yang A, Qian Z, Kong D, Lv F. A Visible Codelivery Nanovaccine of Antigen and Adjuvant with Self-Carrier for Cancer Immunotherapy. ACS Appl Mater Interfaces. 2019 Feb 6;11(5):4876–88.

128. Sanità G, Carrese B, Lamberti A. Nanoparticle Surface Functionalization: How to Improve Biocompatibility and Cellular Internalization. Frontiers in Molecular Biosciences [Internet]. 2020 [cited 2023 May 20];7. Available from: https://www.frontiersin.org/articles/10.3389/fmolb.2020.587012

129. Badten AJ, Ramirez A, Hernandez-Davies JE, Albin TJ, Jain A, Nakajima R, et al. Protein Nanoparticle-Mediated Delivery of Recombinant Influenza Hemagglutinin Enhances Immunogenicity and Breadth of the Antibody Response. ACS Infect Dis. 2023 Jan 6;9(2):239–52.

130. Albin TJ. TLR Tri-Agonist and TLR-Antigen Conjugates as Modulators of Innate Immunity and as Adjuvants in a Q-Fever Vaccine [Internet]. UC Irvine; 2019 [cited 2023 May 20]. Available from: https://escholarship.org/uc/item/6840b8s9

131. Fratzke AP, Jan S, Felgner J, Liang L, Nakajima R, Jasinskas A, et al. Subunit Vaccines Using TLR Triagonist Combination Adjuvants Provide Protection Against Coxiella burnetii While Minimizing Reactogenic Responses. Frontiers in Immunology [Internet]. 2021 [cited 2023 Feb 22];12. Available from: https://www.frontiersin.org/articles/10.3389/fimmu.2021.653092

132. Dziarski R. Recognition of bacterial peptidoglycan by the innate immune system. CMLS, Cell Mol Life Sci. 2003 Sep 1;60(9):1793–804.

133. Mu C, Yang Y, Zhu W. Crosstalk Between The Immune Receptors and Gut Microbiota. Current Protein and Peptide Science. 2015 Nov 1;16(7):622–31.

134. Girardin SE, Philpott DJ. Mini-review: The role of peptidoglycan recognition in innate immunity. European Journal of Immunology. 2004;34(7):1777–82.

135. Ogawa C, Liu YJ, S. Kobayashi K. Muramyl Dipeptide and its Derivatives: Peptide Adjuvant in Immunological Disorders and Cancer Therapy. Current Bioactive Compounds. 2011 Sep 1;7(3):180–97.

136. Höltje JV. Growth of the Stress-Bearing and Shape-Maintaining Murein Sacculus of Escherichia coli. Microbiology and Molecular Biology Reviews. 1998 Mar;62(1):181–203.

137. Vigil A, Ortega R, Nakajima-Sasaki R, Pablo J, Molina DM, Chao CC, et al. Genome-wide profiling of humoral immune response to Coxiella burnetii infection by protein microarray. Proteomics. 2010 Jun;10(12):2259–69.

138. Vigil A, Chen C, Jain A, Nakajima-Sasaki R, Jasinskas A, Pablo J, et al. Profiling the humoral immune response of acute and chronic Q fever by protein microarray. Mol Cell Proteomics. 2011 Oct;10(10):M110.006304.

139. Fratzke AP, Jan S, Felgner J, Liang L, Nakajima R, Jasinskas A, et al. Subunit Vaccines Using TLR Triagonist Combination Adjuvants Provide Protection Against Coxiella burnetii While Minimizing Reactogenic Responses. Frontiers in Immunology [Internet]. 2021 [cited 2023 Feb 22];12. Available from: https://www.frontiersin.org/articles/10.3389/fimmu.2021.653092

140. Davies DH, Chun S, Hermanson G, Tucker JA, Jain A, Nakajima R, et al. T cell antigen discovery using soluble vaccinia proteome reveals recognition of antigens with both virion and non-virion association. J Immunol. 2014 Aug 15;193(4):1812–27.

141. Hernandez-Davies JE, Felgner J, Strohmeier S, Pone EJ, Jain A, Jan S, et al. Administration of Multivalent Influenza Virus Recombinant Hemagglutinin Vaccine in Combination-Adjuvant Elicits Broad Reactivity Beyond the Vaccine Components. Front Immunol. 2021 Jul 14;12:692151.

142. Hernandez-Davies JE, Dollinger EP, Pone EJ, Felgner J, Liang L, Strohmeier S, et al. Magnitude and breadth of antibody cross-reactivity induced by recombinant influenza hemagglutinin trimer vaccine is enhanced by combination adjuvants. Sci Rep. 2022 Jun 2;12(1):9198.

143. Keestra-Gounder AM, Tsolis RM. NOD1 and NOD2: Beyond Peptidoglycan Sensing. Trends in Immunology. 2017 Oct 1;38(10):758–67.

144. Wolf AJ, Underhill DM. Peptidoglycan recognition by the innate immune system. Nat Rev Immunol. 2018 Apr;18(4):243–54.

145. Kühner D, Stahl M, Demircioglu DD, Bertsche U. From cells to muropeptide structures in 24 h: peptidoglycan mapping by UPLC-MS. Sci Rep. 2014 Dec 16;4:7494.

146. Desmarais SM, Cava F, De Pedro MA, Huang KC. Isolation and Preparation of Bacterial Cell Walls for Compositional Analysis by Ultra Performance Liquid Chromatography. JoVE. 2014 Jan 15;(83):51183.

147. Shafa F, Salton MRJ. Disaggregation of Bacterial Cell Walls by Anionic Detergents. Microbiology. 1960;23(1):137–41.

148. Siegrist MS, Whiteside S, Jewett JC, Aditham A, Cava F, Bertozzi CR. d-Amino Acid Chemical Reporters Reveal Peptidoglycan Dynamics of an Intracellular Pathogen. ACS Chem Biol. 2013 Mar 15;8(3):500–5.

149. Kuru E, Hughes HV, Brown PJ, Hall E, Tekkam S, Cava F, et al. In Situ probing of newly synthesized peptidoglycan in live bacteria with fluorescent D-amino acids. Angew Chem Int Ed Engl. 2012 Dec 7;51(50):12519–23.

150. Schudel A, Francis DM, Thomas SN. Material design for lymph node drug delivery. Nat Rev Mater. 2019 Jun;4(6):415–28.

151. Thomas SN, Schudel A. Overcoming transport barriers for interstitial-, lymphatic-, and lymph node-targeted drug delivery. Current Opinion in Chemical Engineering. 2015 Feb 1;7:65–74.

152. Blank F, Stumbles PA, Seydoux E, Holt PG, Fink A, Rothen-Rutishauser B, et al. Size-Dependent Uptake of Particles by Pulmonary Antigen-Presenting Cell Populations and Trafficking to Regional Lymph Nodes. Am J Respir Cell Mol Biol. 2013 Jul;49(1):67–77.

153. Lauer KB, Borrow R, Blanchard TJ. Multivalent and Multipathogen Viral Vector Vaccines. Clinical and Vaccine Immunology. 2017 Jan 5;24(1):e00298-16.

154. Arsiwala A, Castro A, Frey S, Stathos M, Kane RS. Designing Multivalent Ligands to Control Biological Interactions: From Vaccines and Cellular Effectors to Targeted Drug Delivery. Chemistry – An Asian Journal. 2019;14(2):244–55.

155. Bennett NR, Zwick DB, Courtney AH, Kiessling LL. Multivalent Antigens for Promoting B and T Cell Activation. ACS Chem Biol. 2015 Aug 21;10(8):1817–24.

156. Gilmore TD. Introduction to NF-κB: players, pathways, perspectives. Oncogene. 2006 Oct;25(51):6680–4.

157. Moynagh PN. The NF-κB pathway. Journal of Cell Science. 2005 Oct 15;118(20):4589–92.

158. Capparelli R, Nocerino N, Medaglia C, Blaiotta G, Bonelli P, Iannelli D. The Staphylococcus aureus Peptidoglycan Protects Mice against the Pathogen and Eradicates Experimentally Induced Infection. PLOS ONE. 2011 Dec 1;6(12):e28377.

159. Chen Y, Liu B, Yang D, Li X, Wen L, Zhu P, et al. Peptide mimics of peptidoglycan are vaccine candidates and protect mice from infection with Staphylococcus aureus. Journal of Medical Microbiology. 2011;60(7):995–1002.

160. Romero-Saavedra F, Laverde D, Wobser D, Michaux C, Budin-Verneuil A, Bernay B, et al. Identification of Peptidoglycan-Associated Proteins as Vaccine Candidates for Enterococcal Infections. PLOS ONE. 2014 Nov 4;9(11):e111880.

161. Gerritzen MJH, Martens DE, Wijffels RH, van der Pol L, Stork M. Bioengineering bacterial outer membrane vesicles as vaccine platform. Biotechnology Advances. 2017 Sep 1;35(5):565–74.

162. Kashyap D, Panda M, Baral B, Varshney N, R S, Bhandari V, et al. Outer Membrane Vesicles: An Emerging Vaccine Platform. Vaccines. 2022 Oct;10(10):1578.

163. van der Pol L, Stork M, van der Ley P. Outer membrane vesicles as platform vaccine technology. Biotechnology Journal. 2015;10(11):1689–706.

164. Holst J, Martin D, Arnold R, Huergo CC, Oster P, O'Hallahan J, et al. Properties and clinical performance of vaccines containing outer membrane vesicles from Neisseria meningitidis. Vaccine. 2009 Jun 24;27:B3–12.

165. Schild S, Nelson EJ, Bishop AL, Camilli A. Characterization of Vibrio cholerae Outer Membrane Vesicles as a Candidate Vaccine for Cholera. Infection and Immunity. 2009 Jan;77(1):472–84.

166. Kersh GJ, Wolfe TM, Fitzpatrick KA, Candee AJ, Oliver LD, Patterson NE, et al. Presence of Coxiella burnetii DNA in the Environment of the United States, 2006 to 2008. Applied and Environmental Microbiology. 2010 Jul;76(13):4469–75.

167. Lockhart MG, Islam A, Fenwick SG, Graves SR, Stenos J. Comparative sensitivity of four different cell lines for the isolation of Coxiella burnetii. FEMS Microbiology Letters. 2012 Sep 1;334(2):75–8.

168. Chiu CK, Durrheim DN. A review of the efficacy of human Q fever vaccine registered in Australia [Internet]. Database of Abstracts of Reviews of Effects (DARE): Quality-assessed

Reviews [Internet]. Centre for Reviews and Dissemination (UK); 2007 [cited 2023 Feb 22]. Available from: https://www.ncbi.nlm.nih.gov/books/NBK74583/

169. Gefenaite G, Munster JM, van Houdt R, Hak E. Effectiveness of the Q fever vaccine: A meta-analysis. Vaccine. 2011 Jan 10;29(3):395–8.

170. Pasquale AD, Preiss S, Silva FTD, Garçon N. Vaccine Adjuvants: from 1920 to 2015 and Beyond. Vaccines. 2015 Jun;3(2):320–43.

171. Lecrenier N, Beukelaers P, Colindres R, Curran D, De Kesel C, De Saegher JP, et al. Development of adjuvanted recombinant zoster vaccine and its implications for shingles prevention. Expert Review of Vaccines. 2018 Jul 3;17(7):619–34.

172. Campbell JD. Development of the CpG Adjuvant 1018: A Case Study. In: Fox CB, editor. Vaccine Adjuvants: Methods and Protocols [Internet]. New York, NY: Springer; 2017 [cited 2023 Feb 22]. p. 15–27. (Methods in Molecular Biology). Available from: https://doi.org/10.1007/978-1-4939-6445-1_2

173. Wang YQ, Bazin-Lee H, Evans JT, Casella CR, Mitchell TC. MPL Adjuvant Contains Competitive Antagonists of Human TLR4. Frontiers in Immunology [Internet]. 2020 [cited 2023 Mar 9];11. Available from: https://www.frontiersin.org/articles/10.3389/fimmu.2020.577823

174. Nanishi E, Dowling DJ, Levy O. Toward precision adjuvants: optimizing science and safety. Curr Opin Pediatr. 2020 Feb;32(1):125–38.

175. Choubini E, Habibi M, Khorshidi A, Ghasemi A, Asadi Karam MR, Bouzari S. A novel multi-peptide subunit vaccine admixed with AddaVax adjuvant produces significant immunogenicity and protection against Proteus mirabilis urinary tract infection in mice model. Molecular Immunology. 2018 Apr 1;96:88–97.

176. Hawksworth D. Advancing Freund's and AddaVax Adjuvant Regimens Using CpG Oligodeoxynucleotides. Monoclonal Antibodies in Immunodiagnosis and Immunotherapy. 2018 Oct;37(5):195–9.

177. Ihnatko R, Shaw E, Toman R. Proteome of Coxiella burnetii. In: Toman R, Heinzen RA, Samuel JE, Mege JL, editors. Coxiella burnetii: Recent Advances and New Perspectives in Research of the Q Fever Bacterium [Internet]. Dordrecht: Springer Netherlands; 2012 [cited 2023 Mar 9]. p. 105–30. (Advances in Experimental Medicine and Biology). Available from: https://doi.org/10.1007/978-94-007-4315-1_6

178. Skultety L, Hajduch M, Flores-Ramirez G, Miernyk JA, Ciampor F, Toman R, et al. Proteomic comparison of virulent phase I and avirulent phase II of Coxiella burnetii, the causative agent of Q fever. Journal of Proteomics. 2011 Sep 6;74(10):1974–84.

179. Kersh GJ, Fitzpatrick KA, Self JS, Biggerstaff BJ, Massung RF. Long-Term Immune Responses to Coxiella burnetii after Vaccination. Clin Vaccine Immunol. 2013 Feb;20(2):129–33.

180. Soria-Guerra RE, Nieto-Gomez R, Govea-Alonso DO, Rosales-Mendoza S. An overview of bioinformatics tools for epitope prediction: Implications on vaccine development. Journal of Biomedical Informatics. 2015 Feb 1;53:405–14.

181. Zhang L. Multi-epitope vaccines: a promising strategy against tumors and viral infections. Cell Mol Immunol. 2018 Feb;15(2):182–4.

182. López-Siles M, Corral-Lugo A, McConnell MJ. Vaccines for multidrug resistant Gram negative bacteria: lessons from the past for guiding future success. FEMS Microbiology Reviews. 2021 May 1;45(3):fuaa054.

183. Jaydari A, Forouharmehr A, Nazifi N. Determination of immunodominant scaffolds of Com1 and OmpH antigens of Coxiella burnetii. Microbial Pathogenesis. 2019 Jan 1;126:298–309.

184. Samuel JE, Hendrix LR. Laboratory Maintenance of Coxiella burnetii. Current Protocols in Microbiology. 2009;15(1):6C.1.1-6C.1.16.

185. Seshadri R, Paulsen IT, Eisen JA, Read TD, Nelson KE, Nelson WC, et al. Complete genome sequence of the Q-fever pathogen Coxiella burnetii. Proc Natl Acad Sci U S A. 2003 Apr 29;100(9):5455–60.

186. Beare PA, Chen C, Bouman T, Pablo J, Unal B, Cockrell DC, et al. Candidate Antigens for Q Fever Serodiagnosis Revealed by Immunoscreening of a Coxiella burnetii Protein Microarray. Clin Vaccine Immunol. 2008 Dec;15(12):1771–9.

187. Xiong X, Wang X, Wen B, Graves S, Stenos J. Potential serodiagnostic markers for Q fever identified in Coxiella burnetii by immunoproteomic and protein microarray approaches. BMC Microbiol. 2012 Mar 16;12:35.

188. Deringer JR, Chen C, Samuel JE, Brown WC. Immunoreactive Coxiella burnetii Nine Mile proteins separated by 2D electrophoresis and identified by tandem mass spectrometry. Microbiology (Reading). 2011 Feb;157(Pt 2):526–42.

189. Sekeyová Z, Kowalczewska M, Decloquement P, Pelletier N, Špitalská E, Raoult D. Identification of protein candidates for the serodiagnosis of Q fever endocarditis by an immunoproteomic approach. Eur J Clin Microbiol Infect Dis. 2009 Mar 1;28(3):287–95.

190. Hernychova L, Toman R, Ciampor F, Hubalek M, Vackova J, Macela A, et al. Detection and Identification of Coxiella burnetii Based on the Mass Spectrometric Analyses of the Extracted Proteins. Anal Chem. 2008 Sep 15;80(18):7097–104.

191. Vranakis I, Papadioti A, Tselentis Y, Psaroulaki A, Tsiotis G. The contribution of proteomics towards deciphering the enigma of Coxiella burnetii. PROTEOMICS – Clinical Applications. 2013;7(1–2):193–204.

192. Zuo X, Li S, Hall J, Mattern MR, Tran H, Shoo J, et al. Enhanced Expression and Purification of Membrane Proteins by SUMO Fusion in Escherichia coli. J Struct Funct Genomics. 2005 Sep 1;6(2):103–11.

193. Koussa MA, Sotomayor M, Wong WP. Protocol for sortase-mediated construction of DNA–protein hybrids and functional nanostructures. Methods. 2014 May 15;67(2):134–41.

194. Lata S, Reichel A, Brock R, Tampé R, Piehler J. High-Affinity Adaptors for Switchable Recognition of Histidine-Tagged Proteins. J Am Chem Soc. 2005 Jul 1;127(29):10205–15.

195. Nazeri S, Zakeri S, Mehrizi AA, Sardari S, Djadid ND. Measuring of IgG2c isotype instead of IgG2a in immunized C57BL/6 mice with Plasmodium vivax TRAP as a subunit vaccine candidate in order to correct interpretation of Th1 versus Th2 immune response. Experimental Parasitology. 2020 Sep 1;216:107944.

196. Spellberg B, Edwards JE Jr. Type 1/Type 2 Immunity in Infectious Diseases. Clinical Infectious Diseases. 2001 Jan 1;32(1):76–102.

197. Hernandez-Pando R, Rook GA. The role of TNF-alpha in T-cell-mediated inflammation depends on the Th1/Th2 cytokine balance. Immunology. 1994 Aug;82(4):591–5.

198. Andoh M, Zhang G, Russell-Lodrigue KE, Shive HR, Weeks BR, Samuel JE. T Cells Are Essential for Bacterial Clearance, and Gamma Interferon, Tumor Necrosis Factor Alpha, and B Cells Are Crucial for Disease Development in Coxiella burnetii Infection in Mice. Infection and Immunity. 2007 Jul;75(7):3245–55.

199. Bewley KR. Animal Models of Q Fever (Coxiella burnetii). Comparative Medicine. 2013 Dec 1;63(6):469–76.

200. Russell-Lodrigue KE, Zhang GQ, McMurray DN, Samuel JE. Clinical and Pathologic Changes in a Guinea Pig Aerosol Challenge Model of Acute Q Fever. Infection and Immunity. 2006 Nov;74(11):6085–91.

201. Lynn GM, Chytil P, Francica JR, Lagová A, Kueberuwa G, Ishizuka AS, et al. Impact of Polymer-TLR-7/8 Agonist (Adjuvant) Morphology on the Potency and Mechanism of CD8 T Cell Induction. Biomacromolecules. 2019 Feb 11;20(2):854–70.

202. Fratzke AP, van Schaik EJ, Samuel JE. Immunogenicity and Reactogenicity in Q Fever Vaccine Development. Front Immunol. 2022 May 26;13:886810.

203. Blondeau JM, Williams JC, Marrie TJ. The Immune Response to Phase I and Phase II Coxiella burnetii Antigens as Measured by Western Immunoblottinga. Annals of the New York Academy of Sciences. 1990;590(1):187–202.

204. Camacho MT, Outschoorn I, Kovácová E, Téllez A. Distribution of immunoglobulin G (IgG) and A (IgA) subclasses following Q fever vaccination with soluble phase I Coxiella burnetii extract. Vaccine. 2000 Mar 6;18(17):1773–7.

205. WORSWICK D, MARMION BP. Antibody responses in acute and chronic Q fever and in subjects vaccinated against Q fever. Journal of Medical Microbiology. 1985;19(3):281–96.

206. Kishimoto RA, Veltri BJ, Canonico PG, Shirey FG, Walker JS. Electron microscopic study on the interaction between normal guinea pig peritoneal macrophages and Coxiella burnetii. Infection and Immunity. 1976 Oct;14(4):1087–96.

207. Zhang G, Russell-Lodrigue KE, Andoh M, Zhang Y, Hendrix LR, Samuel JE. Mechanisms of Vaccine-Induced Protective Immunity against Coxiella burnetii Infection in BALB/c Mice1. The Journal of Immunology. 2007 Dec 15;179(12):8372–80.

208. Read AJ, Erickson S, Harmsen AG. Role of CD4+ and CD8+ T Cells in Clearance of Primary Pulmonary Infection with Coxiella burnetii. Infection and Immunity. 2010 Jul;78(7):3019–26.

209. Dellacasagrande J, Capo C, Raoult D, Mege JL. IFN-γ-Mediated Control of Coxiella burnetii Survival in Monocytes: The Role of Cell Apoptosis and TNF1. The Journal of Immunology. 1999 Feb 15;162(4):2259–65.

210. Howe D, Barrows LF, Lindstrom NM, Heinzen RA. Nitric Oxide Inhibits Coxiella burnetii Replication and Parasitophorous Vacuole Maturation. Infect Immun. 2002 Sep;70(9):5140–7.

211. Fernandes TD, Cunha LD, Ribeiro JM, Massis LM, Lima-Junior DS, Newton HJ, et al. Murine Alveolar Macrophages Are Highly Susceptible to Replication of Coxiella burnetii Phase II In Vitro. Infection and Immunity. 2016 Aug 19;84(9):2439–48.

212. Sarti L, Lezmi G, Mori F, Giovannini M, Caubet JC. Diagnosis and management of hypersensitivity reactions to vaccines. Expert Review of Clinical Immunology. 2020 Sep 1;16(9):883–96.

213. Marwa K, Kondamudi NP. Type IV Hypersensitivity Reaction. In: StatPearls [Internet]. Treasure Island (FL): StatPearls Publishing; 2022 [cited 2023 Feb 22]. Available from: http://www.ncbi.nlm.nih.gov/books/NBK562228/

214. Moos A, Hackstadt T. Comparative virulence of intra- and interstrain lipopolysaccharide variants of Coxiella burnetii in the guinea pig model. Infect Immun. 1987 May;55(5):1144–50.

215. Hackstadt T. Steric hindrance of antibody binding to surface proteins of Coxiella burnetti by phase I lipopolysaccharide. Infect Immun. 1988 Apr;56(4):802–7.

216. Conti F, Boucherit N, Baldassarre V, Trouplin V, Toman R, Mottola G, et al. Coxiella burnetii lipopolysaccharide blocks p38α-MAPK activation through the disruption of TLR-2 and TLR-4 association. Front Cell Infect Microbiol. 2015 Jan 6;4:182.

217. Dellacasagrande J, Ghigo E, Capo C, Raoult D, Mege JL. Coxiella burnetii Survives in Monocytes from Patients with Q Fever Endocarditis: Involvement of Tumor Necrosis Factor. Infect Immun. 2000 Jan;68(1):160–4.

218. Honstettre A, Ghigo E, Moynault A, Capo C, Toman R, Akira S, et al. Lipopolysaccharide from Coxiella burnetii Is Involved in Bacterial Phagocytosis, Filamentous Actin Reorganization, and Inflammatory Responses through Toll-Like Receptor 41. The Journal of Immunology. 2004 Mar 15;172(6):3695–703.

219. Boucherit N, Barry AO, Mottola G, Trouplin V, Capo C, Mege JL, et al. Effects of Coxiella burnetii on MAPKinases phosphorylation. FEMS Immunology & Medical Microbiology. 2012 Feb 1;64(1):101–3.

220. Saha RN, Jana M, Pahan K. MAPK p38 Regulates Transcriptional Activity of NF-κB in Primary Human Astrocytes via Acetylation of p65. J Immunol. 2007 Nov 15;179(10):7101–9.

221. Pone EJ, Hernandez-Davies JE, Jan S, Silzel E, Felgner PL, Davies DH. Multimericity Amplifies the Synergy of BCR and TLR4 for B Cell Activation and Antibody Class Switching. Front Immunol. 2022 May 19;13:882502.

222. Puffer EB, Pontrello JK, Hollenbeck JJ, Kink JA, Kiessling LL. Activating B Cell Signaling with Defined Multivalent Ligands. ACS Chem Biol. 2007 Apr 1;2(4):252–62.

223. Fan Z, Jan S, Hickey JC, Davies DH, Felgner J, Felgner PL, et al. Multifunctional Dendronized Polypeptides for Controlled Adjuvanticity. Biomacromolecules. 2021 Dec 13;22(12):5074–86.

224. Cho SK, Kwon YJ. Polyamine/DNA polyplexes with acid-degradable polymeric shell as structurally and functionally virus-mimicking nonviral vectors. Journal of Controlled Release. 2011 Mar 30;150(3):287–97.

225. Shah RR, Hassett KJ, Brito LA. Overview of Vaccine Adjuvants: Introduction, History, and Current Status. In: Fox CB, editor. Vaccine Adjuvants: Methods and Protocols [Internet]. New York, NY: Springer; 2017 [cited 2023 Jun 8]. p. 1–13. (Methods in Molecular Biology). Available from: https://doi.org/10.1007/978-1-4939-6445-1_1

226. Bhardwaj N, Gnjatic S, Sawhney NB. TLR AGONISTS: Are They Good Adjuvants? Cancer J. 2010;16(4):382–91.